

Switching Hybrid Polymers with Physically and Covalently Entrapped Organic Photochromes

Dissertation zur Erlangung des
naturwissenschaftlichen Doktorgrades
der Bayerischen Julius-Maximilians-Universität Würzburg

vorgelegt von

Anna Klukowska

aus Olsztyn, Polen

Würzburg 2004

Eingereicht am:

bei der Fakultät für Chemie und Pharmazie

1. Gutachter:

2. Gutachter:

der Dissertation

1. Prüfer:

2. Prüfer:

3. Prüfer:

des Öffentlichen Promotionskolloquiums

Tag des Öffentlichen Promotionskolloquiums:

Doktorurkunde ausgehändigt am:

i. TABLE OF CONTENTS

i. Table of contents	
ii. Index of abbreviations	
1. Abstract	1
2. Introduction	3
3. State of the art	7
3.1 Hybrid polymer matrices	7
3.1.1 The Sol-gel technique	7
3.1.2 Sol-gel derived hybrid nanocomposites and their application	11
3.1.3 Optical and ophthalmic materials and coatings	13
3.2 Photochromism	14
3.2.1 General definition	14
3.2.2 Classes of photochromes	15
3.2.3 Photochromic materials and coatings	29
3.2.4 Commercially available photochromic ophthalmic systems	32
4. Aim of this work	35
5. Experimental part	37
5.1 Measurements and methods	37
5.2 Chemicals and substrates	39
5.3 Preparation methods	42
5.3.1 Preparation of the matrix systems	42
5.3.2 Incorporation of dyes and other additives	45
5.4 Samples preparation	46
5.4.1 Measurement of photochromic activity	46
5.4.2 Measurement of photochromic kinetics	46
5.4.3 Samples for UV-Vis spectrophotometry	47
5.4.4 Samples for EPR and NMR analysis	47

6. Results and discussion	48
6.1 Matrix systems	48
6.1.1 Matrix development	48
6.1.2 Matrix characterisation	51
6.1.3 Polarity of hybrid polymers	62
6.2 Entrapment of photochromic dyes – coloration and photo fatigue	69
6.2.1 Dyes physically incorporated within GG and GB matrices	71
6.2.2 Dyes chemically incorporated within GG and GB matrices	73
6.2.3 Dyes physically incorporated within GA10 and GAD matrices	75
6.2.4 Dyes chemically incorporated within GA10 and GAD matrices	75
6.2.5 Commercially available dyes	79
6.2.6 Alternative matrix systems	81
6.2.7 Other factors that influence coloration and photo fatigue	84
6.3 Kinetics	88
6.4 Electron Spin Resonance Measurements	94
6.5 Optimisation	102
6.5.1 Stabilisers	102
6.5.2 Coating stacks	106
7. Conclusions	118
8. Zusammenfassung - Summary in German	120
9. References	122
Appendix 1	
Appendix 2	
Acknowledgments – Danksagung	
Curriculum Vitae – Lebenslauf	

ii. Index of Abbreviations

ADA – 3-(2-aminoethylamino)propylmethyldimethoxysilane

AMEO – aminopropyltriethoxysilane

AR – antireflective

AS – scratch resistant

CR-39® – plastic made of diallyl diglycol carbonate resin

DABCO -1,4-diazabicyclo[2.2.2]octane

DH – diethoxymethylsilane

ESR – electron spin resonance

ETES - ethyltriethoxysilane

FAS - tridecafluoro-1,1,2,2-tetrahydrooctyltriethoxysilane

GF20 - 3-triethoxysilylpropyl succinic anhydride

GLYMO – 3-glycidoxypropyl trimethoxysilane

HALS - hindered amine light stabiliser

HEPA – cis-hexahydrophthalic anhydride

ICT - intramolecular charge transfer

IR - infrared radiation

NISO – 1,3-dihydro-1,3-dimethylspiro[2H-indole-2,3'-[3H]naphth[2,1-b][1,4]oxazine]

NLO – non-linear optics

MAT – (N-methylaminopropyl)trimethoxysilane

MeOH – methanol

MC - merocyanine

MI – 1-methylimidazole

n-PrOH – n-propanol

PAM – polyacrylamide

PC - polycarbonate

PHA – (aminoethylaminomethyl)phenylethyl trimethoxysilane

PhTMO – phenyltrimethoxysilane

PVD - physical vapour deposition

rpm - revolutions per minute

SP - spiropyrane

SO – spirooxazine

TM 50 – colloidal silica particles, 50 % wt. SiO₂ in water, Ludox®

TMOS - tetramethoxysilane

UV-Vis - ultraviolet and visible light

λ_{max} - absorption maximum

1. Abstract

Hybrid, sol-gel derived poly(organo)siloxanes are well known as materials with tailorable properties for specific fields of application. Low temperature processing makes them suitable for coating of temperature sensitive plastic and many other substrates. Complex shaped objects can easily be dip, spray or spin coated with sol-gel lacquers. Transparent or mat “easy-to-clean” varnishes for metal surfaces or decorative colour coatings for glass are already present on the market. Photopatternable sol-gel materials are very promising for the manufacturing of microelectronic devices. In optics and ophthalmics poly(organo)siloxanes are used as antiscratch (AS) and antireflective (AR) coatings on plastic lenses. Tailorable physical and chemical properties make sol-gel derived materials excellent host materials for organic dyes, e.g. photochromic dyes. Photochromism can be defined as a reversible change in absorption characteristics of a chromophore upon UV light irradiation, for which several different molecular rearrangements depending on the dye class can be responsible. In the case of spirooxazines (SO) and spiropyrans (SP) a heterolytic cleavage of the C_{spiro}-O bond occurs upon UV irradiation. By incorporation of such photochromophores into sol-gel derived inorganic-organic hybrid polymers, versatile coatings with a fast photochromic response and high photochromic activity were obtained. Within the scope of this work, investigations on incorporation, photochromic activity, photo fatigue, switching on/off kinetics and possible ways of stabilisation were carried out with photochromes of the spirooxazine and chromene type and several different matrix systems. Of special interest were silylated dyes capable of participating in the sol-gel process, thus graftable to the polysiloxane backbones.

The resulting thin films showed good photochromic activities and no dye blooming. Their mechanical properties were at least comparable with the pure host material and they were applicable to different glass and plastic substrates. The final photochemical properties were determined by both dye and matrix properties. The chemical differences of the employed matrix materials were identified and characterised in terms of inorganic network connectivity (NMR measurements) and paramagnetic properties (ESR spectroscopy). Solvatochromic dyes were used to probe the polarity of the matrix free volume. The on/off kinetics for different coatings were investigated “in situ”, i.e., during the coloration process. Photodegradation was studied by means of artificial weathering, assessing the factors influencing the fatigue

behaviour of the coatings. A variety of stabilisation concepts were developed, applied and tested. Covalently entrapped dyes showed improved photochemical fatigue resistance. Also the application of stabilisers and oxygen scavengers had a positive influence on the photostability. Inorganic top coatings, usually used for antireflective equipment of ophthalmic lenses, acted as a barrier hindering the migration of ambient oxygen into the underlying photochromic coatings. The effect was a strong stabilisation of the photochromes leading to half life times superior to those of commercial products.

The successful creation of a photochromic coating with outstanding performance was expected to have large potential for many application such as optical switches, filters, UV sensors or sun protection systems, only to mention a few possibilities. The present thesis was focused on the major application field of photochromics i.e. smart ophthalmic lenses, that change their colour depending on the incident UV intensity. Based on the results obtained, an efficient stabilisation concept could be developed for sol-gel derived hybrid photochromic coatings.

2. Introduction

Light with its dual nature – as wave and particle - is essential for the existence of life. UV irradiation was one of the factors that had started the reaction chain leading to the creation of living organisms. Sunlight is the energy resource that enables plants to perform redox processes during the photosynthesis, whereby H₂O and CO₂ molecules are changed into carbohydrates. Cell chlorophyll as a light absorbing molecule is the main centre for the electron transfer process [1]. Many photophysical or photochemical processes are caused by light-matter interactions. Light is absorbed, scattered or transmitted when hitting an object. Absorbed energy is degraded to heat energy or can induce a variety of chemical changes e.g.: isomerisation, photofragmentation, photoaddition - to name only a few [2]. The numerous groups of chemical species that reversibly change their absorption and transmittance characteristics under irradiation (Figure 2.1.) are called photochromes. Most biological photoreceptors belong to this category [3]. Their bleach back reaction is either thermally or photochemically induced.

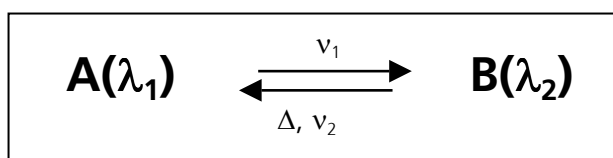


Figure 2.1. Photochromism as a reversible change of the compound A into form B with different absorption characteristics [4].

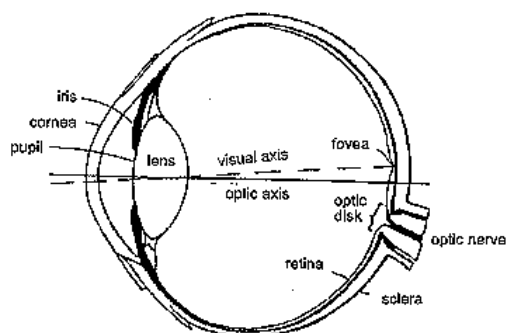


Figure 2.2. Anatomy of the human eye [5].

The human eye (Figure 2.2.) is an instrument that informs the brain about shapes and colours of the world around. The definition of it depends strongly on the

light present. The eye responds to electromagnetic radiation having wavelengths between 360 nm (blue) and 830 nm (red). The light reaching the cornea is composed of photons of various quantum energy values. The light sensitive cells placed in the retina send the information as a neural signal through the optic fibers and nerves. This distribution of wavelengths, interpreted during the process of visual perception, is assigned to a single subjective value: a colour. Colours do not exist independently or naturally, they are a “by-product” of perception. Isaac Newton’s colour circle (1666) gives an insight about complementary colours and additive colour mixing. The work of Thomas Young (1802) and James C. Maxwell (1860) can be considered as the basis for modern colorimetry. The colours were defined by the “Commission Internationale de l’Eclairage” (CIE) in 1931, and were improved in 1976, by means of the colour matching functions. The CIE standard system (known as the CIE chromaticity standard) is the basis for most quantitative colour measurements. When the light hits the eye with sufficient intensity, it irritates the light-sensitive cones. There are three types of cones, which are sensitive to red, green and blue light, respectively. Together they create a certain colour. The rods, the rhodopsin containing second type of the receptors in the human retina, are responsible for the monochrome vision.

UV radiation (UVR), as one part of the sunlight, is dangerous for human beings; e.g. the rate of deaths caused by skin cancer increases each year in Australia [6]. Awareness of the hazards of UVR has increased. The currently available knowledge of potential hazards to the eye (Figure 2.3.) proves that exposure to a very intense visible radiation source potentially harms the retina. Excessive UVR can be hazardous to the cornea and lens. The greatest retinal

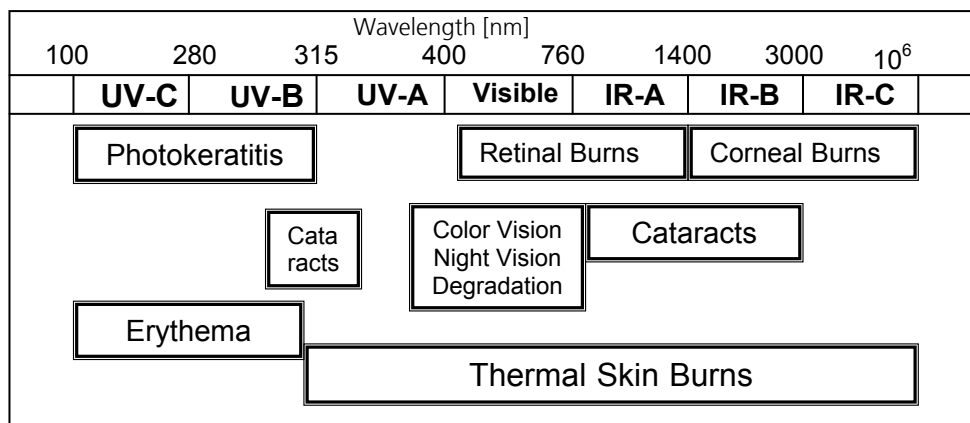


Figure 2.3. The optical spectrum and ocular effects [adopted from 7].

exposure to blue light and to UVR is most likely to occur when one is standing or walking outside in a field of snow without eye protection [7].

Therefore, sunglasses should have no significant transmittance in the UVR region according to the innovative Australian and New Zealand standards (Sunscreen products – evaluation and classification, Report No. AS 2604) [8]. Also protecting eyes from unwanted high intensity scenic, scattered or reflected visible light - “glare” – is a requirement for these lenses [9]. However, a complete blocking of the UV region is not the proper solution, because it would disturb human dye rhythm.

Already in the 60's first “intelligent” sunglasses were invented [4]. The colourless glasses changed reversibly into coloured ones upon UV irradiation. Active investigations in the last few decades on the “chameleon effect” of organic photochromic materials succeeded in a branch of new photochromic dyes. Their main disadvantage is the lack of sufficient photostability. Some examples of photochromes with a good to very good fatigue are spirooxazines, spiropyrans and chromenes [10]. The whole branch of colours, additionally to the traditional ophthalmic grey and brown hues, can provide a promising approach e.g. concerning an improvement of the reading fluency [11]. Proper host materials allowing a low temperature procedure for the incorporation of the dye are indispensable for the fabrication of photochromic optical materials. Hybrid polymers derived by the sol-gel process are one of the most promising possibilities. The matrices, combining features of inorganic and organic materials, offer some practical advantages for synthesis, doping and further application of the photochromic systems. Such a task-tailored photochrome-matrix combination could provide an improved effective protection of the human eye.

Appropriate sunglasses should have the following characteristics:

- adequately low transmittance for the visible light and UVR;
- the bleached hue should be nearly colourless (high luminous transmittance, above 80 %);
- the activated hue should have wide consumer acceptance;
- the activation and bleaching should have adequate kinetic behaviour, which is perceptible to the user;
- degradation of the photochromic effect must be sufficiently slow during the eyewear lifetime.

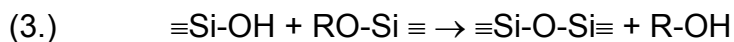
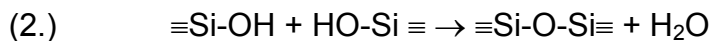
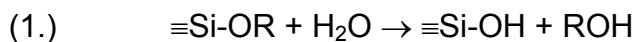
Low cost and reliable production of such sunglasses require an application system based on minimised amounts of dyes and low energy consumption. Coating of plastic lenses with sol-gel derived lacquers doped with photochromic dyes could fulfil the conditions named above.

3. State of the art

3.1 Hybrid polymer matrices

3.1.1 The Sol-gel technique

Sol-gel chemistry is based on the polycondensation of molecular precursors such as metal alkoxides $M(OR)_n$. The classical sol-gel route takes advantage of a sequence of reactions: hydrolysis of the alkoxy groups (1) and condensation (water condensation – 2 and alcohol condensation - 3). Precursors react in a liquid medium and lead to partially crosslinked three dimensional particulates suspended in the liquid, which is called the “sol” state. Further reactions, during aging and curing of the sol, lead to the solid amorphous state referred to as “gel”. Hydrolysis and condensation are then largely completed. Remaining solvents and water evaporate, before the amorphous material is built up. Hydrolysis and condensation of the alkoxides lead to the formation of metal-oxo polymers [12]:



Hydrolysis and condensation are influenced by many parameters. The complexity of the simultaneous processes and the multiplicity of the possible products is still a topic of continuous investigation. Changing the temperature, pH, catalyst, solvent, and water-to-silane ratio influences the formation of many intermediate states such as dimers, oligomers or higher condensation products. A number of different gradually hydrolysed species condense with each other. A specific direction of a reaction can be favoured upon appropriate choice of parameters. E.g. in a basic environment condensation is much faster than in acidic media, which preferably leads to three dimensional oligomer intermediates. The whole characteristics of the final coating or bulk material also depend on the storage time (aging) of the lacquer, curing manner, and properties of the substrate surface [13, 14].

The amorphous materials originating from a low temperature process are serious competitors for organic polymers as well as for inorganic glasses in many practical application fields. Using siloxane matrices instead of organic plastic materials has some potential advantages, also for new photochromic coatings:

- sol-gel glasses are transparent in the near UV;
- plastics deteriorate both thermally and photochemically, losing their mechanical strength and becoming opaque;
- the excited state of the trapped photoactive molecule is capable of reacting with organic polymers;
- sol-gel matrices isolate the trapped molecule from the external environment, plastics are much more permeable to e.g. oxygen;
- decomposition products are efficiently isolated in the sol-gel matrix.

Sol-gel derived materials are not as heavy and brittle as the classic inorganic glasses [15].

The unification of organic and inorganic properties in one material was the goal of numerous investigations in the past few decades. The flexibility and functionality of organic polymers combined with the transparency and hardness of inorganic glasses, gives the chance to create a lot of new material property combinations. The sol-gel process is the most convenient reaction method to achieve this unification. The mild reaction conditions offered by the hydrolysis and condensation reactions allow the introduction of organic molecules or even biomolecules into an inorganic network [16]. Inorganic and organic components can be mixed on a nanometric scale (supramolecular level). The organic and inorganic networks in composite materials can exist separately without any chemical bonding (Figure 3.1. a, b, e) or with strong chemical bonds linking the organic and inorganic components (Figure 3.1. c, d, f). Various strategies for the formation of sol-gel derived hybrid nanocomposites can be applied:

- a.) mixing of the precursors for the sol-gel process with the organic polymer followed by the inorganic polycondensation reaction,
- b.) polymerisation of an organic monomer in the inorganic gel,
- c.) simultaneous formation of the organic and inorganic networks, and
- d.) using dual network materials in which the molecular precursors for the formation of the two networks are covalently linked to each other (Figure 3.1. f) [17].

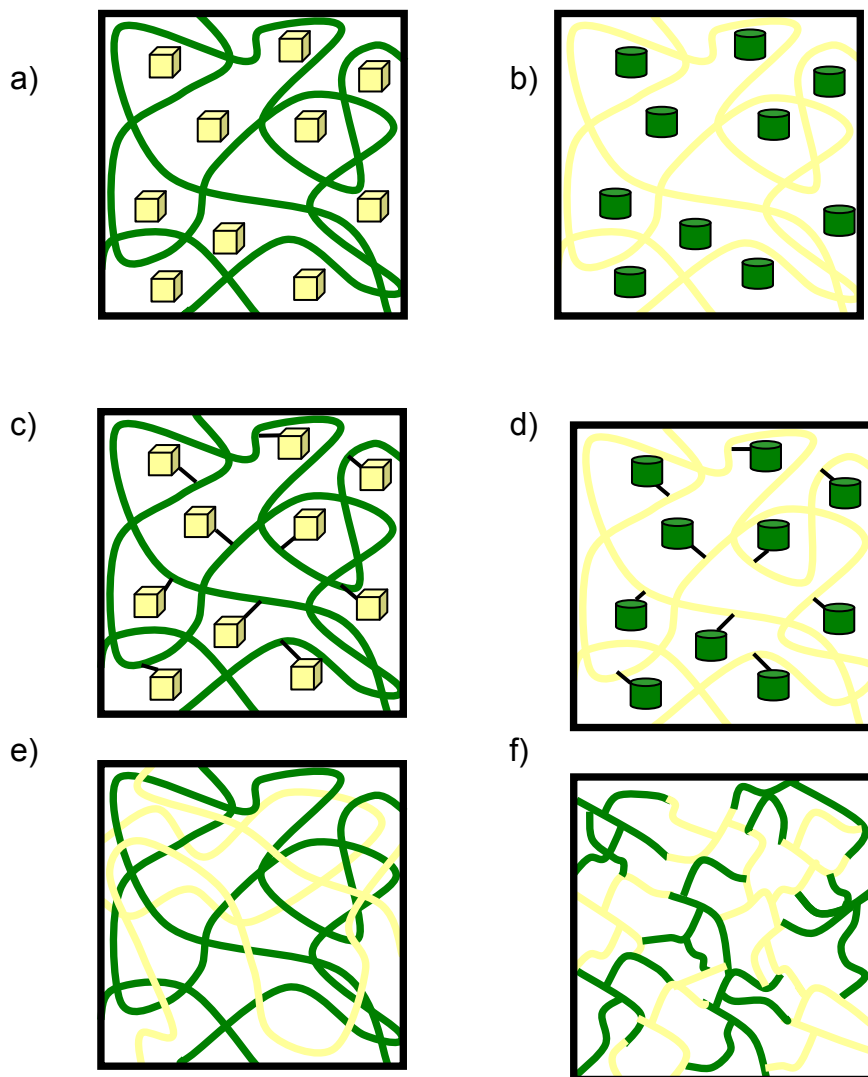


Figure 3.1. Different kinds of inorganic-organic composite materials: a) and b) embedding of the inorganic (yellow) moieties into the organic (green) polymer and vice versa; c) inorganic moieties bonded to the organic polymer; d) organic moieties bonded to the inorganic network; e) interpenetrating networks and f) dual inorganic-organic hybrid polymer.

Inorganic-organic hybrid polymers have been successfully developed and investigated at the laboratories of the Fraunhofer-Institut für Silicatforschung [18]. Because of the stability of the Si-C bond, silicon offers a very large variety of organic functionalisations. Inorganic-organic polymers consisting of organically cross-linked heteropolysiloxanes (ORMOCER[®]s [19]) are a materials class with many possible applications. These systems combine the properties of organic polymers

(functionalisation, low temperature processing, flexibility) with properties of glass-like materials (hardness, chemical and physical stability, transparency). Silicone-like units provide the sufficient thermal stability. Non-reactive organic groups may be used for the design and control of some material properties, e.g. polarity. To introduce the organic components organo-substituted silicic acid esters of the general formula $R'_n\text{Si}(\text{OR})_{4-n}$ can be employed. R'_n represents any organofunctional group, that can be bonded to the inorganic network as network modifier or network former (Figure 3.2). As network modifier any simple non-hydrolysable group can be selected. Network formers can polymerise, co-polymerise or undergo hydrolysis and condensation. The presence of network modifiers and formers change the physical properties (mechanical, hydrophobic, electrochemical, optical, etc.) of the material [18, 20, 21]. For the investigation of the partially or fully hydrolysed and condensed stages and the final materials, vibrational spectroscopy (Raman spectroscopy, Raman microscopy, IR spectroscopy) and nuclear magnetic resonance (especially ^{29}Si -NMR) [22, 23, 24] are most useful.

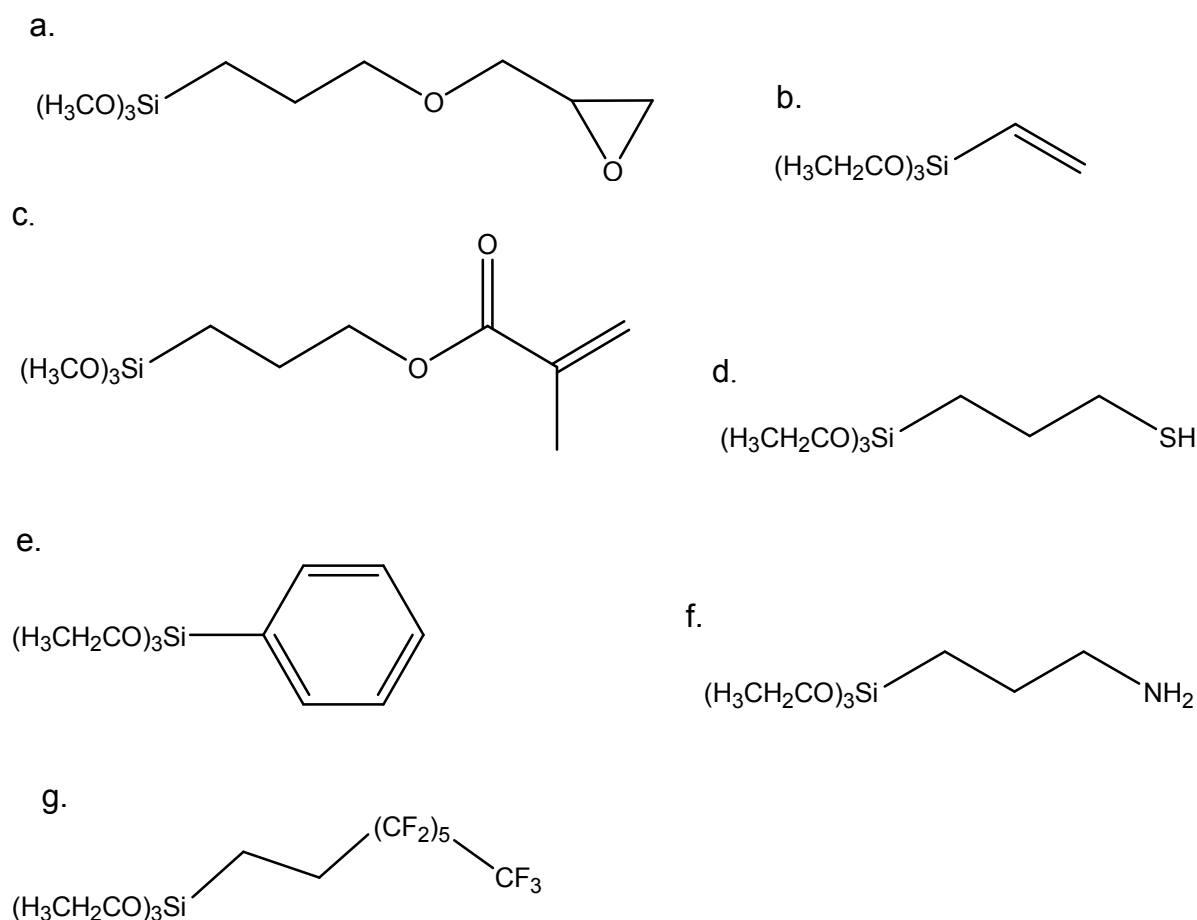


Figure 3.2. Examples for network modifiers (e, f and g) and formers (a, b, c, d and f).

The most popular inorganic components for hybrid materials, apart from Si compounds, are Al, Ti and Zr alkoxides. The more ionic the M-C bond (M: transition metal) the less stable it is. It breaks down upon hydrolysis. In order to introduce such structures into the sol-gel reaction, strong complexing ligands may be used. Ligands such as acetoxyethylmethacrylate or methacrylamidosalicylic acid contain a strongly chelating part and a highly reactive methacrylate group and thus are appropriate [21]. Low-viscous hybrid sols may be applied by nearly any conventional wet-coating technique, such as dipping, spraying, flow-coating, spinning, roll-coating, screen-printing, etc. Ease of processing and transparency are great advantages of inorganic-organic hybrid polymers for a use as coatings, combined with high mechanical strength, hardness and abrasion resistance [20].

3.1.2. Sol-gel derived hybrid nanocomposites and their application

Sol-gel based optical materials include hybrid siloxane matrices doped with photoactive dyes, transition metal oxide based gels doped with luminescent chromophores, and rare earth doped hybrid polymers. Through addition of self organised nano-building blocks (e.g.: oligosilsesquioxanes, polyoxometalates, transition metal oxo-clusters), the control over the growth and morphology of inorganic materials can be achieved [16, 25].

Luminescent materials based on sol-gel hybrid matrices can be obtained through embedding of rare earth ions (Nd^{3+} , Eu^{2+} , etc.), also in combination with organic dyes (e.g.: rhodamine 6G). Because of the presence of OH quenchers complexation or encapsulation of the metal ions is usually required. Nanocomposites built from siloxane polymers cross-linked with metal oxo species allow the introduction of high concentrations of the lumophore without affecting the synthesis and transparency of the created thin films. Despite of the low quantum efficiency values and weak emission, sol-gel materials open many possibilities for the creation of room temperature processed luminescent films.

Non-linear optics (NLO) can also be based on the sol-gel technique. Combination of π -electron rich organic polymers with silica leads to new materials with superior NLO properties [21, 26, 27].

Photochromic systems emphasise in how far a good tuning between the nature of the matrix and the dye can optimise the optical response. It can be strongly

modified by the presence of polar groups (i.e. Si-OH), complexation, protonation, matrix rigidity and steric hindrance [15, 28]. The grafting of the photochromic dyes on the inorganic backbone has also been investigated in order to increase the dye content without aggregation. Strong interactions between the dye and the host matrix reduce the dye mobility and thus the thermal decoloration rate.

Matrices made from hydrophobic polydimethylsiloxane species and cross-linked with hydrophilic zirconium oxopolymers were used as a host for SO and SP dyes. The amount of the coloured form after irradiation depended on the molar percentage of the zirconium oxopolymer domains. In the hydrophobic domains where the Si-OH groups are fully condensed, direct and very fast photochromism was observed [21].

Hybrid polymers can be used in a variety of application fields besides the optical materials mentioned above [20, 29, 30]. Functional transparent coatings e.g. anti-scratching, anti-adhesive, anti-fogging or anti-reflective etc. represent the most exploited applications for hybrid polymers. The last two examples have been realised by microstructuring with the so called “moth-eye” structure [14, 31, 32]. Dye-doped hybrid layers also allow a very flexible glass design for a wide range of different glass types (soda lime glass, crystal glass or lead crystal glass). Despite of the low thickness in the range of 5-20 μm , which is characteristic for inorganic-organic polymer coatings, the concentration of the dyes and pigments is high enough to achieve good colouration depth [33]. Very good compatibility of certain organic molecules with sol-gel derived host materials allows to create sensors (pH-sensors, bioactive materials, light dosimeters, etc.) [30, 34, 35, 36]. The controllable properties such as gas permeability, hydrophilicity and density of the network make this class of materials also attractive in the design of membrane systems or barrier layers for polymer foils [37] as well as for corrosion protection for brass or bronze surfaces [38]. Hybrid polymers can be applied in optical interconnection technology. Microelectronics, micro-optics and photonic materials as wave guides, as well as photopatternable dielectric or passivation layers can be created from these materials, whereby 3D lithography via two-photon polymerisation allows patterning with a resolution of down to 100 nm [39-41].

Hybrid polymer products are already present on the market. Screens coated with hybrids made of indigo dyes embedded in a silica-zirconia matrix (Toshiba), organically doped sol-gel glassware (Spiegelau) or sol-gel entrapped enzymes (Fluka) [42 - 44] should be mentioned just as examples.

3.1.3 Optical and ophthalmic materials and coatings

The purpose of coatings for ophthalmic lenses (glass or plastic) is the modification of the optical, electrical, chemical and mechanical properties of the lens surface.

Coatings are needed on polymer ophthalmic lenses to enhance both the mechanical durability of the relatively soft plastic surface and the optical performance of the lens [45]. The low abrasion resistance of uncoated standard ophthalmic plastics (PC, CR39®) is a great disadvantage. Hard, abrasion resistant coatings are used to overcome this problem. Hybrid polymer materials, usually obtained by the sol-gel process, have been introduced into the market in the last years [30, 46]. Also other properties such as oxygen permeability, reflectivity or hydrophilicity / hydrophobicity can be produced by the proper coating. For polymers that are UV degradable, UV light absorbing coatings would be desirable. Derived from co-hydrolysis of tetramethoxysilane, 3-glycidoxypropyltrimethoxysilane and titanium-tetraethylate coating materials have been commercially available for more than 15 years. The high mechanical resistance of that system is achieved through in situ formation of titanium oxo clusters and a high degree of organic cross-linking. Additives such as zirconium or aluminium alkoxides, colloidal silica, or boehmite (AlOOH) nanoparticles, can further improve the scratch and abrasion resistance of hybrid polymers. Sol-gel based hybrid coatings are also suitable base coatings for different types of antireflective metal oxide layer stacks deposited by vacuum techniques [33]. In the field of scratch resistant coatings on plastic lenses hybrid sol-gel based materials, play a major role, but still compete against evaporated films of titania, silica, alumina or some mixed oxides [47].

3.2 Photochromism

3.2.1 General definition

The term photochromism (suggested by Hirshberg in 1950) consists of two parts: “photo” (light) and “chrom” (colour), the suffix “-ism” indicates a phenomenon, so it means literally “colouration by light”. The first description of an observed photochromic reaction is already dated from the second half of the 19th century. The case of the strange gate post that was black during the day and became white at night (probably some kind of lithophone) was described by Phison [48]. Ter Meer [49] observed the change of the colour of potassium salt when exposed to exciting radiation. Photochromism was first recognised by Marckwald (1899) as a new phenomenon and called “phototropy”, which was followed by about 20 years of active research in that field [4]. The development in chemistry helped to define basic mechanisms for photochromism for the rising amount of new compounds, both organic and inorganic. The second “gold age” of photochromism had started in the 1940s. Finally, in the 1960s the first photochromic glasses were manufactured (Corning Glass Work). With the discovery of time-resolved or flash spectroscopy and the aid of sophisticated techniques (NMR, ESR, Raman, IR, UV-Vis absorption and laser technology) a refined insight into the nature of photochromic molecules, their reactivities, transients and excited states, has become possible [50].

“Photochromism can be defined as a reversible change of a single chemical species between two states having distinguishably different absorption spectra, such change being induced in at least one direction by the action of electromagnetic radiation” (Figure 2.1) [4].

The typical response of a photochromic compound A to activating irradiation (t_0) is an increase of the amount of the coloured molecular form B; when the radiation disappears or changes (t_1), the reaction equilibrium favours the colourless form A (Figure 3.3.). Depending on the system mono- or bimolecular back reactions can occur. The thermally sensitive reverse reaction generally has kinetics of first or second order. With the photochromic reaction, reversible changes also in the optical, chemical, electrical and bulk properties of the molecular and supramolecular (matrix) structures may occur.

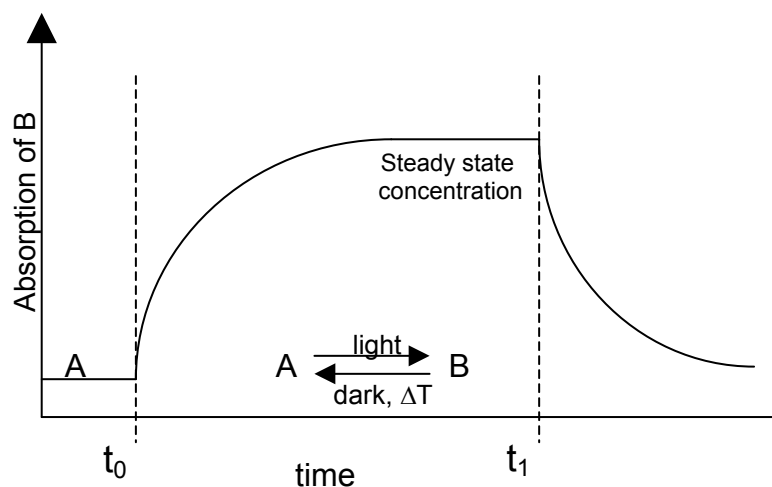


Figure 3.3. Typical behaviour of a photochromic substance A, activated by light to form B (adapted from [4]).

The molecular rearrangement responsible for the reversible colour change may be caused by the following chemical transformations: E-Z isomerisation of double bonds (stilbenes, azo compounds, polymethines, indigoids etc.) [51], electron transfer (cell chlorophyll, Fe(II) thiazines etc.) and hydrogen transfer (metal dithizonates, N-salicylidene anilines etc.) [52], photodissociation (triarylmethanes) [53], pericyclic reactions such as intramolecular electrocyclic reactions (spiropyrans, spirooxazines, fulgides etc.) [54] and cycloaddition reactions [55]. The properties of photochromic molecules are dependent not only on the structure but also to a large extent on their environment. Clear differences are to be expected if solutions or solid phases (supramolecular systems, liquid crystalline phase, polymer containing photochromic systems etc.) of photochromic molecules are compared [56]. All photochromics are temperature dependent in the sense that the activated equilibrium transmittance increases as the temperature increases [9]. Practical applications such as data recording and storage, optical filters, sunglasses, to name only a few examples, require photochromes with good colourability and acceptable long durability.

3.2.2 Classes of photochromes

The extensive studies of the photochromism phenomena in the past few decades have generated considerable information about the chemistry of the known

photochromes and have also brought completely new families of photochromic compounds. It should not be forgotten that besides numerous organic photochromes, also some inorganic systems change their optical properties when irradiated.

Inorganic Systems

Glasses doped with metal halides (AgCl, CuCl) nanocrystals have long been known for their photochromic properties [57]. They are used in special glasses as active materials for ophthalmic applications, although they offer only a limited colour range [58]. When exposed to UV light, the silver halides dissociate to form colloidal silver which is not transparent. Without radiation, recombination to the transparent halides takes place. Powders and thin films of photochromic glasses containing AgBr or AgCl microcrystals were synthesised also via sol-gel processing. Compared with molten photochromic glasses, the specific advantages of the sol-gel process, i.e., low preparation temperature and a higher variability in terms of matrix compositions, allows the production of materials with higher concentrations (up to 10 wt. %) of photoactive components, but fairly long bleaching times were observed [59].

Another interesting group of compounds are polyoxometallates. Polyoxometallates are a class of molecularly defined inorganic metal-oxide clusters. Their properties such as catalytic activity for chemical transformations, molecular conductivity, magnetism, electrochromism, luminescence and photochromism, additionally good compatibility with sol-gel derived materials as well as with organic polymers, make them attractive for developing new functional materials [60, 61]. A series of photochromic hybrid films were prepared through entrapping tungsten heteropolyoxometallate ($\text{PW}_{12}\text{O}_{40}^{3-}$) and molybdenum heteropolyoxometallate ($\text{PMo}_{12}\text{O}_{40}^{3-}$) in a polyacrylamide (PAM) matrix [62]. Irradiated with UV light, the transparent films changed from colourless to blue. The bleaching process occurred when the films were in contact with air or O_2 in the dark and was finished after about 30 days for the tungsten heteropolyoxometallate system, which is the faster one. When the film was heated to 50 °C in the presence of oxygen, the coloured species returned to their original colour already after 2 h. The photochromic process is associated with the reduction of the polyoxometallates ($\text{M}^{6+} \rightarrow \text{M}^{5+}$, Figure 3.4.) and oxidation of the organic matrix, which is driven by a radical mechanism [62, 63].

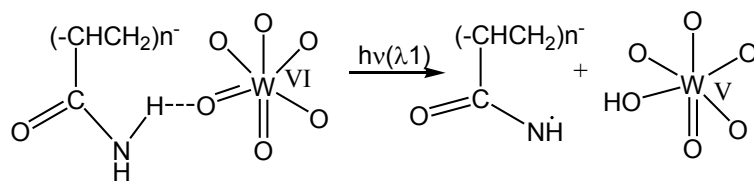


Figure 3.4. The photochromic reaction of a polyoxometallate complex [63].

Also molybdenum and tungsten oxides show photochromism. Irradiated MoO_3 turns from colourless to blue due to charge separation (production of electron-hole pairs). The photochromic phenomena are stronger in thin films than in single crystals or crystalline films. Once the coloured films have been bleached thermally in oxygen, they cannot be coloured again by UV irradiation. However, the films bleached by electrochemical polarisation demonstrate the reversibility of the photochromism. WO_3 nanoclusters in water give good photochromic response, which even improves when a TiO_2 sol is added presumably due to interfacial charge transfers between those two types of clusters [64]. Some composite and hybrid systems involving inorganic photochromes have already been fabricated. However for broad technical applications such as erasable optical storage media, large-area displays, chemical sensors, control of radiation intensity or self-developing photography, the variety of colours and the kinetics of coloration and fading still needs to be improved [65].

Organic photochromic compounds

Many scientific research groups focused their work on the development of commercially available and utilisable stable photochromic systems based on organic dye with adequate photofatigue resistance. Many photochromes were investigated. Among others, also spirooxazines and spiroopyrans, which turned out to be the most relevant ones for this study, underwent dynamic progress in the last few decades.

A. Chromenes

The colourless naphthopyrans or 2,2-dialkyl-2*H*-benzopyrans exhibit photochromism through the electrocyclic opening of the pyran ring (Figure 3.5.).

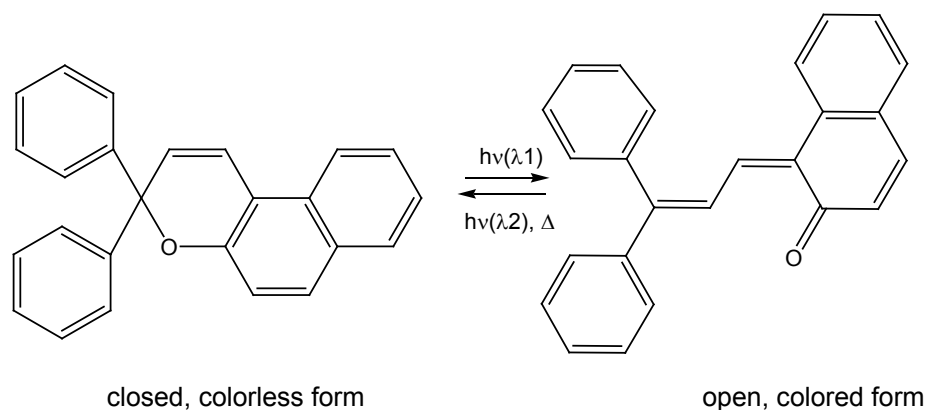


Figure 3.5. Photochromic reaction of chromene (3,3-diphenylnaphthopyrane).

Incorporation of electron-withdrawing groups (e.g.: fluorine), especially in the *p*-position, causes a blue shift of the absorption band, whereas electron donating groups are leading to a red shift [66, 67]. The kinetic and optical yield of the photochromic process, as well as the absorbance of the activated open form of diarylnaphthopyranes can be extensively influenced by substituents [68, 69]. Also fluorescence is caused by the presence of substituents [70]. Some bis-naphthopyranes linked at C(3) through a bis-thiophene moiety have been examined. These molecular systems are sensitive to the energy of incident light, as well as to the duration and intensity of the stimuli, which simulates the response in living systems to light [71].

B. Fulgides and fulgimides

Photochromism of fulgides is a molecular phenomenon based on the photocyclisation of substituted bis-methylenesuccinic anhydrides or fulgides to 1,8a-dihydronaphthalene (Figure 3.6.) [72].

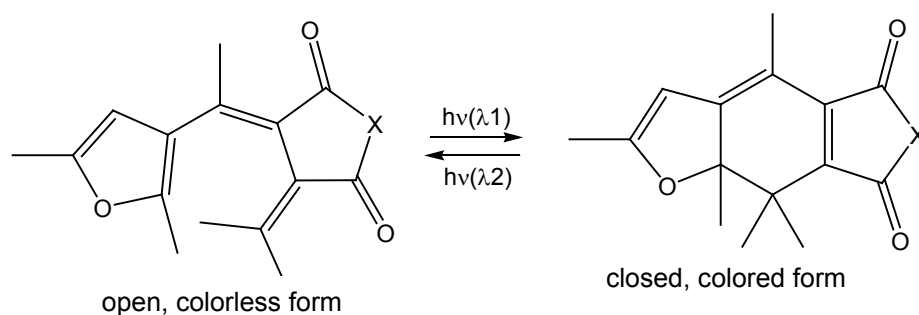


Figure 3.6. Photochromic reaction of the fulgides (X = O) and fulgimides (X = NR) [73].

The fulgides (2,3-dialkylidenesuccinic anhydrides) and fulgimides (2,3-dialkylidenesuccinimides) show good photochromic behaviour, and both forms are thermally stable and photoreversible. Fulgimides have also good chemical stability [74]. However, it should be noted, that the anhydride functionality undergoes slow and irreversible hydrolysis to esters, especially in alcohols, which contributes to dye degradation [72]. The majority of fulgides undergo extensive photochemical fatigue upon repeated coloration-decoloration cycles in spin coated polymer films. Besides a very good photochromic response, the photostability of thienyl and oxazolyl fulgides is distinctly higher than for the parent compounds. Molecular modifications [75, 76], addition of stabilisers or exclusion of oxygen are effective to improve fatigue resistance [77]. This extensively investigated photochromic family is interesting for many electronic applications, such as optical memories or optical switches.

C. Diarylethenes and related compounds

Diarylethenes having a central perfluorocyclopentane moiety show low fatigue during photocyclisation (Figure 3.7.).

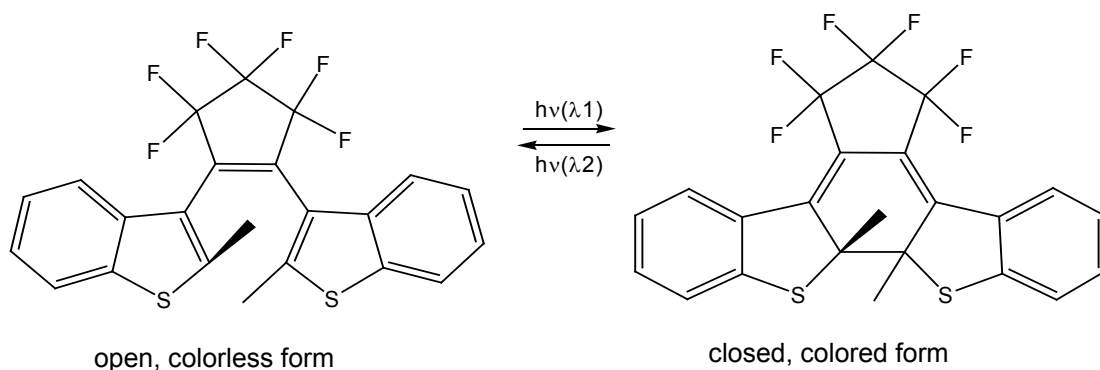


Figure 3.7. Photochromic reaction of the diarylethenes [73].

The thermal stability of the coloured closed ring isomers is dependent on the type of aryl group, whereby the dipyrrolylethenes also show good photochromic response and kinetics [78]. Nanoparticle aggregates of the diarylethenes showed changes in absorption spectra, emission efficiency and photoisomerisation rate [79]. The photoactivity of dithienylethene can be optimised with respect to the reaction quantum yield, resistance to photo fatigue or thermal stability [80]. Photochromic silsesquioxanes (empirical formula $\text{RSiO}_{3/2}$; R = H, alkyl or aryl group) having dithienylethene pendant groups are potentially useful for optoelectronic devices [81].

D. Dihydroindolizines, spirodihydroindolizines and related systems

The characteristic structural feature of dihydroindolizine-based molecules is a five-membered ring, typically a cyclopentene anion. The photochemically induced opening reaction (1,5-electrocyclisation) leads to zwitterionic or neutral heteropentadienes, whereby spirodihydroindolizines form the zwitterionic species only (Figure 3.8.).

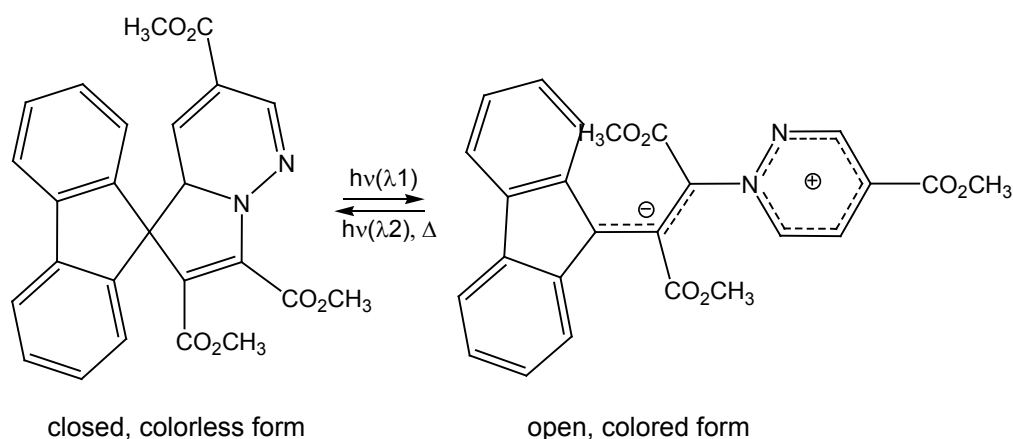


Figure 3.8. Photochromic reaction of a spirodihydroindolizine [73].

The photochromic family involves numerous compounds built on the basis of pyrroline, pyrazoline, triazoline, and pentadienyl anions, with one or more heteroatoms, such as spirodihydroindolizine, tetrahydroindolizines and hexahydroindolizines. Irradiation with long-wavelength UV or visible light ($\lambda_{\text{max}} = 400 - 450 \text{ nm}$) produces the coloured betaine form that shows a thermal or photochemical reverse process. The products can only exist in the zwitterionic form. Dihydroindolizines can be dissolved in or linked to many polymer matrices (e.g. poly(thiourethane), polycarbonate, poly(methyl) methacrylate), which results in promising materials for information recording or ophthalmic lenses [56, 82].

E. Azo compounds

The azo (diazene) group $-\text{N}=\text{N}-$ has given its name to a large group of compounds. There is a great number of substituents that can be attached to the azo group. Trans-cis (E-Z) isomerisation can be reversibly induced by light and heat (Figure 3.9.).

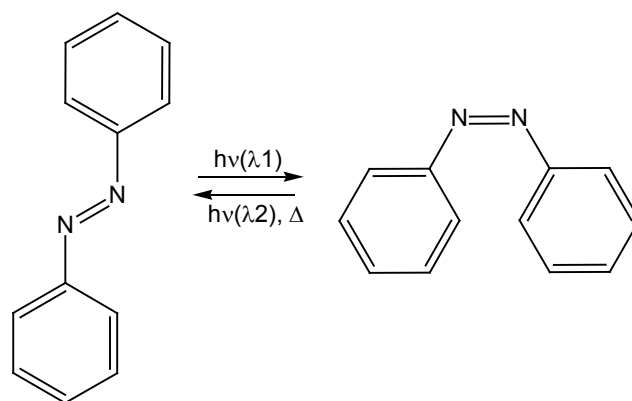


Figure 3.9. Isomerisation of diphenyldiazene [73].

The E (trans) form is thermodynamically more stable than the Z (cis) form. When oxygen is excluded, the UV initiated photochromic reaction occurs for days in hydrocarbon (e.g.: n-hexane) solution. The excited and ground state energies in the isomerisation process are not very different, which favours very fast radiationless deactivation. The application of azo compounds is seldom based on the colour change, but rather on the UV-visible light switching of other properties. The geometrical transformation of azobenzene units in larger molecules causes structural changes in the latter or in supramolecular systems. They have also been used for diagnostic purposes. Azobenzene units in the backbone of a polymer (e.g. methacrylate), or as pendants, can reversibly change the properties of the polymer material (wettability, viscosity, solubility, membrane properties, refractive index, dipole moment) [83, 84].

F. Polycyclic aromatic compounds

That family of compounds shows a photochromic reaction based on 1,3-electrocyclisation ($4n$ systems). Compounds from that molecular mechanism family can be used as actinometers. This means that their chemical system determines the number of photons in a beam integrally or by unit time. The repeatability of the photochromic actinometers is an advantage compared to physical devices. Heterococordianthrone endoperoxide (HECDPO) is a suitable actinometer in the 248 – 334 nm region (Figure 3.10.).

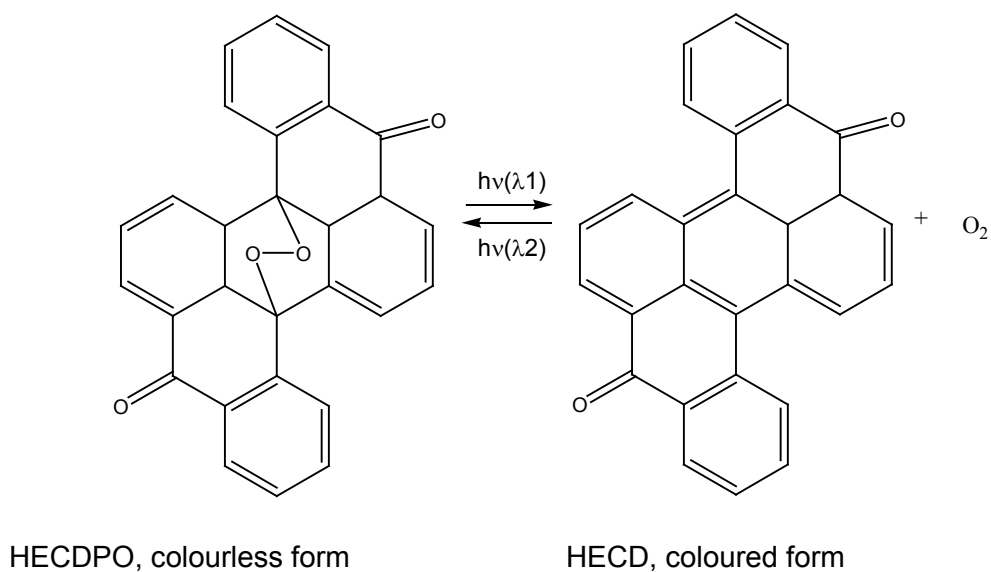


Figure 3.10. The photochromic reaction of heterocoerdianthrone endoperoxide (HECDPO) in methylene chloride leads to heterocoerdianthrone (HECD), red [73].

The photochromic response of the oxiranes and aziridines depends on the polarisation of the activating light. The isomerisation of nitrones to oxaziridines stores up to 100 kJ mol^{-1} , that is why they are suggested as energy storage material [85].

G. Spiropyrans and Spirooxazines

The first references to photochromic spirooxazines (SO) appeared in the 1970 [86, 87]. Since then they have been considered, together with spiropyrans (SP), as very promising photochromic dyes, which have extensively been studied both in academia and industry.

The synthesis of the SO, SP and structurally related photochromics can be based on a thermal condensation reaction (Figure 3.11.) of the corresponding alkylidene heterocycle or conjugate acid with ortho-hydroxyformyl or alternatively ortho-hydroxynitroso aromatic derivatives [67, 88].

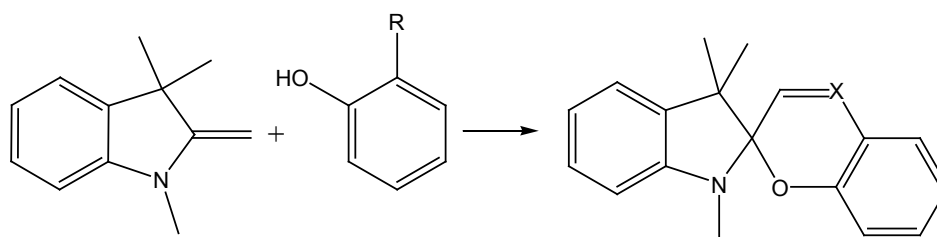


Figure 3.11. The synthesis reaction scheme for spirooxazines (R = NO₂; X = N) and spiropyrans (R = CHO; X = C) [9].

Later, many uncomplicated processes were employed to create novel compounds [89 - 93]. The replacement of the benzopyran ring in a spiropyran molecule by a naphthoxazine ring (spironaphthoxazine) greatly improves the photostability.

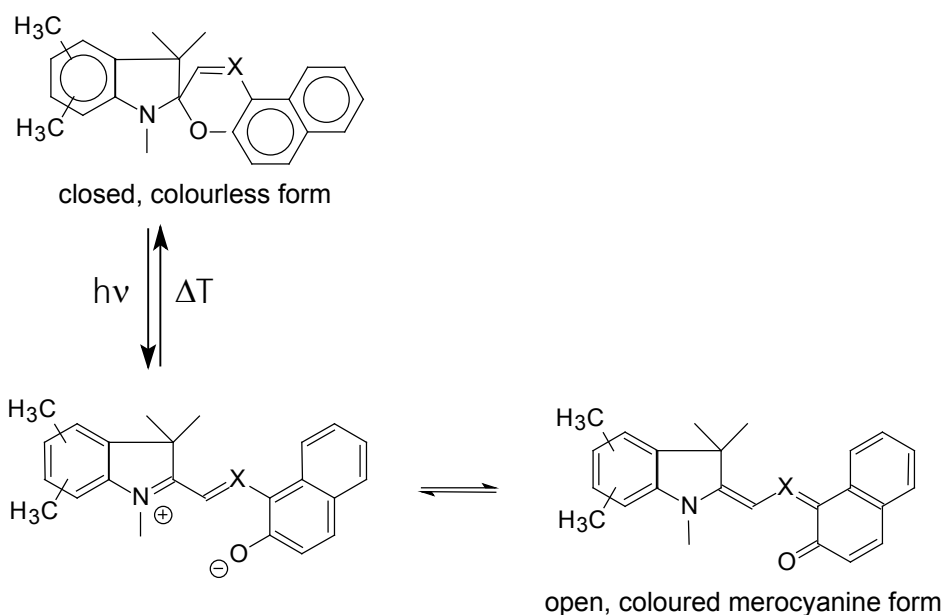


Figure 3.12. The photochromic reaction of SP (X = C) and SO (X = N).

The photochromic reaction features the dissociation of the C_{spiro}-O bond, leading to an open merocyanine-like form (MC) (Figure 3.12.). Spiropyranes bearing a nitro group photo-degrade rapidly due to the involvement of triplet states in the chemical ring opening process. The presence of a nitro group as a substituent changes the photocolouration process from dominated by excited singlet states, ¹SP, to triplet states, ³SP_{NO₂}. The decay processes initiated by UV irradiation of SP and SO both in

a solvent and in a polymer matrix can involve intermediate states of different multiplicity and/or geometry. Also photooxidation must be considered. In 1962, Fisher et al. proposed the existence of an open cis-cisoid isomer, that evolves as an unstable isomer after UV irradiation [10]. The geometry of the X form is very close to that of the parent spirooxazine (Figure 3.13.) [72].

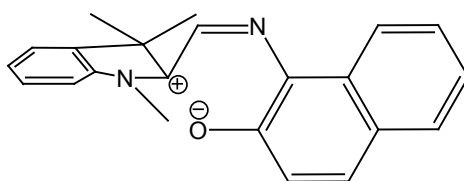


Figure 3.13. Isomer X with cis-cisoid conformation of the central C3=C4 bond [72].

The formation of the cis-cisoid opened-ring non planar intermediate X was investigated with picosecond transient absorption spectroscopy and nanosecond time resolved spontaneous coherent anti-Stokes Raman scattering. Its existence is much better documented for nitro-spiropyrans than for spirooxazines.

For practical applications, high photochromic activity and excellent resistance to photofatigue by light exposure are required. Unfortunately, SP and SO degrade after prolonged or repeated UV irradiation.

Gautron et al. showed in pioneering studies that it is the cleavage of the C_{spiro}-O bond that leads to the formation of the merocyanine. Substitution of SP indoline or chromene moieties influences the photodegradation. Introduction of electron-donor groups (CH₃, CH₃O, etc.) at any position of the molecule, except for the C3' of the bridging C3'=C4' bond, decreases photofatigue. Electron-withdrawing groups (NO₂, Cl, Br, etc.) accelerate photodegradation. In general, the more polarised the C_{spiro}-O bond is, the higher the degradation quantum yield [94]. The reaction of the cis-cisoid X isomer with the solvent and impurities leads to degradation. The open photomerocyanine form can be quinonic, zwitterionic or biradical. Oxidation of these forms (or one of them) plays an important role in the degradation process (Figure 3.14.) [95].

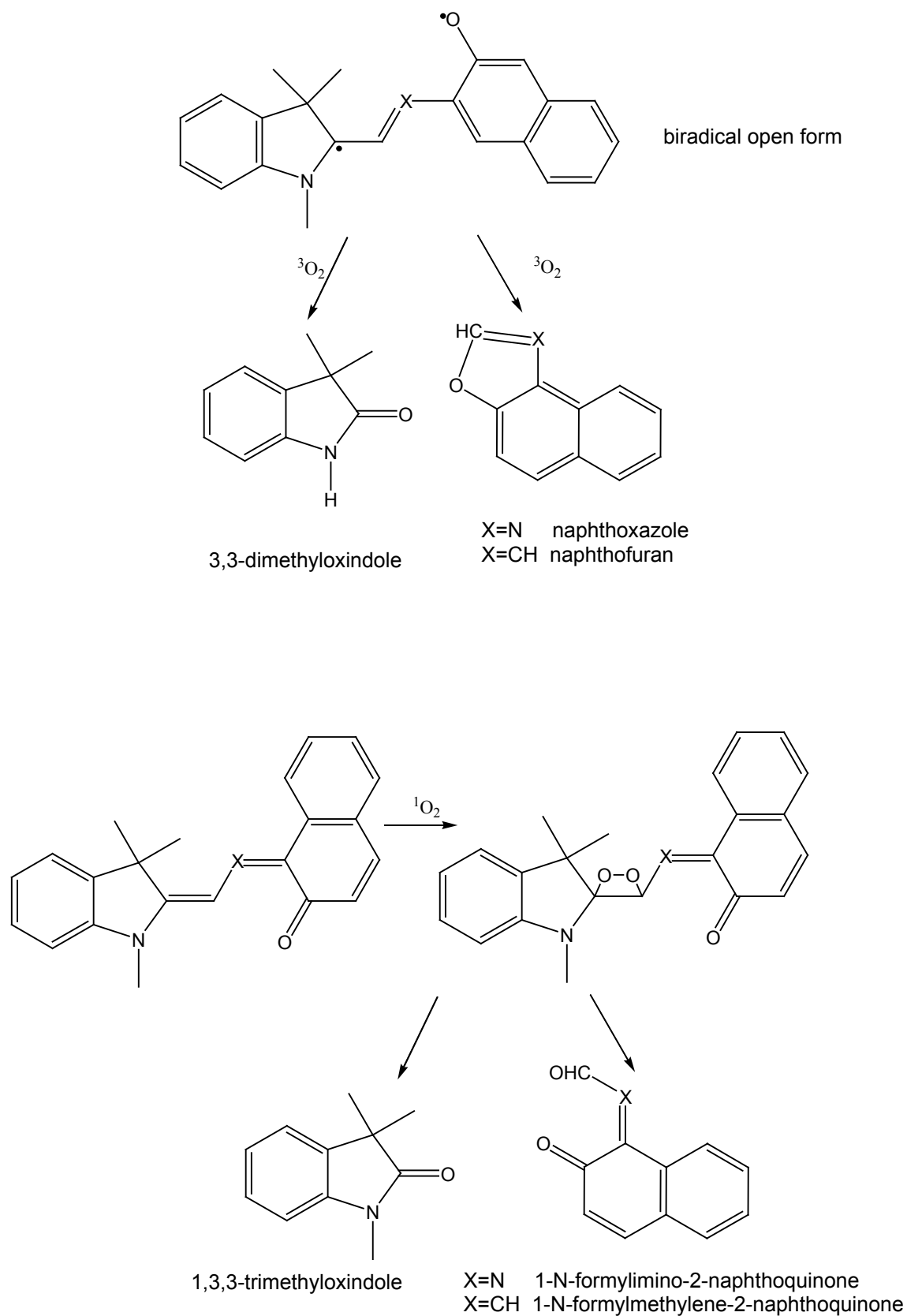


Figure 3.14. Different oxidation processes of photomerocyanines [95].

However, for many SPs having intermediate triplet-states with life-times shorter than microseconds, photodegradation is not affected by the presence of oxygen. The degradation takes place also in the absence of oxygen [96]. Excited state quenchers (among others amines such as 1,4-diazabicyclo[2.2.2]octane (DABCO)) or sensitisers affect the fatigue resistance of SP. In non-polar solvents strong intermolecular interaction could accelerate degradation. The degradation products can react with the nonactivated as well as with the activated form of the dye molecule. An increased concentration of them can change the chemical characteristics of the system.

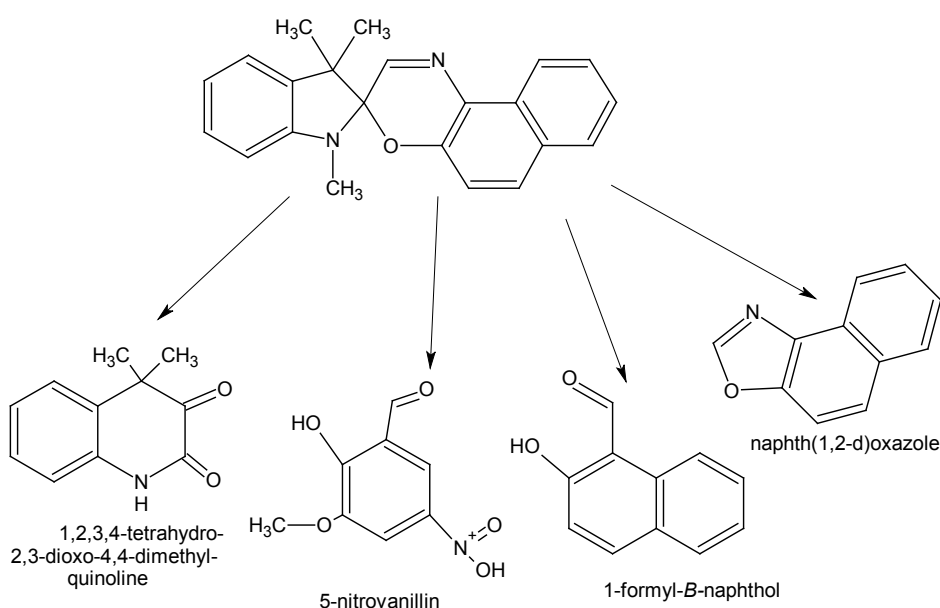


Figure 3.15. Main photodegradation products for spirooxazine Blue A [97].

The photofatigue of spirooxazines (Figure 3.15.), in contrary to SP, is not considerably affected by the polarity of the solvent. SO are characterised by a better photostability than SP or spironaphthopyrans. Photodegradation and colourability change in opposite ways. It could be generalised that organic photochromes having high colourability are less photostable. More dilute solutions have a better colourability and poorer fatigue resistance.

The role of oxygen in the photodegradation was explained with a merocyanine-oxygen interaction. A polar intermediate (charge-transfer complex) is considered to be responsible for the higher degradation rate in polar solvents.

The ability of SO and SP to induce sensitised formation of singlet oxygen was investigated. It was suggested that $^1\text{O}_2$ is produced through the reaction between the photomerocyanine in its triplet state and ground state oxygen. The opinions in that field are very divergent. Nevertheless, the presence of a singlet-oxygen quencher (DABCO) in the reaction solution leads to the stabilisation of the photochromes and degradation products occur different from those in the absence of it. That is because SP, SO and chromenes can also act as photosensitiser of singlet oxygen [95, 98]. The kinetics of the bleaching reaction of many SO in toluene solution can also influence the degradation processes. For compounds having fast bleaching kinetics the fading rate increases during photodegradation, whereas those characterised by slower kinetics exhibited a reduction of the fading rates.

Thermal dark reaction of SO, which can be involved in irreversible electron-transfer processes, leads to the same intermediates as for the photooxidation [99]. The merocyanine form easily reacts with free radicals giving diamagnetic products.

Some investigations about chelation of a photochromic spiropyran with Cu (II) in solution were performed. Kopelman et al. reported the synthesis of a series of stable spiro[indolinephenanthrolineoxazine]-metal (II) complexes. The metal is bound to a ligand-functionalised spirooxazine and remains bound in both the open and the closed form. The complexation leads to a significant stabilisation of the photomerocyanine form, a decrease in thermal fading and an increase in photoresponsivity. The changes were dependent on the nature of the metal centre. The improved colourability may be a result of the metal cation stabilisation of the photomerocyanine form [100].

The coloured opened-ring form of SP or SO interacts with its environment. The maximum absorbance occurs at shorter wavelengths ("blue shift") in a polar solvent [15]. Also the characteristics of the free volume surface in a sol-gel derived material alter with embedded, trapped or bonded organic molecules. The photochromic behaviour of dyes incorporated in the pores of a matrix system is dependent on the characteristics of the molecular structure surrounding the dye (Figure 3.16.) [56, 101, 102].

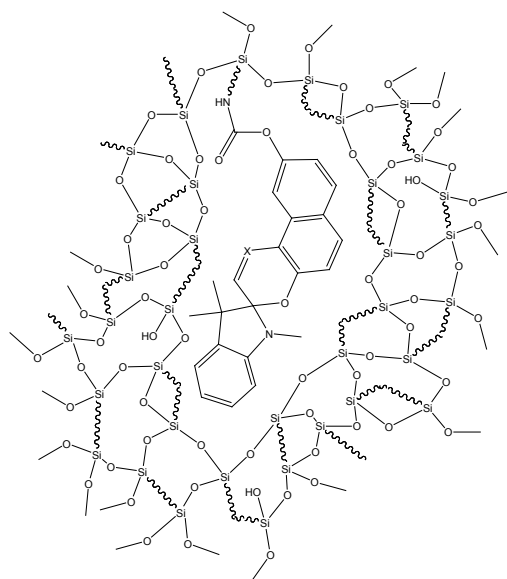


Figure 3.16. A covalently bonded dye molecule situated within a hybrid polymer matrix .

The dye-matrix interaction was first investigated on bulk samples by Levy et al. [15, 28]. The continuous environmental changes along the gel/xerogel process (post condensation and drying) were reflected by the changes of the photochromic behaviour of the trapped molecules. At a certain point photochromism changed to reversed photochromism, which is also known for liquid systems [103]. In those materials the “dark” form was the coloured one and bleached upon irradiation, so that the normal colourless to coloured transitions were reversed. The photochromic behaviour of the investigated spiropyrans suggested that the open zwitterionic coloured form of the dye was stabilised in hydrophilic matrix domains (residual Si-OH groups, possible strong hydrogen bonding). Through a change in the percentage of the hydrophilic and hydrophobic domains in the matrix the controlled balance between reversed and normal photochromism can be achieved [104]. For the photochromic activity the free volume within the host material is important. When the matrix becomes too rigid, no molecular movements of the trapped molecule are possible. The photochromic reaction cannot take place. This phenomenon is observed in pure SiO₂ xerogel matrices. When they are modified with ethylene

groups, sufficient flexibility for molecular movements is induced and full scale photochromism can be achieved in the final glass [28].

Both, the closed and the activated forms of SP/SO dyes are easily degraded by UV radiation, OH-attack, oxidation (O_2 from air or activated oxygen species), interaction with solvent, matrix and impurities, as well as their degradation products. In order to improve the photostability of the photochromics, different additives like antioxidants, HALS and organo-nickel UV light stabilisers were successfully used [95, 105, 106].

3.2.3 Photochromic materials and coatings

Photochromic molecules may be dissolved in, adsorbed on, or bound to a suitable polymer. When considering polymeric matrices for exploitation of the photochromic effect, soft polymers are not applicable because of their poor mechanical properties. On the other hand, in hard polymers the switching behaviour of the photochromic dyes is hindered. A certain inner free volume of the host material is required to avoid sterical hindering of the switching process. Moreover, an as impermeable as possible host is desired to prevent the reaction of photochromics with moisture and oxygen migrating from the environment which leads to a decay of the photochromic activity.

For a diluted system with passive absorbing dyes, the absorbance is a linear function of the dye concentration and the thickness of the layer (Lambert – Beer law). For active systems like photochromic dyes absorbance of the exciting irradiation is also a function of the coating thickness (the UV light is strongly absorbed in the upper part of the coating) and the dye concentration [107].

The amount of a typical photochrome necessary to produce a photochromic lens with good response and a reasonable wearer lifetime performance (fatigue resistance) is from 0.15 to 0.35 mg / cm³ [108, 109]. This means that the dye concentration equals approximately 25-50 % of the film composition [9].

The great interest in photochromic materials and devices has provoked intensive research in that field. Many new photochromic species were synthesised. Some of them exhibit photochromic properties not only in the dissolved (solution or embedded in a matrix) but also in the pure crystalline state [110, 111], e.g. self-assembled monolayers [112] or liquid crystal materials [113]. The presence of the

electron-withdrawing N-methyl pyridinium ring allows intra-molecular rearrangement of an unsolved SP dye probably due to the sufficient free volume around the spiropyran [114]. Those cationic SP are also photoactive in solution as well as in silica matrices. The incorporation of organic photochromes into magnetic systems is one of several new strategies to realise photoresponsive magnetic materials. Combination of photochromism and molecular magnetism has succeeded in increasing the magnetisation value of magnetic vesicles of SP containing iron oxide particles, and in photocontrol of its magnetic properties at room temperature [114 - 116]. Incorporation of spirooxazines or spiroyrans in membrane materials, such as polysulfones, allow to control the membrane potential with UV light [103].

Sol-gel derived matrices can serve as stable environment for active species, especially dye molecules, preventing them from self-aggregation and interaction with the degradation products. The optical transparency in both the UV and visible light region, as well as low temperature processing make this kind of material attractive for the incorporation of photochromic dyes [9, 117, 118].

Menning et al. developed a photochromic organic-inorganic nanocomposite (Nanomer[®]) coating system. Surface modified SiO₂ nanoparticles were incorporated into an organic-inorganic matrix in order to obtain macroscopically “hard” properties without changing the photochromic kinetics. Organic spacers were added to the matrix to create a sufficiently high free pore volume. That system was claimed to be compatible with different photochromic dyes, like oxazines, pyranes and fulgides. The long term stability of the photochromic dyes in this matrix system was considerably improved by the addition of antioxidants, hindered amine light stabiliser (HALS) and UV stabilisers [58, 119, 120].

Also other ideas for a decrease of the photodegradation rate were attempted. A silylated spirooxazine was introduced into “organically modified ceramic” coatings prepared by the sol-gel method. The silylation on the N-atom (Figure 3.17.) of the indoline domain has little influence on the spectroscopic properties and the photochromic intensity of the silylated dye, though the decoloration rate of the dye is reduced. The slower fading kinetics strongly indicate a restricted mobility for the silylated dye molecules in the matrix [121, 122]. Besides N-silylation, the silylation of the naphthooxazine domain is also known [123] as well as a whole series of spiro-indolino-oxazines [124].

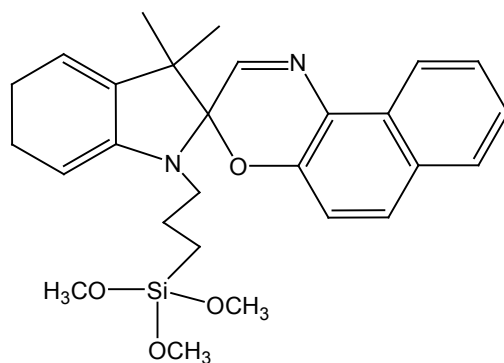


Figure 3.17. Structure of a N-silylated SO [121] .

Photochromic molecules trapped in various SiO_2 and chemically modified SiO_2 matrices have been suggested, among others, as chemical switches for signal processors, reusable information storage media, micro-imaging materials, protective materials against irradiation, displays, camouflage, decoration, photomasking and photoresisting materials [15, 111, 125]. Photoactive materials have served for a variety of information recording applications. Besides, the photochrome-matrix system has to have good thermal stability, high quantum yield for activation and bleaching reactions and possible low degradation rate [126].

Not only sol-gel derived inorganic or hybrid polymer matrices are used for entrapping photochromics. Also, purely organic matrices can be attractive as media for new photoactive materials. The interaction between dispersed photochromic and polymer matrix was investigated in the case of thin films containing spiropyran dyes. Polymethyl methacrylate (PMMA), polyethyl methacrylate (PEMA), poly(n-butyl)methacrylate (PnBMA) and styrene-butadiene-styrene copolymer (SBS) caused differences in the coloration rate and kinetics of photochromic processes. A polar PMMA matrix was found to have a higher coloration rate and slower bleaching kinetics. The zwitterionic photomerocyanine form of the SP was more stable than in the non-polar SBS [127]. The optical properties of the photomerocyanine form of spirophenanthroxazine dispersed in polystyrene varies with laser wavelength, intensity, irradiation time and the sequence of photoirradiation [128]. UV sensor devices of the optical waveguide type composed of the spirooxazine derivative and PMMA matrix thin film showed 64 times greater sensitivity than the conventional transmittance method [129].

3.2.4 Commercially available photochromic ophthalmic systems

Photochromic sunglasses should be essentially colourless under low-light conditions but convert rapidly to a coloured form under intense lighting. The fading process should be fast, when the UV light is absent. All phenomena should happen over a wide temperature range and with sufficient life-time of the eyewear [130].

A few processes for the incorporation of photochromics within plastic or glass substrates can be distinguished. Coating approaches have great advantages being universal application methods. An optical film containing a photochromic dye can be used independently from the shape and for most compositions of the plastic ophthalmic lenses. The liquid lacquer (organic resin, polysiloxane etc.) with the dissolved photochrome can be applied by dip coating, spray coating, spin coating, flow coating etc. By the “in-mould coating” process the fluid photochromic intermediate is applied to the mould surface onto which the lens is cast (Toray Industries). Injection moulding is essentially a single step process for the photochromic lens fabrication from thermoplastic resins. American Optical has used injection moulding of cellulose acetate butyrate with the NISO photochrome to produce a 1.5 mm thick goggle-type sunglass lens [105]. Internal casting with catalysed monomers as a possible single step process is not compatible with the chemical sensitivity of oxazines. Strong oxidants or radical initiators necessary in the polymerisation process decompose photochromic dyes. This problem can be solved through incorporation of the photochrome into the polymer backbone, which could also be an advantage for the polymer, as in the case of the polyacetylene or polysulfone polymer containing spirooxazine moieties [103, 131] or acrylate- and styrene-derived polymers having pendant photochromic quinone moieties [132].

The photochromic dye can permeate into the lens surface. Solvent dyeing, aqueous dispersing and vapour-liquid transfer as lens surface treatment processes lead to the migration of the dye into the lens subsurface via a dissolution-diffusion mechanism (“imbibing”) [9]. Unfortunately, the production of a photochromic polymer by the thermal transfer technique is connected with relatively high processing costs [58].

The first commercially successful [57] photochromic ophthalmic lenses appeared already in 1964. They were based on silver halide crystallites suspended in an inorganic glass matrix. The usually grey or brown (when irradiated) lenses are

relatively heavy (specific gravity up to 2.65 g/cm^3 [133]). They found their way into the market, and about 10 million pairs of silver based photochromic prescription lenses (e.g.: Photogray Extra[®], Corning Co.) were dispensed in the United States in 1989 (Optical Manufactures Association, 1990). In the same time the light and easy to handle plastic lenses have gained 70 % percentage of the U.S. prescription eyewear market [9].

American Optical has commercialised an oxazine dye based photochromic lens in the early 80s, that was rated not attractive by the customers, who compared it with the more stable glass based photochromic lenses.

In the 1990s the plastic photochromic lenses have already been commercialised on the US prescription eyewear market, whereby most of them utilised the indolinospirooxazine dyes. Rodenstock US Lens Division still distribute some photochromic lenses. The first marketed brand name was Colormatic[®], followed by Colormatic[®] Hard Resin lens, both with a indolinospirooxazine based photochromic coating and brownish tint. Photocolor[®] was a trademark for three fashion coloured lenses.

Transitions[®] Lenses marketed by PPG Industries, are made from light plastic material (specific gravity 1.32 g/cm^3 [133]) and presumably indolino spironaphthooxazines and spiropyranes. The dyes are thermally transferred (“imbibed”) into the surface of the clear lens to a depth of 0.15 mm. The Transitions[®] product required an application of a polysiloxane hard-coat. The permanent investigation in the field of photochromic materials, their stabilisation and application made PPG Industries (Transitions Optical, Inc.) one of the leading suppliers of ophthalmic photochromic lenses [134 - 136]. One of the actual products of PPG Industries is a poly(urea-urethane) resin lens with a spiropyran type dye doped coating, equipped additionally with protective hard and AR coatings [137], whereby development work at Transitions Optical, Inc. laboratories is concerned with the improvement of the optical and mechanical properties of produced laminated lenses [138]. Besides the above mentioned, also other photochromic products such as Ogaver and Photolite (American Optical Co.), Photoblue-Lite (Nikon), Attiva (Interlenti), Perfalit Colormatic (Rodenstock) and Sola Sunstive (Sola) are present on the ophthalmic lens market (Table 3.1) [139, 140].

Table 3.1. Examples of market available photochromic lenses and their characteristics.

	Photochromic Activity	Activation Speed	Bleaching Rate	Half-life Time
Photogray Extra® Corning Co.	From 90 % to 45 % ($\Delta Y = 45\%$)	60 s to achieve 50 % (at 22 °C)	120 -140 s lost 50 % of max. luminous transmittance change	Not available
Transitions® Lens [fisher] PPG Industries	from 82 % to 28 % (at 22 °C) ($\Delta Y = 54\%$)	30 s to achieve 57 % of max. luminous transmittance change	115 s lost 50 % of max. luminous transmittance change	50 % of usability in more than 2 years
Colormatic®, Colormatic® Hard Resin; Rodenstock	$\Delta Y = 75\%$	120 –135 s to achieve 50 % (at 22 °C)	Not available	Relative loss of 10 % in photochromic activity under normal eyewear condition per year

Little is known concerning the role of the photochromic dye-matrix interactions in the kinetics of coloration and thermal fading. The interaction of the matrix systems with incorporated dyes are mostly complicated and systematic investigations of the influence of some additives could help to define it.

The ophthalmic market is further characterised by photochromic lenses either based on silver halides incorporated within silicate glasses or on organic dye mass tinted plastic lenses. Despite several research efforts to incorporate the dyes into sol-gel based hybrid coatings, no products have appeared so far [32]. The development of photochromic coatings with satisfactory coloration activity and degradation fatigue would decrease the energy needed and the cost related to the process, and it would increase the spectrum of the substrates on which such a coating could be applied. The low temperature process and variety of the coating methods are suitable also for temperature sensitive materials as well as for complex shaped substrates.

4. Aim of this work

The aim of this research was to develop, characterise and optimise new photochromic hybrid polymer coating systems.

A number of photochromic dyes (brand name Variacrol®) and special products created by Great Lakes Chemical, Italy, were to be tested with respect to their compatibility with hybrid polymer materials. Also the application procedure of the fluid intermediates and the curing conditions, as well as the photostability during artificial weathering and kinetics of the coatings were to be investigated.

New sol-gel materials as hosts for the photochromic dyes were to be developed. For the optimisation of the dye-matrix systems, information about the matrix material itself had to be gained. By chemical control of all the synthesis intermediates (FT-Raman and FT-IR spectroscopy) the properties of the end product were to be defined. The physical characterisation of the coatings (proper thickness, high microhardness and very good adhesion on different substrates) should also be taken into account. The analysis of the cross-linking within the material (NMR measurements) and the determination of the presence of radicals (EPR measurements) as well as the polarity of the matrix free volume (solvatochromic investigations) were considered important in order to learn about the relation between dyes and their host materials. The change of matrix properties under different curing conditions was supposed to be used to optimise the host materials.

To achieve systems with a low degradation rate (and consequently long lifetimes of the photochromic coating) was the main goal of this work. In weathering devices the photostability of the systems was to be tested. Also the photochromic kinetics of samples coated with photochromic sol-gels were to be analysed.

The influence of the different type of entrapment (physically entrapped non-silylated and chemically bonded silylated dyes) into the sol-gel derived host materials was to be investigated with respect to the photodegradation rate during artificial weathering, considering also kinetics and matrix effects.

In order to improve the photostabilisation of the achieved photochromic materials some stabilisation techniques were to be tested:

- physical incorporation and chemical bonding as two different concepts of dye entrapment;
- application of excited state quenchers, UV absorbers and radical scavengers;
- shielding from ambient O₂;

- shielding from excessive UV radiation .

The development of high performance photochromic coatings that can be synthesised at low temperature was the main purpose of this investigation. Their photodegradation rates and physical properties should be comparable with market products and acceptable for commercial use. Small dye concentrations within the materials were favoured. Matrix characterisation as well as informations about matrix-dye effects and their dependence on multiple factors were expected to contribute to reach the goal.

5. Experimental Part

5.1 Measurements and methods

For the characterisation of the liquid intermediates as well as of the coated substrates a variety of methods were applied:

To study the hydrolysis of precursors FT-Raman spectroscopy was applied. A Bruker spectrometer *model RFS 100* was used with a Nd-YAG laser (Coherent) as excitation light source with an emission wavelength of 1064 nm.

FT-IR spectroscopy was performed on a Nicolet Magna 750 spectrometer; usually the transmittance spectra (pulverised sample 5 %wt. within a KBr pellet) were acquired. Solid state MAS-NMR spectra were kindly recorded at the Faculty of Inorganic Chemistry, Würzburg University, Germany by means of a Bruker *DSX 400* device, the measurement temperature being 298 K.

Paramagnetic properties (EPR) were investigated by means of a standard SE/X *Radiopan* spectrometer at the Institute of Experimental Physics, Gdansk University, Poland. The sample holders were sealed quartz capillaries (1 mm diameter). The magnetic field was calibrated by using diphenylpicrylhydrazyl (DPPH) free radicals and modulated at 100 kHz. The EPR spectra were obtained at 9.4 GHz (X-band) and displayed as the first derivative of the absorption curve.

The optical absorption of solvents and solutions of the solvatochromic dyes were investigated by UV-Vis absorption spectroscopy on a Shimadzu UV 2501 PC, spectrophotometer.

Transmittance spectra (spectral transmittance τ and luminous transmittance Y) were measured by means of a colorimeter BYK-Gardner, model *The Color Sphere*. A Tungsten-Halogen lamp connected with an IR-filter has served as light source; by means of a 35 Channel TCS polychromator the spectra in the 380 – 720 nm range were recorded with 10 nm intervals. Prior to each measurement of the photochromic response, the samples were activated and manually transferred into the measurement chamber of the spectrometer, and the spectra measured with a 2 seconds delay. For the activation a commercial face tanner (Philips, *model HB170*) with Philips CLEO 15 W UV-A bulbs was used. Integrated power density was 44 W/cm²min between 250 – 410 nm. The bulb-sample distance was 12 cm. After

each irradiation interval and prior to initial measurements all samples were subjected to a bleach-back procedure comprising a heat treatment (75 °C, 20 minutes) and irradiation with visible light (1 h), followed by storage in the dark (at least 2 h). This procedure was used in order to ensure all photochromic centres were in the bleached state before activity measurements. There were always four samples prepared and tested in order to achieve meaningful average values. Nevertheless, some irregularities within the photochromic activity measurements can be noticed e.g. for the degradation curves. These might have been partially caused by the manual and therefore not strictly defined sample transfer into the measurement chamber of the spectrometer. The chamber was not thermostated, which also have been a source of some disturbance (temperature depending bleaching kinetics). The temporary increase of photochromic activity observed in some cases after a short UV irradiation period instead of immediate activity dropping is a common phenomenon observed not only for samples investigated within the present work [141].

Kinetic measurements were performed “in situ” by means of an experimental set-up consisting of a HBO 200 W Hg lamp, a water IR filter, a colorimeter and a sample holder allowing a sample fixing with an angle of 45°.

For the preparation and testing of coatings the following equipment was employed:

Spin coating was performed by means of a KSM Karl Süss spin coater model RC8. After manual application of the fluid sol onto the substrate, the sample was rotated for 30 s at 600 rpm, and finally 10 s at 1200 rpm. Thermal curing was done by means of Heraeus drying ovens.

The universal micro hardness was determined by means of a Berkovich indenter (*Fischerscope H 100*). It was ensured the penetration depth did not exceed 10 % of the coating thickness.

The adhesion of the coatings was measured by the cross cut and tape test. After the coating is cross cut a standardised tape is placed and removed from the grid after 1 minute. The resulting detaching and flaking of the coating is optically classified according to ASTM D 3359 [142].

The surface polarity was assessed via contact angle measurements with an Automatic Contact Angle System *ACA 50* produced by Data Physics Instruments GmbH.

The coating thickness was measured by means of a Laser Profilometer UBM, equipped with a microfocus device.

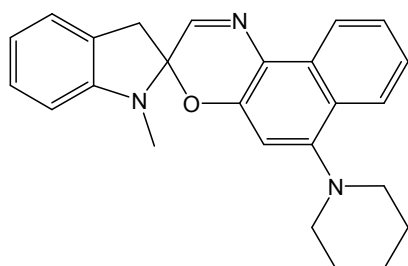
Artificial weathering was performed in an air cooled Suntest chamber (ATLAS Material Testing Technology BV, model *Suntest CPS+*) with a 1100 watt Xenon arc lamp as the light source (according to DIN ISI 9000ff specification). The average irradiance was 750 W/m^2 . Also the Weathering Tester Q-Panel model QUV/Se with UV-A bulbs (emission maximum 351 nm) was used. For irradiation of EPR samples a HBO 200 W mercury lamp was used. The powders were irradiated with a lamp-sample distance of 0.5 m for 4 h.

5.2. Chemicals and Substrates

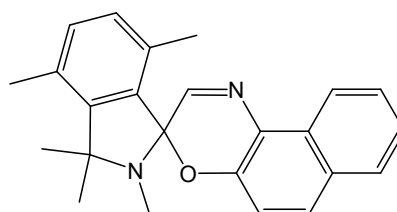
The chemicals used for all experiments were commercially available from several companies, such as ABCR, Aldrich, Fluka and Sigma.

As test substrates microscope slides (glass, quartz) as well as plastic lenses (PC, CR39®) were selected. Before coating they were cleaned for 5 min in a NaOH bath (50 °C), and afterwards rinsed with distilled water. After a 3 min treatment in an ultrasonic water bath, the substrates were thoroughly rinsed again and dried.

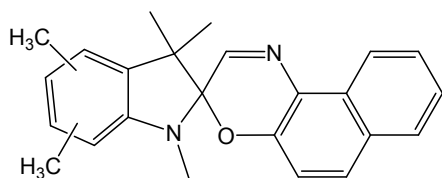
The structures of photochromic dyes selected for this work are shown in Figure 5.1. a)-h).



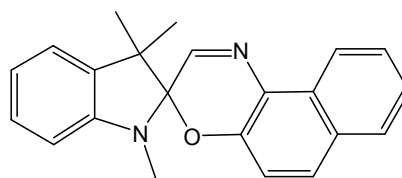
a) Red PNO



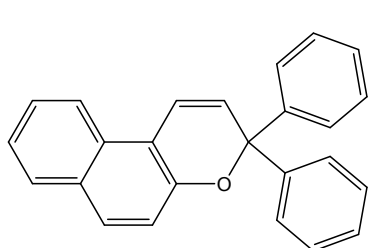
b) Blue C



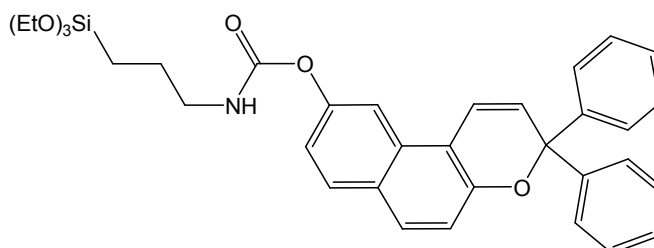
c) Blue D



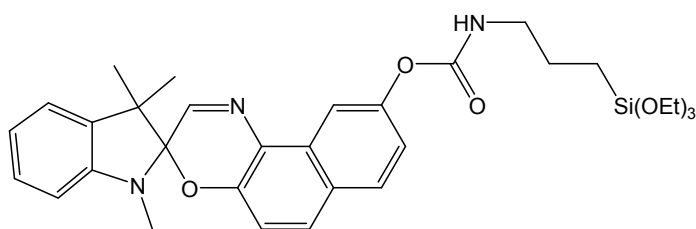
d) Blue A



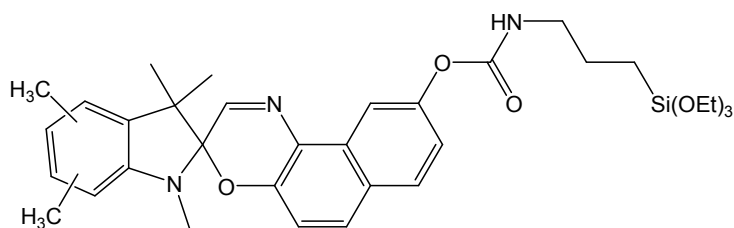
e) Photo L



f) graftable Photo L



g) graftable Blue A



h) graftable Blue D

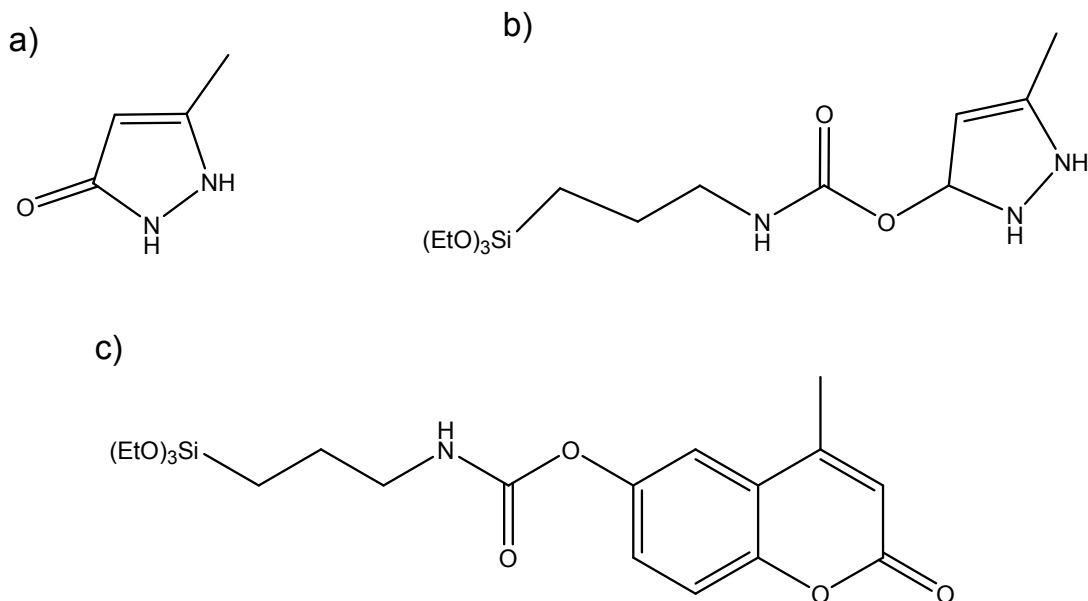
Figure 5.1. Photochromic dyes used in this study: a) 5'-morpholino-1,3,3-trimethyl substituted spiro-indolinoxazine (Red *PNO*); b) 1,1,2,4,7-pentamethylspiro-[isoindolino-naphthoxazine], (*Blue C*, *BC*); c) Variacrol® *Blue D* (1,3,3,5,6-pentamethylspiro-[indolino-naphthoxazine], *BD*); d) *Blue A* (1,3-Dihydro-1,3,3-trimethylspiro[2H]-indol-2,3'-[3H]naphth[2,1-b][1,4] oxazine), CAS-No. 27333-47-7); e) 3,3-diphenyl-3H-naphtho[2,1-b]pyran (Variacrol® *Photo L*, *PhL*); f) silylated

derivative of PhL called *graftable Photo L*, *SPhL*; g) silylated derivative of Blue A called *graftable Blue A*, *SBA*; h) silylated derivative of Blue D called *graftable Blue D*, *SBD*. Dyes a), b), c), e) as well as the silylated analogues f), g) and h) and a red-switching chromene with proprietary structure (WW) were kindly supplied by Great Lakes Chemical Italia, s. r. l. Blue A was purchased from Aldrich.

Besides the above mentioned products also Reversacol® dyes, i.e. Ruby, Midnight Grey and Misty Grey, commercially available from Robinson Co., UK were tested for their compatibility with hybrid polymers. According to the manufacturer's information these dyes belonged to the spironaphthoxazine and naphthopyran compound families.

For solvatochromic measurements ethyl-4-(methoxycarbonyl)pyridinium iodide, 4-methoxynitrobenzene and 4-(2,4,6-triphenylpyridinium)-2,6-diphenylphenoxide purchased from Fluka Co were used.

The stabilising additives (Figure 5.2.) were of different origin: 3-methylpyrazoline, silylated 3-methylpyrazoline, graftable 3-methylcoumarine, Enam 121 and 129, Lowillite Q84 nickel complex were supplied by Great Lakes Chemical, Italia, s. r. l., Tinuvin 770 and 1,8-diazabicyclo[5.4.0]undec-7-ene (DABCO-I) were products of Ciba-Geigy and Fluka, respectively.



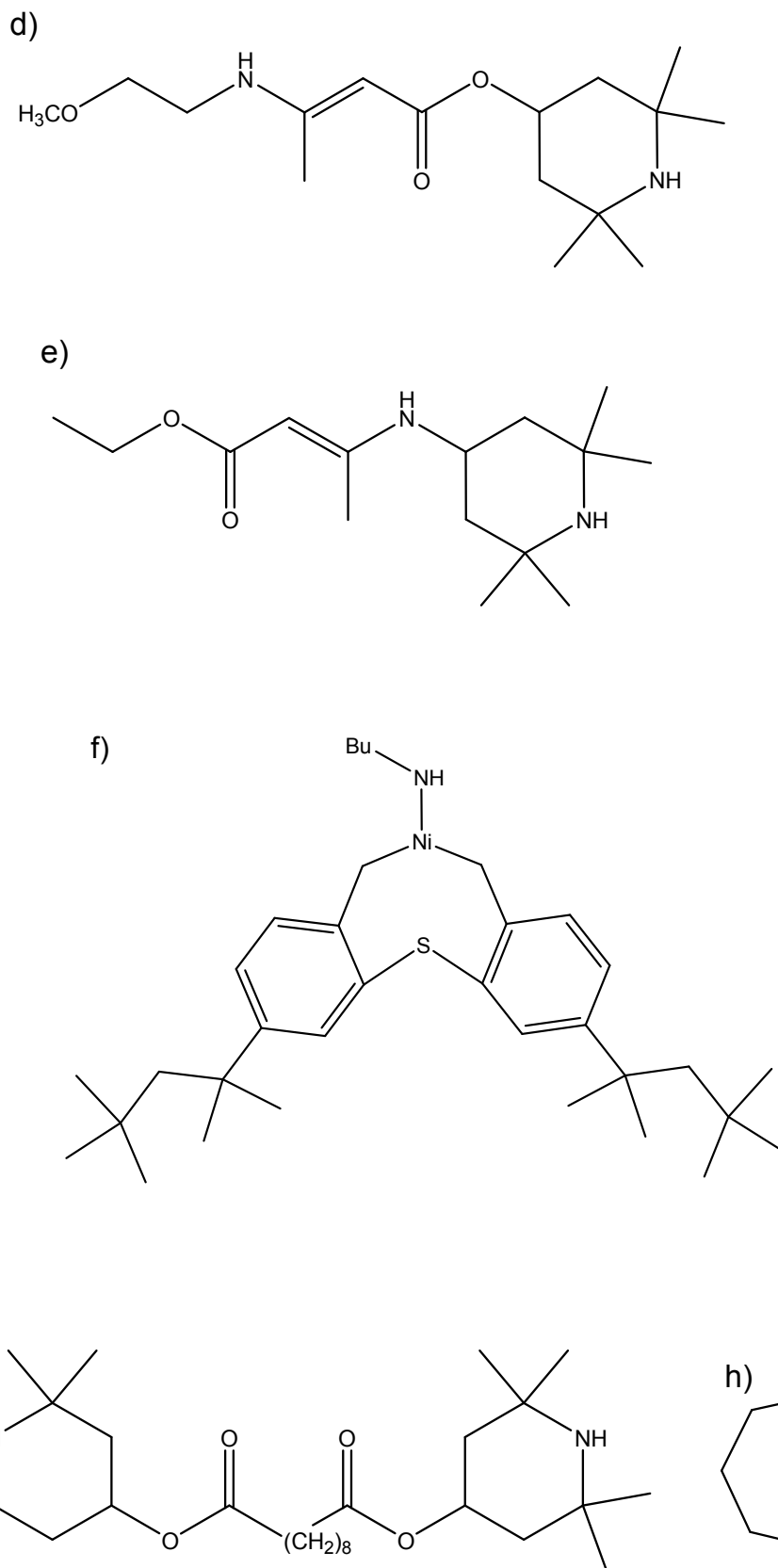


Figure 5.2. Additives used in this work: a) 3-methylpyrazoline (MP), b) silylated 3-methylpyrazoline (gr. MP), c) graftable 3-methylcoumarine, d) Enam 121, e) Enam 129, f) Ni-organocomplex (Q84), g) Tinuvin 770 (T770) and h) 1,8-diazabicyclo[5.4.0]undec-7-ene (DABCO-I).

5.3. Preparation methods

5.3.1. Preparation of the matrix systems

Preparation of matrix GG: To ice-cooled 3-glycidoxypropyl trimethoxysilane (GLYMO) placed in a round bottom flask H₂O and methylimidazole (MI) as the catalyst were added in a molar ratio of GLYMO : H₂O : MI = 1 : 1.5 : 0.05, and the mixture was stirred. After completion of the hydrolysis as determined by Raman spectroscopy [143], n-PrOH (100 g per mole of GLYMO) and 3-triethoxysilylpropyl succinic anhydride (GF20) in a molar ratio of GLYMO : GF20 = 1 : 0.5 were added. After stirring for 1 h the mixture was in a ready-to-apply condition.

Preparation of matrix GB: GLYMO and phenyltrimethoxysilane (PhTMO) in a molar ratio 0.75 : 0.25 were placed in a round bottom flask, ice-cooled and stirred. Subsequently, H₂O and MI in a molar ratio of GLYMO : H₂O : MI = 0.75 : 1.5 : 0.0375 were added and the mixture was stirred until the hydrolysis was complete. Finally, n-PrOH (100 g per mole of GLYMO) and cis-hexahydrophthalic anhydride (HEPA) in a molar ratio of GLYMO : HEPA = 0.75 : 0.375 were added. After stirring for 1 h the sol was in a ready-to-apply condition.

Preparation of matrix GA10: To ice-cooled GLYMO placed in a round bottom flask H₂O and MI were added in a molar ratio of GLYMO : H₂O : MI = 1 : 1.5 : 0.05, and the mixture was stirred. After completion of the hydrolysis as determined by Raman spectroscopy, n-PrOH (100 g per mole of GLYMO) and aminopropyltriethoxysilane (AMEO) in a molar ratio of GLYMO : AMEO = 0.9 : 0.1 were added. After stirring for 1 h the mixture was in a ready-to-apply condition. **GA5** is a variation of that system with a molar ratio of GLYMO : AMEO = 0.95 : 0.05.

Preparation of matrix GAD: To ice-cooled GLYMO placed in a round bottom flask H₂O and MI were added in a molar ratio of GLYMO : H₂O : MI = 1 : 1.5 : 0.05, and the mixture was stirred. After completion of the hydrolysis and cooling down (5 °C), AMEO in a molar ratio of GLYMO : AMEO = 0.9 : 0.1 was added. After stirring for 1 h diethoxymethylsilane (DH) (under ratio GLYMO : DH = 0.9 : 0.25) was dropped to the mixture. n-PrOH (100 g per mole of GLYMO) was added. After 30 minutes of stirring the mixture was in a ready-to-apply condition.

Preparation of matrix GEB: GLYMO and ethyltriethoxysilane (ETES) in a molar ratio of GLYMO : ETES = 0.7 : 0.3 were placed in a round bottom flask, ice-cooled and briefly stirred. Subsequently, H₂O and MI in a molar ratio of silanes : H₂O

: MI = 1 : 1.5 : 0.05 were added. The mixture underwent sonification with ultrasound for 20 minutes. Finally n-PrOH (100 g per mole of silanes) was added. After 1 h of stirring the mixture was in a ready-to-apply condition.

Preparation of matrix BIF: GLYMO and ETES in a molar ratio of GLYMO : ETES = 0.7 : 0.3 were placed in a round bottom flask, ice-cooled and briefly stirred. Subsequently, H₂O and MI in a molar ratio of silanes : H₂O : MI = 1 : 1.5 : 0.05 were added and the mixture underwent sonification with ultrasound for 20 minutes. n-PrOH (100 g per mole of silanes) and tridecafluoro-1,1,2,2-tetrahydrooctyltriethoxysilan (FAS) (molar ratio silanes : FAS = 1 : 0.015) was added. Afterwards the mixture was stirred for 20 h.

Preparation of matrix GPHA: To ice-cooled GLYMO placed in a round bottom flask H₂O and MI were added in a molar ratio of GLYMO : H₂O : MI = 1 : 1.5 : 0.05, and the mixture was stirred. After completion of the hydrolysis n-PrOH (100 g per mole of GLYMO) and (aminoethylaminomethyl)phenylethyl trimethoxysilane (PHA) in a molar ratio of GLYMO : PHA = 0.8 : 0.2 were added. After stirring for 1 h the mixture was in a ready-to-apply condition.

Preparation of matrix GADA: To ice-cooled GLYMO placed in a round bottom flask H₂O and MI were added in a molar ratio of GLYMO : H₂O : MI = 1 : 1.5 : 0.05, and the mixture stirred. After completion of the hydrolysis n-PrOH (100 g per mole of GLYMO) and 3-(2-aminoethylamino)propylmethyldimethoxysilane (ADA) in a molar ratio of GLYMO : ADA = 0.8 : 0.2 were added. After stirring for 1 h the mixture was in a ready-to-apply condition.

Preparation of matrix GMAT: To ice-cooled GLYMO placed in a round bottom flask H₂O and MI were added in a molar ratio of GLYMO : H₂O : MI = 1 : 1.5 : 0.05, and the mixture was stirred. After completion of the hydrolysis n-PrOH (100 g per mole of GLYMO) and (N-methylaminopropyl)trimethoxysilane (MAT) in a molar ratio of GLYMO : MAT = 0.8 : 0.2 were added. After stirring for 1 h the mixture was in a ready-to-apply condition.

Preparation of matrix PL (nanoparticle lacquer): To GLYMO and MI placed in a round bottom flask (molar ratio GLYMO : MI = 1 : 0.05) the aqueous silica sol TM50 was added dropwise in a molar ratio silanes : TM50 (water amount) = 1 : 1.1875, and the mixture stirred for ca. 15 minutes. Tetramethoxysilane (TMOS) (molar ratio GLYMO : TMOS = 0.75 : 0.25) was slowly dropped to the mixture. After

stirring for 1 h, n-PrOH (100 g per mole of GLYMO) and GF20 in a molar ratio of GLYMO : GF20 = 1 : 0.5 were added. After stirring again for 1 h the synthesis was complete. Before coating application the sol was filtered (1 µm membrane filter) and diluted with 30 wt.% of n-PrOH.

Preparation of the SiO₂-matrix: To TMOS placed in a round bottom flask MI was added in a molar ratio of TMOS : MI = 1 : 0.05, and the mixture was stirred for 1 h. Thereafter, MeOH (25 g per mole of TMOS) and H₂O in a molar ratio of TMOS : H₂O = 1 : 2 were added. After stirring for 20 minutes and addition of the additives the mixture was left for gelation. Byk301®, BYK Chemie was added in 0.2 wt.% to the PL laquer if it was applied as the top coat.

5.3.2 Incorporation of dyes and other additives

The dyes, depending on their chemical properties, were added at different steps of the reaction. Generally they were pre-solved in 1 g THF and 0.5 g n-PrOH, when incorporated into 5 g of sol.

Physically incorporated dyes (unsilylated) were mixed with the final coating solution. In the case of the chemically incorporated dyes (silylated Blue A, silylated Blue D and silylated Photo L) an additional amount of water was added for dye hydrolysis at the beginning of the sol synthesis (molar ratio graftable dye : H₂O = 1 : 1.5). The dissolved dye was incorporated at the final stage of the GLYMO hydrolysis.

The concentration of the dyes was calculated with respect to the solids content counted as weight percent of liquid phase of each sol (Table 5.1). This way of the dye amount calculation, allowed to achieve defined chromophore concentrations within the cured coating materials. For the silylated dyes only the molecular weight of the photochromic moieties was taken into consideration in order to ensure identical chromophore concentrations were present in the cured coating.

Table 5.1. Solids content for different matrices.

Matrix	Solids content [%]
GG	57
GB	57

GA05	45
GA10	45
GEB	45
BIF	45
GAD	45
GPHA	48

The UV stabilisers were added with respect to the molar amount of the photochromes. The absolute amounts of the stabilisers used are given in chapter 6.5.1 .

In all cases ready-to-apply coating solutions were filtered (1 μm membrane filter) in order to remove gel particles and other solid impurities that could be harmful for the optical quality of the coating.

5.4. Samples preparation

5.4.1 Measurement of photochromic activity

The sols with incorporated dyes and additives were applied to properly cleaned substrates by spin coating. The glass microscope slides were the most common, but also PC sheets, as well as CR39[®] sheets and lenses were used as substrates. Prior to coating, the glass slides, plastic sheets and lenses were immersed in NaOH ($c = 15\%$) for 5 minutes ($50\text{ }^{\circ}\text{C}$), thereafter washed with deionised water, treated in an ultrasonic water bath for 3 minutes, washed again with deionised water and subsequently dried with compressed air. In the spin coating process, the substrate spins around an axis and thus the deposited coating material

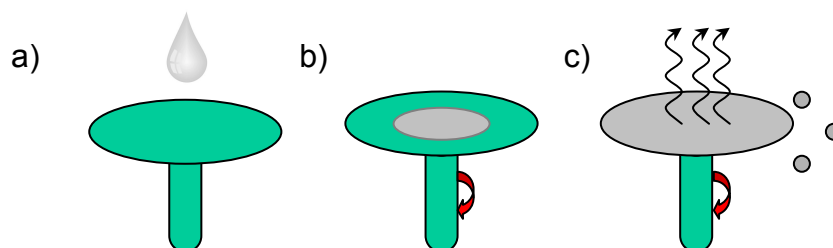


Figure 5.3. Spin coating process: a) deposition of the coating solution, b) spreading and c) spin off and solvent evaporation.
is spread on

the substrate surface (Figure 5.3. a) and b)). The remaining coating solution is spun off and the solvent evaporates (Figure 5.3. c)) [144]. The coatings were spun on at 600 revolutions per minute (rpm) for 30 seconds and spun off for 10 seconds at 1200 rpm. Thereafter, the wet coatings were cured. If not noted explicitly, the standard curing schedule was 20 minutes at 125 °C.

5.4.2 Measurement of photochromic kinetics

The dyes Blue A, Blue C, Blue D, gr. Blue D, Photo L, Red PNO, WW, Ruby, Misty Grey and Midnight Grey were added to freshly synthesised GG, GB, GA10 and GAD sols in a concentration of 3 wt. %. The samples were spin-coated on properly cleaned glass microscope slides.

5.4.3 Samples for UV-Vis spectrophotometry

The ready-to-apply sols were dip coated on properly cleaned quartz microscope slides (AlfaAesar).

5.4.4 Samples for EPR and NMR analysis

The samples were made from freshly prepared sols. The dyes were added in a concentration of $c = 10^{-4}$ mole per 1 g of dried gel, in case of the SiO₂-matrix photochromes concentration was calculated with respect to 1 g of SiO₂. The sols were poured in small portions (to achieve a simulation of the coating process) into aluminium vessels, cured at 125 °C for 20 minutes and powdered.

The powders that were investigated by NMR did not contain any additives. Besides the standard conditions, also other curing temperatures (between 100 and 225 °C) and times (2, 5, 20 and 40 minutes) were used.

6. Results and discussion

6.1 Matrix systems

6.1.1 Matrix development

Organically modified sol-gel systems were used as host materials for photochromic dyes. They allow convenient processing by means of spin or dip coating on most polymer and glass substrates.

The development of matrix systems was directed to achieve a proper chemical and physical environment for dyes that were supposed to have high photochromic activity and show low photo fatigue when enclosed within a matrix free volume. Photochromic dyes from spirooxazine and chromene compound families undergo a UV light initiated cleavage reaction, which is associated with a symmetry modification. It is important to secure sufficient dye mobility for an undisturbed on/off reaction. On the other hand, the degree of cross-linking of the matrix network has to be tight enough to immobilise physically incorporated dye molecules, as well as to reduce negative effects from possible impurities, degradation products, water molecules or ambient oxygen migration. Acidic or basic functionalities that could be enclosed within the matrix, should be limited to concentration, that do not attack (and lead to degradation of) the open form of the photochromes. A prolonged life time of the zwitterionic form of the photomerocyanine is considered to be hazardous, because in that molecular form the photochromes are most easily affected by degradation factors. A fast bleach back reaction will take place within a non polar matrix that favours the uncharged closed form of the compounds studied in this work. Moreover, purely organic photochromes should be protected against aggressive reaction conditions or very high processing temperatures.

Sol-gel derived materials seemed to be very promising. The wide range of organosiloxane precursors and cross-linkers allows to control chemical and physical properties of the synthesised material. Mild reaction conditions and relatively low processing temperatures are an appropriate choice for treatment of organic dyes.

The main interest of this work were sol-gels based on 3-glycidoxypropyl-trimethoxysilane (GLYMO). The epoxy moiety of GLYMO can react to form a polyether type network at moderately elevated temperature independent of the alkoxy silane part of the molecule. The alkoxy silane part undergoes a sol-gel reaction (hydrolysis and condensation) to build up the inorganic polysiloxane backbone. The

resulting hybrid material comprises organic and inorganic cross-linkers. To form matrices of different rigidity and polarity different cross-linkers were used (Figure 6.1), i.e., the silylated cross-linker 3-triethoxysilylpropyl succinic anhydride (GF20) to form matrix GG and the organic cross-linker cis-hexahydrophthalic anhydride (HEPA) to form matrix GB. As the latter would not contribute additional inorganic cross-linking, its use should enhance the flexibility of the matrix. Phenyltrimethoxysilane (PhTMO) inserts aryl moieties that were supposed to increase the hydrophobic character and loosen the network.

Aminopropyltriethoxysilane (AMEO) was used as inorganic and organic cross-linker (matrix GA10) to produce carboxyl free systems.

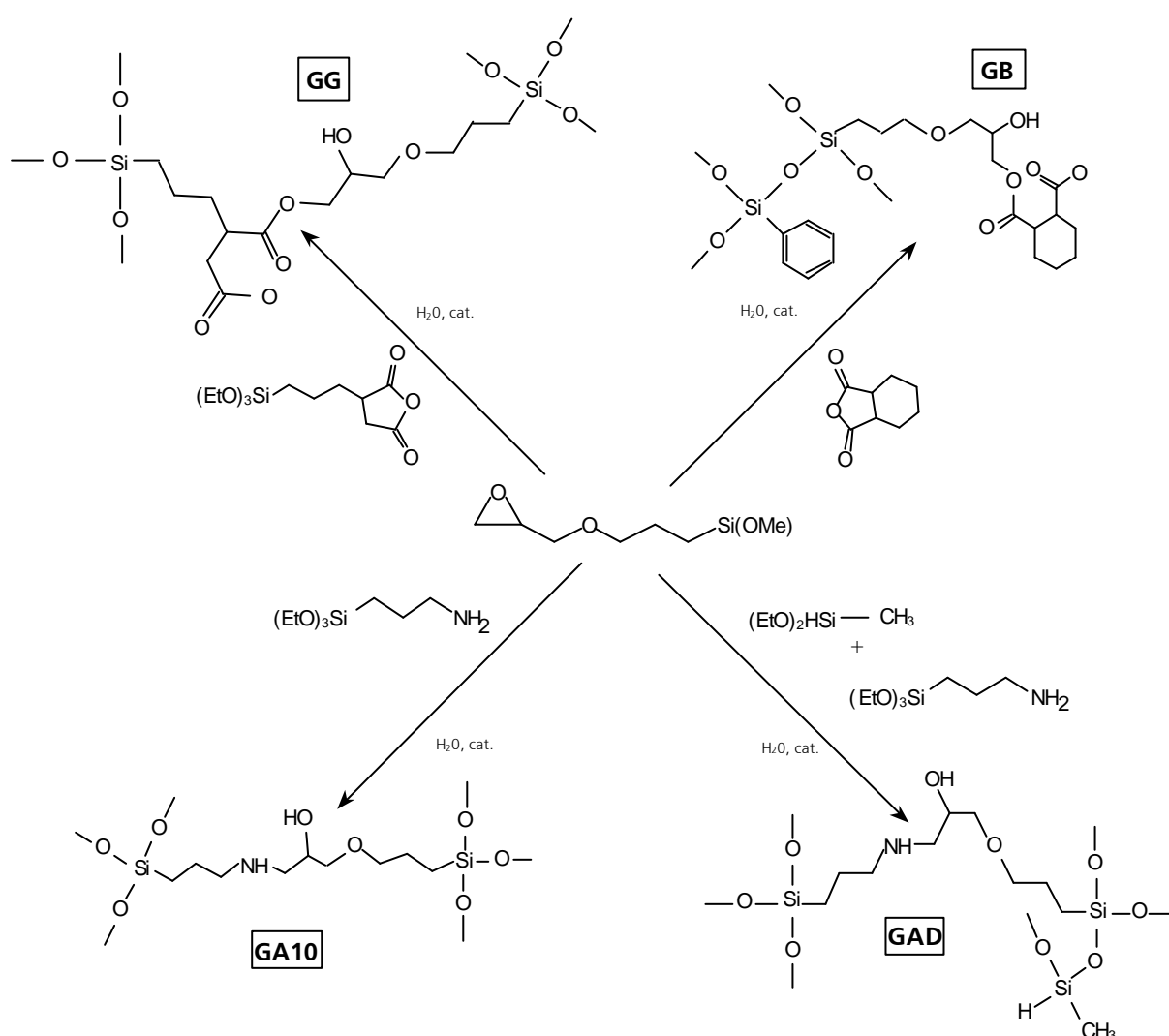


Figure 6.1. Reaction scheme for the mostly used matrix systems.

The precursor diethoxymethylsilane (DH) (matrix GAD) known to be reactive against -OH functionalities [145] is expected to lead to fully condensed polysiloxane networks with high amounts of uncharged methyl groups.

The material synthesis was carried out in two steps. In the first one 3-glycidoxypropyltrimethoxysilane (GLYMO) being the main component of all tested matrices (Figure 6.1 and paragraph 5.3.1), was pre-hydrolysed with 0.5 moles of water per mole alkoxy group and methylimidazole (MI) as basic catalyst. The half-stoichiometric amount of water is sufficient for a complete hydrolysis of the alkoxy groups and does not introduce any unnecessary water, whose presence would potentially be harmful for incorporated dyes (Si-OH formation). The decreasing concentration of alkoxy groups was followed by means of Raman spectroscopy (Figure 6.2). The signals at 643 cm^{-1} and 612 cm^{-1} both due to vibrations of the trialkoxysilyl moiety [143] disappear during the reaction.

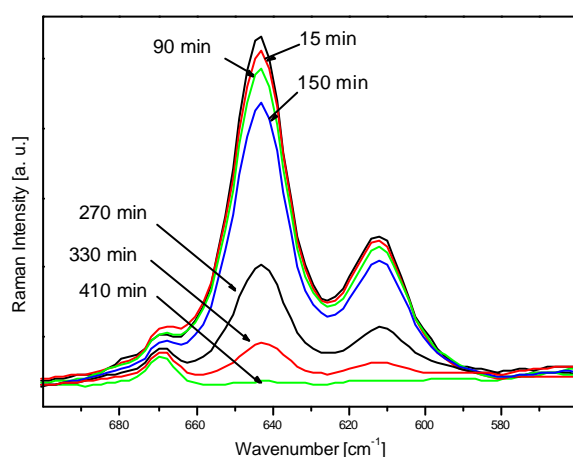


Figure 6.2. The investigation of the hydrolysis of GLYMO methoxy groups by means of Raman spectroscopy during the synthesis of the GG matrix system.

In the case of a methoxysilane such as GLYMO one can observe a signal arising at about 1030 cm^{-1} , which is due to methanol released during the reaction (Figure 6.3). The signal at 480 cm^{-1} is due to polycondensation products [146]. Cross-linking of silanes proceeds with condensation of the inorganic network. Formation of the organic network occurs during the curing step. Upon heating to temperature above $100\text{ }^{\circ}\text{C}$ the epoxy ring vibration at about 1256 cm^{-1} decreases in

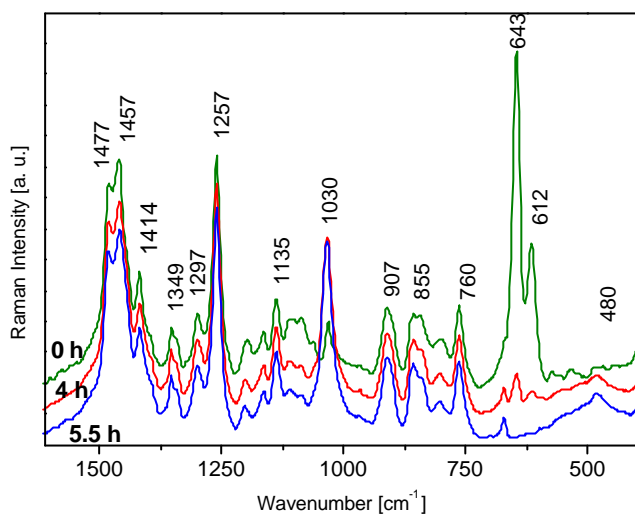


Figure 6.3. Observation of the hydrolysis reactions of GLYMO by means of Raman spectroscopy.

intensity, as well as do the signals at 2157 cm^{-1} and 2120 cm^{-1} which indicates that $=\text{Si-H}$ bonds break down and $=\text{Si-CH}_3$ groups are incorporated within the matrix network during the synthesis of the GAD system (spectra not shown).

6.1.2 Matrix characterisation

The physical properties of coatings spun on glass, polycarbonate (PC) and CR39® were characterised (Table 6.1). The average thickness was in the range between $2.5\text{ }\mu\text{m}$ and $10\text{ }\mu\text{m}$ depending on the system, dilution and spinning conditions.

Table 6.1. Average thickness, microhardness and adhesion characteristics for selected matrices (standard deviations in parentheses).

Matrix	Thickness [μm]	Hardness [N/mm^2]	Adhesion PC, CR39®, glass
GG	4 - 5	~80	Gt. 0, Gt. 0, Gt. 0
GB	3.5 - 5	~60	Gt. 0, Gt. 0, Gt. 0
GA10	4.5 - 5.5	~40	Gt. 0, Gt. 0, Gt. 0
GAD	7.7 (0.56)	58.6 (8.42)	Gt. 0, Gt. 0, Gt. 0
PL	4.8	143.2	Gt. 0, Gt. 0, Gt. 0
GEB	2.1 (0.13)	102.9 (3.96)	Gt. 4, Gt. 5, Gt. 1
BIF	14.8 (0.12)	187 (12.42)	Gt. 0, Gt. 4, Gt. 5

The universal microhardness of the systems depended on the amount of organic components and on the curing conditions. For the GG, PL and GAD systems the curing temperature range was between 100 and 225 °C and curing times from 2 minutes to 40 minutes were employed. In the case of the GG system (Figure 6.4) curing at 200 °C for 10 was sufficient to achieve a maximum of hardness, i.e., approximately 130 N/mm². The minimum value of 38 N/mm² was measured for coatings cured at 100 °C for 5 minutes.

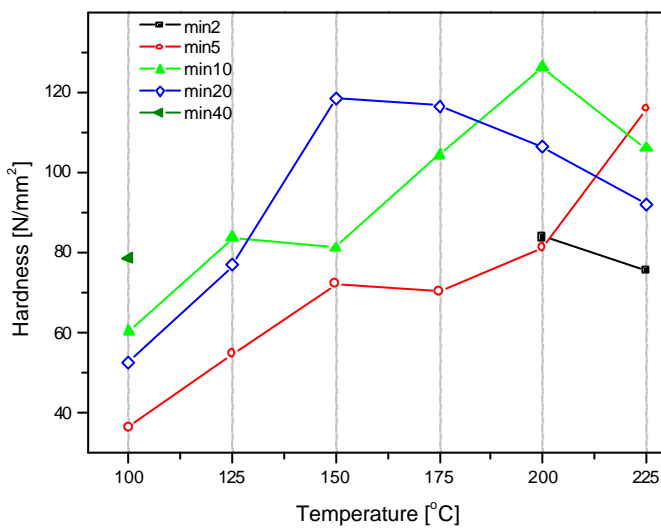


Figure 6.4. Universal microhardness of GG coatings depending on different curing times and temperatures.

However, coatings cured at 200 and 225 °C, were yellowish and cracked, respectively, thus indicating that thermolysis took place under these conditions. Curing at 150 °C for 20 minutes seemed to be the optimum in order to achieve the highest hardness without affecting the optical quality and integrity of the coating. In all cases adhesion on glass was very good (Gt. 0), with exception of samples cured at the highest temperature (Gt. 2 – 4). For the particle lacquer (PL, Figure 6.5) which was supposed to be used as a scratch-resistant non-photochromic top coat the hardness of samples cured at 100 °C and 225 °C for 5 and 10 minutes differs about 100 N/mm², whereby curing for 20 minutes yields a difference of 200 N/mm².

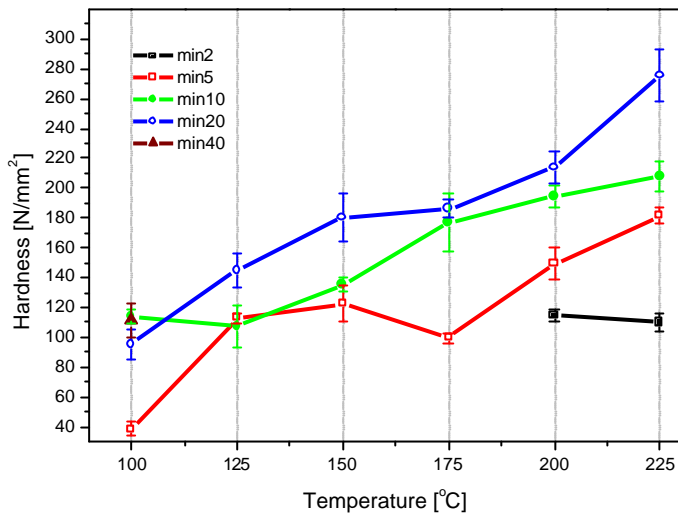


Figure 6.5. Universal microhardness of PL coatings depending on different curing times and temperatures.

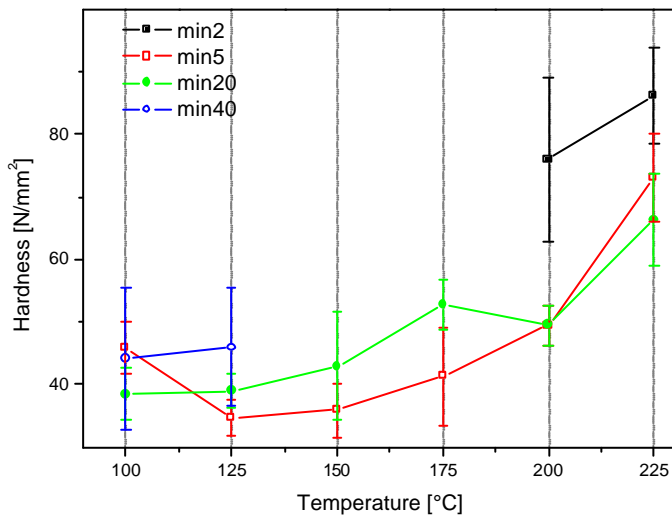


Figure 6.6. Universal microhardness of GAD coatings depending on different curing times and temperatures.

The hardening behaviour of the GAD matrix (Figure 6.6) was rather similar for curing times of 5 and 20 minutes. In that particular case a 2 minutes curing step at the highest temperature gave the best results in terms of hardness.

The mobility of dye molecules within the host materials was expected to depend on the connectivity of the matrix network. Quantitative solid state ^{29}Si MAS-NMR spectroscopy was employed to gain insights into the level of inorganic connectivity and determine the concentration of relevant silicon structural units.

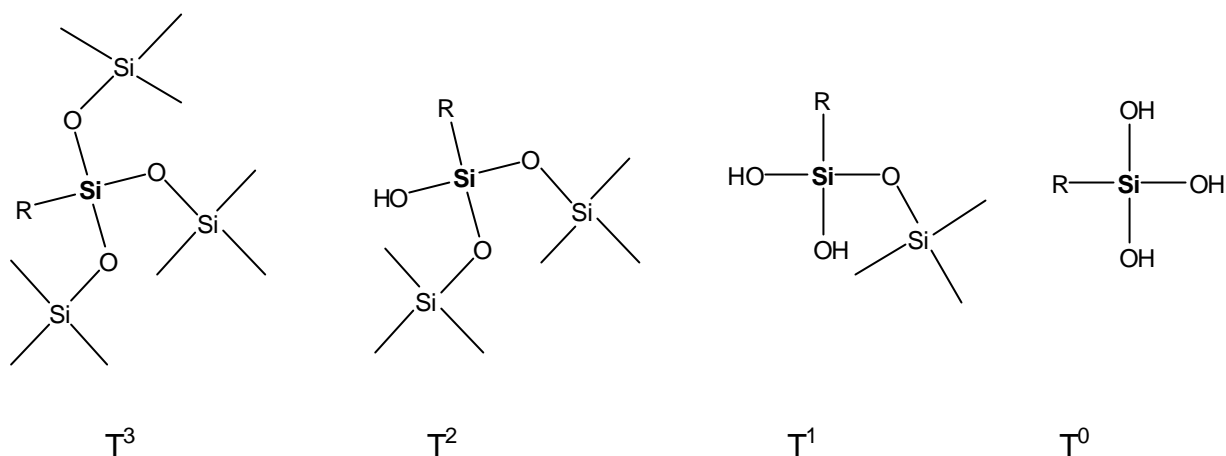


Figure 6.7. Nomenclature popularly used for the different condensation states of trialkoxysilanes.

The widely accepted nomenclature, which describes possible connectivities of poly(organo)siloxanes, is presented in figure 6.7 for trialkoxysilanes [12, 147]. T^0 is defined as a silanetriol species, with no other silicon atoms connected via oxygen bridges. In the case of T^1 , T^2 and T^3 groups there are one, two or three siloxane bonds consequently. The inorganic network connectivity was measured for powdered bulk samples (Table 6.2). The quantitative solid state ^{29}Si MAS-NMR spectra provided information about the composition of the polysiloxane backbone. The signal with a chemical shift δ around -67 ppm in the ^{29}Si -NMR spectrum can be assigned to the completely hydrolysed and polycondensed species T^3 that form a three-dimensional polysiloxane network. In GG, GB and GAD matrices T^3 species were detected to a maximum of 79 %. Partially condensed T^2 and T^1 species, bearing residual alkoxy or OH groups [12, 147] were found to be present to a maximum of 23 %. Only matrix GB behaves somewhat differently, in that solely T^3 could be found. The resonance at -80.9 ppm can be attributed to T^3 groups with the substituent on the silicon atoms being phenyl groups originating from the PhTMO component in the GB system [148]. Thus, unlike GG, GA10, and GAD, which contain residual hydroxyl or even alkoxy groups, the GB matrix essentially consists of a fully hydrolysed and completely condensed polysiloxane network.

Table 6.2. ^{29}Si solid state MAS-NMR chemical shifts and inorganic network connectivity (samples cured at 125 °C for 20 minutes).

GG		GB		GA10		GAD	
δ [ppm]		δ [ppm]		δ [ppm]		δ [ppm]	
-66.5	T^3 (~74 %)	-80.9	Si-Ph (~21 %)	-67.5	T^3 (~77 %)	-67.8	T^3 (~78 %)
-60.1	T^2 (~22 %)	-67.3	T^3 (~79 %)	-59.9	T^2 (~23 %)	-60.1	T^2 (~22 %)
-52.8	T^1 (~4 %)						

Hardening at different temperatures for various periods changed the physical properties of the coatings. The chemical characteristics of the polysiloxane backbone was also altered, which can be seen from the ^{29}Si solid state MAS-NMR measurements. There was no evidence for the presence of T^0 groups. Thus, all species are incorporated in the polycondensate network. Percentage ratios between possible condensation states for GG (T^1 , T^2 and T^3 ; Figure 6.8 A) and GAD (T^2 and T^3 ; Figure 6.8 B) depend rather on the curing temperature than on the curing times, with this effect being more pronounced for the GG matrix.

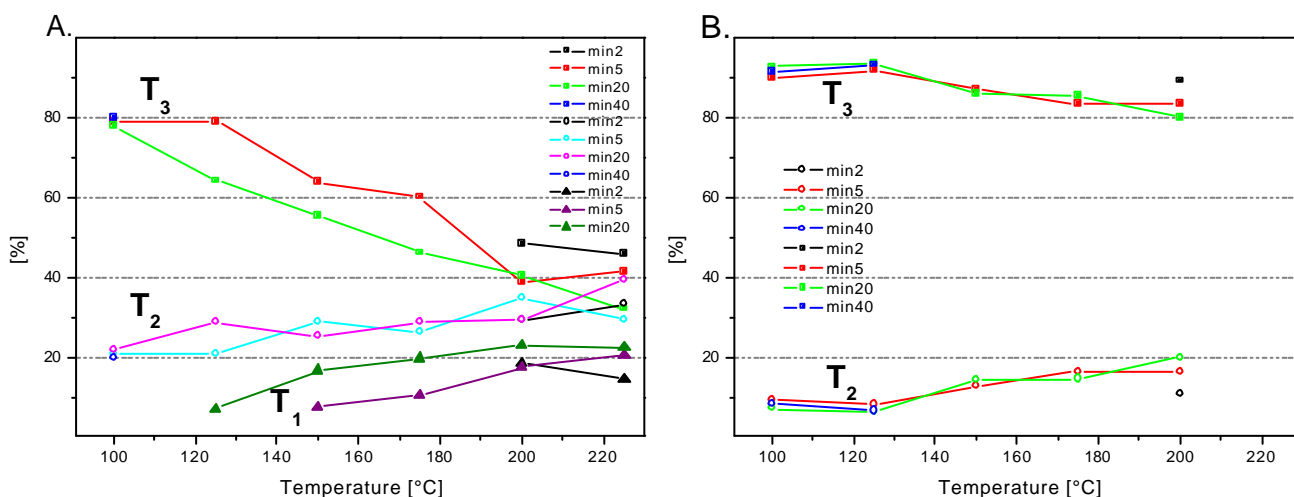


Figure 6.8. Network connectivity of **A.** GG and **B.** GAD matrices depending on the curing conditions as revealed by ^{29}Si MAS-NMR spectroscopy.

Interestingly, in the case of samples cured at 100 °C 80 % T^3 groups with no T^1 groups, were present, thus indicating a three dimensional polysiloxane network predominantly present. T^1 groups occurred at curing temperatures higher than 125 °C. After curing at 150 °C for 20 minutes they covered almost 20 % of the total amount of the silicon species. Under additional consideration of the 20 % of T^2 groups present under these conditions this clearly suggests a transition towards a more planar, two dimensional network occurring at elevated temperatures. The same tendency was observed also for higher temperatures. For gels cured at 200 °C and 225 °C T^1 and T^2 groups comprised over 20 % and almost 40 % of all silicon species, respectively, so the inorganic network can be considered to be chain-like under these conditions. In contrast to the matrix connectivity, the coatings' hardness developed as expected with the change of the curing conditions.

The GAD matrix did not fully follow the “GG pattern” of backbone formation (Figure 6.8 B). The influence of temperature on the network connectivity was similar, but not so distinct. Possibly, the mobility of the chemical species was hindered already after a very short time in this system. Only an increase by about 10 % of T^2 groups and accordingly less T^3 groups was measured for 100 °C curing as compared to 225 °C cured samples.

Ageing of the coating solution also influenced the condensation process. After storing for four months at -18 °C the GG system seemed to be in a precondensed state. A gel directly processed after synthesis contained less T^2 groups than a gel that has been stored for four months, when curing at lower temperatures was performed. At higher curing temperatures the difference between both systems appeared to be less marked (Figure 6.9). That would suggest that a certain amount of two dimensional linkages already existed in the fluid stadium.

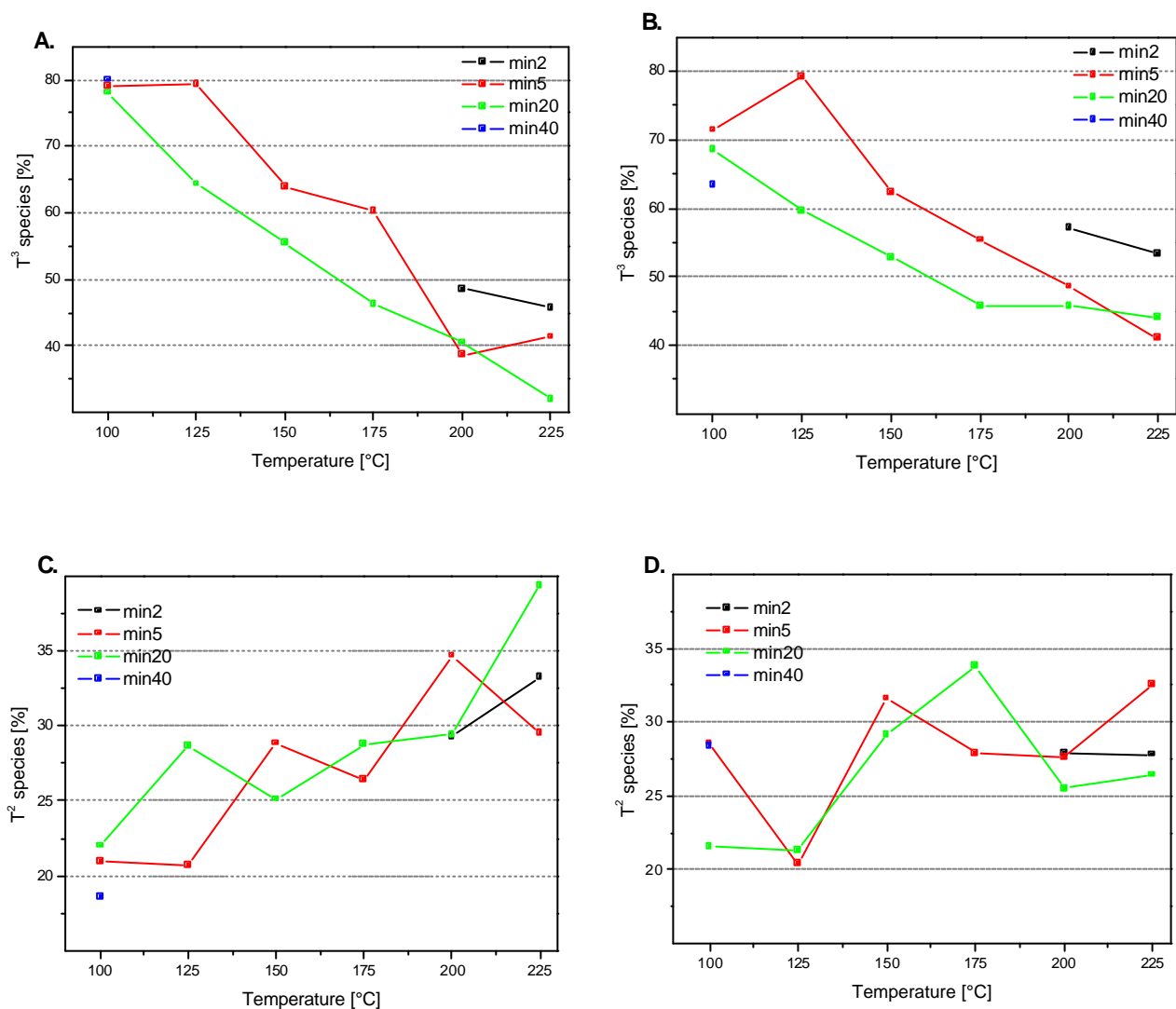


Figure 6.9. Network connectivity of the GG matrix investigated by means of ^{29}Si -MAS-NMR spectroscopy in percents of T^3 (A. and B.) and T^2 groups (C. and D.), processed directly after synthesis (A. and C.) and after 4 months storage (B. and D.) depending on the curing conditions.

IR spectrometry, combined with NMR spectroscopy, is a powerful tool that enables the observation of the structural evolution of the entire system in a sol-gel derived formulation [24, 149]. IR spectra recorded for the same GG sample series as reported above showed that the $\nu(\text{CO})$ absorption bands of the GF20 anhydride ring (1864 and 1785 cm^{-1}) already disappeared at $100\text{ }^\circ\text{C}$ (Figure 6.10). The amount of $-\text{OH}$ (3458 cm^{-1}) groups compared to hydrocarbon groups (2938 and 2877 cm^{-1}) decreased for the $225\text{ }^\circ\text{C}$ cured sample. Some changes in the polysiloxane network Si-O-Si vibrations were seen at 1028 and 1110 cm^{-1} . The signals were significantly stronger for the sample cured at higher temperature. The signal at 1588 cm^{-1} , that

was clearly observed for a sample cured at 100 °C disappeared at higher curing temperatures. It is assumed to originate from uncondensed Si-OH or SiOR moieties, which has to be proven yet. With increased temperature the signal disappears presumably as a result of the proceeding condensation.

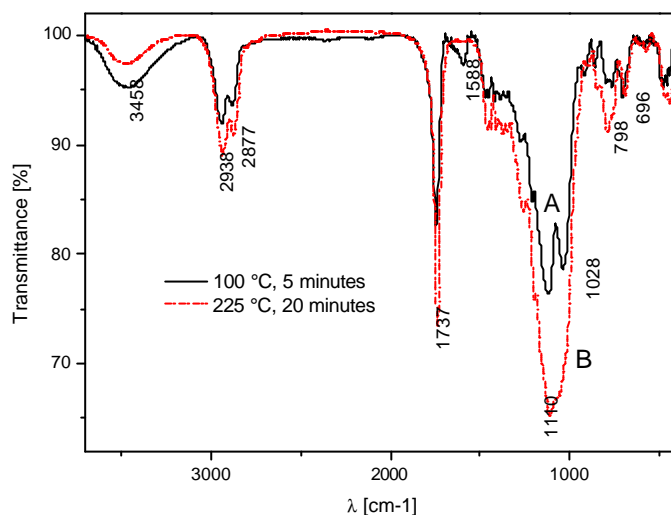


Figure 6.10. IR absorption spectra of the GG system cured at 100 °C for 5 minutes (A.) and 225 °C for 20 minutes (B.), measured in KBr pellets.

Another spectroscopic method used to get information about the structural evolution is solid state ^{13}C NMR spectroscopy. Typically, such ^{13}C NMR spectra cannot be quantitatively interpreted because carbon atoms with long relaxation times may not completely return to the thermodynamic equilibrium state between the magnetic pulses. Besides, an interaction with neighbouring H nuclei changes the signal intensities. Nevertheless, by cautious estimation of carbon nuclei intensities the assessment of concentrations is possible when similar chemical conditions are given [148,150].

GG samples (direct synthesis and after 4 months storage at -18 °C) were cured at temperatures between 100 °C and 225 °C for time intervals between 2 and 40 minutes. According to the ^{13}C NMR spectra there was almost no difference between samples cured at 200 °C and 225 °C for each series. Thus, the sample cured at 100 °C for 5 minutes was compared with the sample cured at 200 °C for 20 minutes (Figure 6.11 and 6.12). Those two extreme examples shall demonstrate the tendency, which was found for the whole series of ^{13}C NMR measurements.

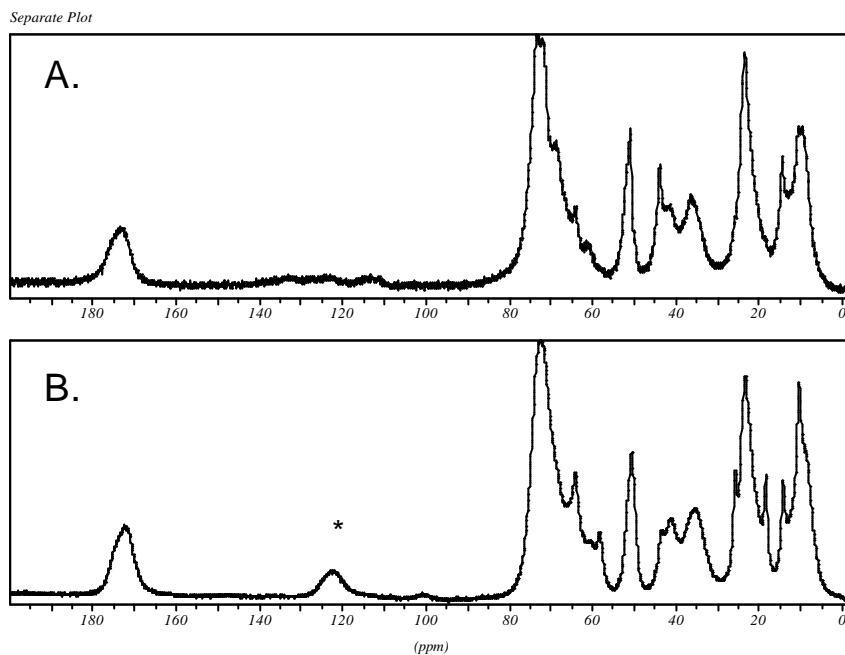


Figure 6.11. Solid state ^{13}C NMR spectra for samples cured at $100\text{ }^{\circ}\text{C}$ for 5 minutes (upper, sample A) and for samples cured at $200\text{ }^{\circ}\text{C}$ for 20 minutes (lower, sample B); the coating solution was used directly after preparation; * - rotation side band.

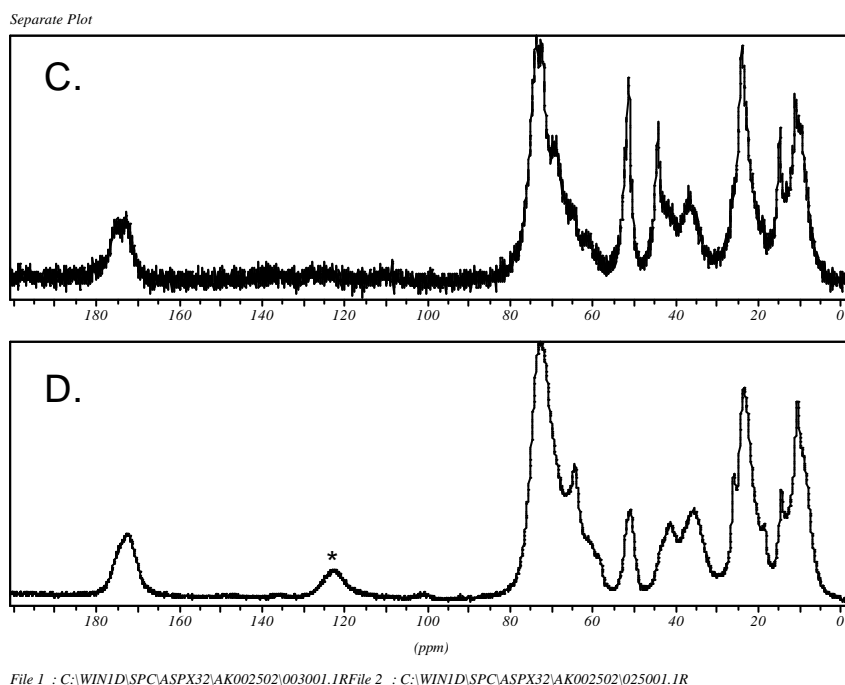
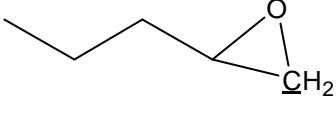
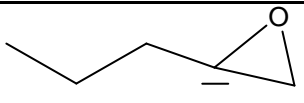


Figure 6.12. Solid state ^{13}C NMR spectra for samples cured at $100\text{ }^{\circ}\text{C}$ for 5 minutes (upper, sample C) and for samples cured at $200\text{ }^{\circ}\text{C}$ for 20 minutes (lower, sample D); the coating solution was stored for 4 month at $-18\text{ }^{\circ}\text{C}$; * - rotation side band.

Table 6.3. ^{13}C solid state MAS-NMR chemical shifts and their assignment.

δ [ppm]	
10.2, 18.2	$-\underline{\text{C}}\text{H}_3$
14	$-\text{CH}_2-\underline{\text{C}}\text{H}_3$
23.3	$-\text{O}-\text{CH}_2-\underline{\text{C}}\text{H}_2-\text{CH}_2-\text{Si}=\text{}$
25.5	$-(\text{O})\text{C}-\underline{\text{C}}\text{H}_3$
44.0	
51.5	
58.1	$-(\text{O})\text{C}-\text{O}-\underline{\text{C}}\text{H}_2-\text{CH}_3$
64	$-\underline{\text{C}}\text{H}_2-\text{O}-, =\underline{\text{C}}\text{H}-\text{O}-$
72, 74	$-\underline{\text{C}}\text{H}_2-\text{O}-\underline{\text{C}}\text{H}_2-$
172	$-\text{CH}_2-\underline{\text{C}}(\text{O})\text{O}-\text{CH}_2-$

In the case of samples cured directly after preparation (Figure 6.11), the main differences consisted of a sharp signal at 44.0 ppm for the sample cured at 100 °C (sample A), and signals at 10.2, 18.2, 25.5, 58.1, and 64.2 ppm, that were all present for the sample cured at higher temperature (sample B). For signals assignment see Table 6.3. The signal at 44.0 ppm proved the presence of closed epoxy rings, which indicated that no full cleavage occurred at 100 °C. Sample B could be characterised to have a higher concentration of $-\underline{\text{C}}\text{H}_2-\text{O}-$ and $=\underline{\text{C}}\text{H}-\text{O}-$ groups (64.2 ppm) as well as more terminal methyl groups or groups that are connected with a carbonyl carbon atom ($\underline{\text{C}}\text{H}_3-(\text{O})\text{C}-$, 25.5 ppm; $-\text{CH}_3$, 10.2 and 18.2 ppm). The band at 58.1 ppm signalled the presence of ethyl groups connected with an ether bond ($-(\text{O})\text{C}-\text{O}-\underline{\text{C}}\text{H}_2-\text{CH}_3$), whereas the concentration of epoxy ring carbon atoms (at 44.0 ppm) was extremely low. For the samples that were made from stored coating solution (sample C cured at 100 °C for 5 minutes and sample D cured at 200 °C for 20 minutes; Figure 6.12) the same tendencies were observed, however, in the case of sample C the very high intensity of the signal at 51.3 ppm is taken as an evidence for a high epoxy ring concentration, higher than found for sample A. Increased band intensity at approx. 14 ppm suggests some uncondensed ethoxy groups to be

present. The ^{13}C NMR spectrum of sample D showed no signal at about 44 ppm (still observed for sample B) and also a very weak signal at about 58 ppm, which suggests that complete opening of the epoxy ring and possibly also condensation with the anhydride moiety occurred. The higher intensity at approx. 18 ppm for sample B as compared to D indicates a higher condensation rate for the stored sol. Cleavage of the organic functionalities during storage of the GG system can also be seen by comparing for example samples cured at 100 °C for 40 minutes. The stronger resonances at approx. 10, 26 and 64 ppm are due to the presence of the cleaved but not yet polyadded carboxyl species. For the sample cured at 150 °C for 20 minutes the signal at ca. 44 ppm (epoxy ring) has a much lower intensity when prepared from the pre-stored solution. Nonetheless, the time of hardening was an important factor: there was found a higher epoxy ring concentration for samples cured at 175 °C for only 5 minutes than for samples cured for a longer time (20 minutes) at 150 °C.

Measurements were also performed for the GAD system. There, a ^{13}C NMR signal at 63.8 ppm marked the main difference between samples cured at 100 °C for 5 minutes and at 200 °C for 20 minutes. The very distinct and intensive resonance found for the sample cured at higher temperature is an evidence for the presence of methyl groups that are connected to oxygen atoms in chain-like domains [151, 152].

The spectroscopic investigations gave an indication of the degree of hydrolysis and condensation. The hardness of the investigated coatings not only depended on the inorganic connectivity but also on the degree of organic polymerisation in the poly(organo)siloxane network, which was indicated by ^{13}C NMR measurements performed on sample series cured at different conditions.

6.1.3. Polarity of hybrid polymer materials

Many characteristics of embedded organic chromophores are affected by their direct environment in the matrix, i.e., by the so-called microenvironment [26]. Its characterisation can provide valuable information for the development of photochromic materials. The polarity of the matrix free volume, in which the photochromic dyes are entrapped, is very important. Among others, the kinetics of the thermal bleaching also depends on the polarity of the medium [153].

The surface energy measured through the contact angle method is one indication for the material polarity. A droplet of water or diiodomethane placed on the coating forms a contact angle that reflects the wetting behaviour of the surface. The free surface energy, σ_s comprises a polar, σ_s^p and non polar (dispersive) part, σ_s^d :

$$\sigma_s = \sigma_s^p + \sigma_s^d$$

These can be calculated by means of the Owens-Wendt theory, which associates fluids surface tension properties and measured contact angle:

$$\sigma_s^p = \frac{\sigma_w(1 + \cos\Theta^{DM}) / (\sigma_w^d)^{1/2}}{(\sigma_w^p / \sigma_w^d)^{1/2} - (\sigma_{DM}^p / \sigma_{DM}^d)^{1/2}}$$

$$\sigma_s^d = \frac{\sigma_{DM}(1 + \cos\Theta^W) / (\sigma_{DM}^d)^{1/2}}{[(\sigma_w^p / \sigma_w^d)^{1/2} - (\sigma_{DM}^p / \sigma_{DM}^d)^{1/2}][(\sigma_{DM}^p / \sigma_{DM}^d)^{1/2}]}$$

Where σ_w is the surface tension of water ($\sigma_w = 72.8$ mN/m);

σ_w^d and σ_w^p are the non polar and polar parts of the surface tension of water, respectively ($\sigma_w^d = 26.0$ mN/m, $\sigma_w^p = 46.8$ mN/m);

σ_{DM} is the surface tension of diiodomethane ($\sigma_{DM} = 50.8$ mN/m);

σ_{DM}^d and σ_{DM}^p are the non polar and polar parts of the surface tension of diiodomethane, respectively ($\sigma_{DM}^d = 48.5$ mN/m, $\sigma_{DM}^p = 2.3$ mN/m);

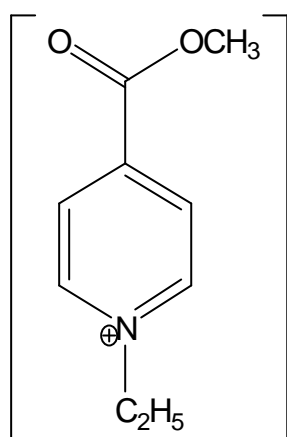
Θ^W and Θ^{DM} are the contact angles of water and diiodomethane on investigated surface, respectively.

For materials used in the present work, GAD films had the lowest surface energy with a very small fraction of the polar component (σ_s^p) (thus being the least hydrophilic surface). The introduction of =Si-CH₃ or =Si-H groups makes the material more hydrophobic [154]. GB films had the highest surface energy (σ_s) but GG films showed the largest fraction of σ_s^p (thus being the most hydrophobic surface) (Table 6.4).

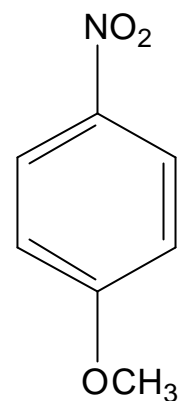
Table 6.4. Contact angles and surface energy for GAD, GG, GA10 and GB films.

Sample	Θ^W [°] (contact angle, H ₂ O)	Θ^{DM} [°] (contact angle, CH ₂ I ₂)	σ_s^p [mN/m]	σ_s^d [mN/m]	σ_s [mN/m]
GAD	94.2	58.1	0.86	28.89	29.75
GG	77.6	49.5	5.57	30.25	35.83
GA10	81.0	40.0	2.59	37.10	39.69
GB	80.9	38.5	2.49	37.91	40.40

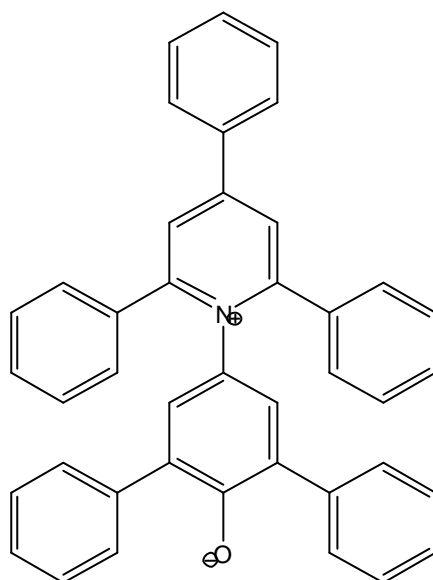
For dye doped materials the determination of the matrix free volume polarity is more interesting on a molecular microscopic level. For that purpose solvatochromic dyes are a convenient means. Solvatochromism can be defined as a reversible variation of the spectroscopic properties (absorption, emission) of a chemical species, induced by solvents. Halosolvatochromism is a colour change upon increasing ionic strength of the medium without a chemical change of the chromophore [73]. Many studies in that area were made [155 - 158] and negative and positive solvatochromes defined and described in the literature. A hypsochromic (blue) shift of the UV/vis/near-IR absorption band with increasing solvent polarity is usually called negative solvatochromism. On the other hand, positive solvatochromism leads to a bathochromic (red) shift with increasing solvent polarity. Two dyes of the former type have been used in this investigation: ethyl-4-(methoxycarbonyl)pyridinium iodide (charge transfer absorption type; Figure 6.13 a) and 4-(2,4,6-triphenylpyridinium)-2,6-diphenylphenoxide ($\pi \rightarrow \pi^*$ with intramolecular charge transfer (ICT) absorption type; Figure 6.13 c) belong to the negative solvatochromes. The third one, 4-methoxynitrobenzene ($\pi \rightarrow \pi^*$ absorption type; Figure 6.13 b) is a positively solvatochromic compound. All three were chosen because of their universal qualities and well documented solvatochromic properties [159, 160 and references therein]



a) Ethyl-4-(methoxycarbonyl)pyridinium iodide



b) 4-Methoxynitrobenzene
(4-nitroanisole)



c) 4-(2,4,6-Triphenylpyridinium)-
2,6-diphenylphenoxide

Figure 6.13. Solvatochromic dyes: ethyl-4-(methoxycarbonyl)pyridinium iodide (a), 4-methoxynitrobenzene (b), 4-(2,4,6-triphenylpyridinium)-2,6-diphenylphenoxide (c) [160, 161].

Many quantitative relationships between chromophore light absorption and physical solvent properties, based upon different models for solute/solvent interaction, were established. In any case, the empirical scales are the more useful ones (as Z [161], π^* [159] or $E_T(30)$ scale), based on the spectral data of a single (or more) standard probe molecule, after systematic correlation and analysis of chemical

and physicochemical properties in solution or in microheterogeneous media. The $E_T(30)$ scale of Dimroth and Reichardt was initially based on the solvatochrome *c* (Figure 6.13) and, afterwards, has been adapted also for other solvatochromes e.g. solvatochrome *a* (Figure 6.13). It is defined as the molar electronic transition energies (E_T) of dissolved compound *c* in kilocalories per mole at room temperature and normal pressure:

$$E_T(30) \text{ (kcal mol}^{-1}\text{)} = hc\nu_{\max}N_A = 28591/l_{\max}(\text{nm})$$

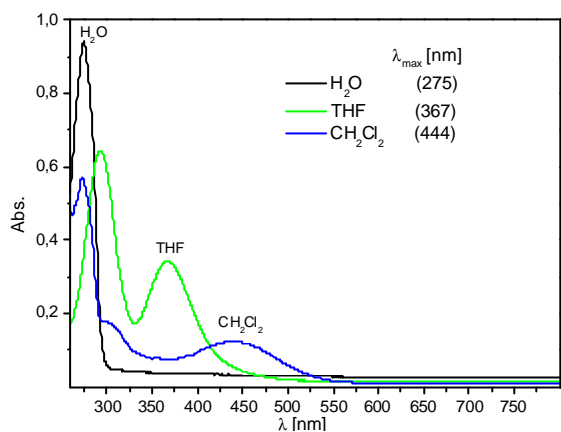
where: ν_{\max} is the frequency and l_{\max} is the wavelength of the longest wavelength ICT absorption band of the dye.

To make it more suitable for use the $E_T(30)$ is usually normalised to E_T^N that is based on the absorption characteristics of dye *c* in both water ($E_T^N=1.000$) and tetramethylsilane (TMS; $E_T^N=0.000$), representing extremely polar and nonpolar solvents, respectively.

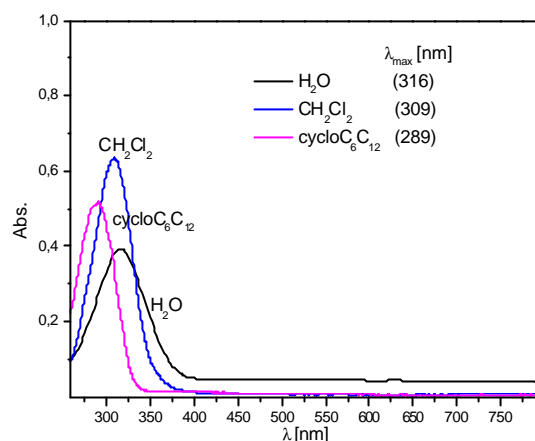
$$\begin{aligned} E_T^N &= [E_T(\text{solvent}) - E_T(\text{TMS})] / [E_T(\text{water}) - E_T(\text{TMS})] \\ &= [E_T(\text{solvent}) - 30.7] / 32.4 \end{aligned}$$

Compounds *a* and *c* work well in the above mentioned scales. Compound *b* is one of the compounds on which the π^* scale was based. It considers also the solvation energy and gives an indication of dipolarity and polarizability of the solvent.

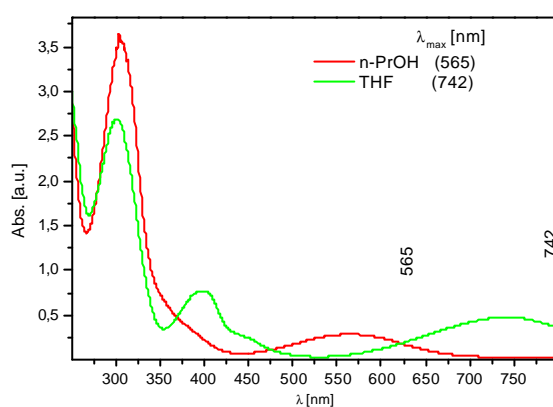
For absorbance measurements by means of UV-vis spectrometry solutions of the three solvatochromic compounds were prepared (the concentrations for the solutions of *a* and *b* were in the range of $c = 5 \times 10^{-5}$ moles/dm³ up to $c = 5 \times 10^{-4}$ moles/dm³, for *c* the concentration was about $c = 5 \times 10^{-6}$ moles/dm³). The solvatochromes were dissolved in solvents with different polarity. The absorption spectra of the solutions, correlated well with their solvatochromic properties (Figure 6.14 A-C) [160].



A. Absorption spectra of ethyl-4-(methoxycarbonyl)pyridinium iodide in different solvents.



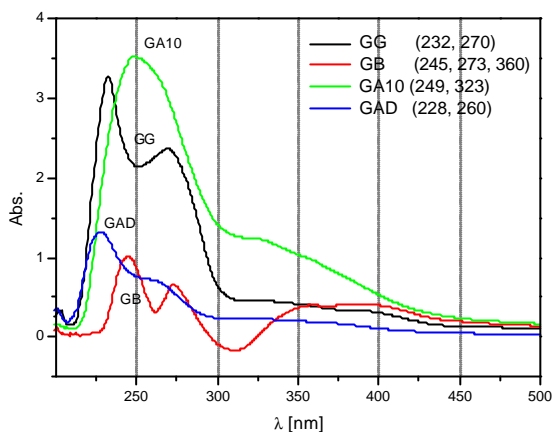
B. Absorption spectra of 4-methoxynitrobenzene in different solvents.



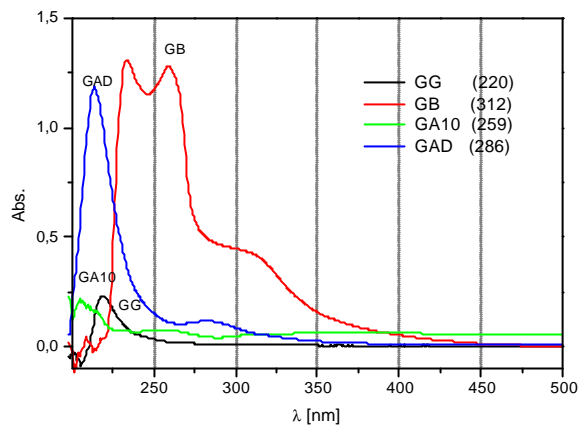
C. Absorption spectra of 4-(2,4,6-triphenylpyridinium)-2,6-diphenylphenoxide in two different solvents.

Figure 6.14. Absorption spectra of solvatochromes in different solvents: **A.** ethyl-4-(methoxycarbonyl)pyridinium iodide, **B.** 4-methoxynitrobenzene and **C.** 4-(2,4,6-triphenylpyridinium)-2,6-diphenylphenoxide.

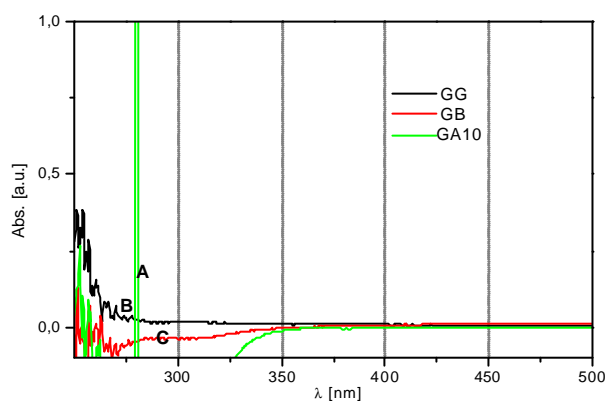
The solvatochromes were added to the ready-to-apply coating solutions in a concentration of 1×10^{-4} moles per 1 g of solution. The goal was to achieve the highest possible concentration of the dye within the coating. In the case of 4-(2,4,6-triphenylpyridinium)-2,6-diphenylphenoxide the solvatochrome showed very low solubility and the concentration $c = 1 \times 10^{-5}$ moles per 1 g of solution was obviously (Figure 6.15 C) too low to introduce enough of the dye to produce a perceptible absorption. The sols were sprayed on quartz slides in order to realise higher film thicknesses as usually obtained in spin coating. 20 μm were a typical value for sprayed samples. The two other solvatochromes showed much better solubility in the coating fluids.



A. Absorption spectra of GG; GB, GA10, GAD coatings doped with ethyl-4-(methoxycarbonyl)pyridinium iodide.



B. Absorption spectra of GG; GB, GA10, GAD coatings doped with 4-methoxynitrobenzene.



C. Absorption spectra of GG; GB, GA10 coatings doped with 4-(2,4,6-triphenylpyridinium)-2,6-diphenylphenoxide.

Figure 6.15. Absorption spectra of GG, GB, GA10, GAD coatings doped with solvatochromes: ethyl-4-(methoxycarbonyl)pyridinium iodide (A.), 4-methoxynitrobenzene (B.) and 4-(2,4,6-triphenylpyridinium)-2,6-diphenylphenoxide (C.).

Unfortunately, hardly interpretable information was obtained. On one hand, when probed with ethyl-4-(methoxycarbonyl)pyridinium iodide (Figure 6.15 A), matrix GA10, with its first absorption maximum being around 325 nm appeared to be the least polar. The GB system appeared to be a bit more polar, while the GAD matrix appeared to be the most polar, even more than the GG material according to the absorption data. On the other hand, the spectra for coatings doped with 4-methoxynitrobenzene, a positively solvatochromic dye, showed the shortest wavelength absorption for the GA10 film (least polar). The GB matrix appeared to be

the most polar one, whereas the GAD matrix should be more polar than the GG matrix according to absorption spectra of 4-methoxynitrobenzene (Figure 6.15 B). Interestingly, in both cases the GA10 matrix can be characterised to be the least polar. The GAD matrix, which was by far the least polar one according to contact angle measurements, belongs to the more polar materials according to the absorption spectra of incorporated solvatochromic dyes.

Remarkably, the absorption spectra of GB matrix doped with solvatochromes showed more than one maximum. The same was observed for the GG system, but only in the case of samples doped with ethyl-4-(methoxycarbonyl)pyridinium iodide (Figure 6.15 A and B). That phenomena might suggest that the solvatochromes were immobilised within different microenvironments. If photochromes would also be entrapped in free volume of different polarity, different kinetics depending on the surrounding milieu would be expected. Nothing like this was observed in the present work (see paragraph No. 6.3 Kinetics), however, more detailed investigations are considered to be necessary in order to get full information about polarity of the used hybrid materials.

It was assumed that a possible reason for the inconsistency could be residual amounts of solvents or water within the ready-to-apply system, that might influence directly the solvatochromes entrapped within matrix free volume. To verify that possibility, the water amount was determined by means of the Karl-Fischer titration (Table 6.5).

Table 6.5. The amount of water in ready-to-apply coating solutions of four matrix systems (Karl-Fischer titration).

	[%]
GAD	1.13 +/-0.01
GA10	1.19 +/-0.2
GB	0.66 +/-0.01
GG	0.00

The residual water concentrations were found to be very low for all four systems. Therefore, it is considered unlikely that this was the reason for the observed differences between polarity data determined by contact angle and by use of solvatochromes.

6.2 Entrapment of photochromic dyes – coloration and photo fatigue

The photochromic activity of the dyes and their photo fatigue not only depend on the dye itself, but also on the properties of solvent or host material in which they are situated. The polarity of the carrier substance, its free volume, rigidity, presence of impurities or some reactive chemical groups such as OH- or carboxylic moieties do change the photochromic kinetics. The characterisation of dye microenvironments and their optimisation to achieve the highest possible photostability and photocolourability was one main goal of this work. To find proper matrix-dye combinations many different systems (Table 6.6 and Figure 5.1) were investigated.

Table 6.6. Photochromes used at this work.

Dye	also called:
1,3-dihydro-1,3,3-trimethylspiro[2H]-indolino-2,3'-[3H]naphth[2,1-b][1,4]oxazine	Blue A; BA
silylated 1,3-dihydro-1,3,3-trimethylspiro[2H]-indolino-2,3'-[3H]naphth[2,1-b][1,4]oxazine	graftable Blue A; GBA
1,1,2,4,7-pentamethylspiro-[isoindolino-naphthoxazine]	Blue C; BC
silylated 1,1,2,4,7-pentamethylspiro-[isoindolino-naphthoxazine]	graftable Blue C; GBC
1,3,3,5,6-pentamethylspiro-[indolino-naphthoxazine]	Blue D, BD
silylated 1,3,3,5,6-pentamethylspiro-[indolino-naphthoxazine]	graftable Blue D, GBD
5'-morpholino-1,3,3-trimethyl substituted spiro-indolinoxazine	Red PNO
3,3-diphenyl-3H-naphtho[2,1-b]pyran	Photo L; PhL
silylated 3,3-diphenyl-3H-naphtho[2,1-b]pyran	graftable Photo L; GPhL
red-switching chromene with proprietary structure	WW

Also, commercially available dyes (Ruby, Midnight Grey and Misty Grey) from Robinson Co., UK were tested concerning their compatibility with host materials used in this work.

The dyes were incorporated via two different routes, depending on their chemical character. Photochromes without trialkoxysilyl functionalities were added to ready-to-apply coating solutions, that is to say as additives (Figure 6.16). Those with trialkoxysilyl functions (and the chromene WW containing a hydroxy ethyl group) were added to prehydrolysed (organo)siloxane solutions, usually prepared from GLYMO. In this way, the graftable dyes were allowed to hydrolyse and bond covalently to the polysiloxane network. The principle is demonstrated in Figure 6.16.

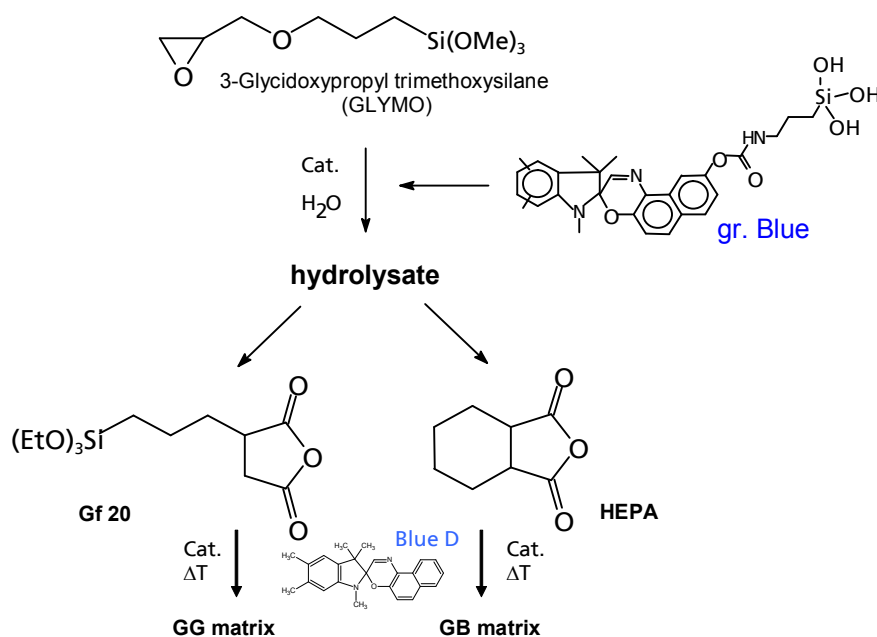


Figure 6.16. Incorporation pattern for non silylated and silylated dyes, e.g.: synthesis scheme of GG and GB matrices doped with Blue D and graftable Blue D.

Dye colorability and photostability after prolonged Suntest irradiation were the first line selection criteria. Initially, all dyes were tested in the **GG** system that seemed to be the most suitable matrix. Concentrations of 1 wt% and 3 wt% were chosen (calculated with respect to the solids content of the coating solutions). For all samples the spectral transmittance (τ , transmittance at a given wavelength) and the

luminous transmittance (Y) were determined. The luminous transmittance is an integrated transmittance parameter corrected to the human eye's response to solar light. It is often used in ophthalmology and for the characterisation of photochromic articles (lenses):

$$Y [\%] = 100 \times \frac{\int_{380 \text{ nm}}^{780 \text{ nm}} \tau(\lambda) \cdot V(\lambda) \cdot S_{D65\lambda}(\lambda) \cdot d\lambda}{\int_{380 \text{ nm}}^{780 \text{ nm}} V(\lambda) \cdot S_{D65\lambda}(\lambda) \cdot d\lambda}$$

where $\tau(\lambda)$ is the spectral transmittance of the tinted spectacle lens;

$V(\lambda)$ is the spectral luminous efficiency function for dye light (ISO/CIE 10527);

$S_{D65\lambda}(\lambda)$ is the spectral distribution of radiation of CIE standard illuminant D65 (ISO/CIE 10526).

The UV irradiation time span resulting in a loss of 50 % of the photochromic activity (half life time, $T_{50\%}$) was also evaluated for samples with promising photo fatigue resistance. Before activity measurements the bleach back procedure was applied (see paragraph No. 5.1 Measurements and methods). As an exception, in the case of Blue A doped coatings, the extremely low coloration depth and extraordinarily fast (see paragraph No. 6.3 Kinetics) bleach back reaction makes the achieved results questionable.

In the following, colorimetric results obtained from unweathered coatings (initial state) and from such weathered in a Suntest device will be discussed. Luminous transmittance changes ΔY will be referred to as “photochromic activity” or “colorability”. Coatings with y % of dye Z based on matrix X shall be termed as [X / y % Z].

6.2.1. Dyes physically incorporated within GG and GB matrices

Red PNO ($\lambda_{\text{max}} = 590 \text{ nm}$) and **Photo L** ($\lambda_{\text{max}} = 430 \text{ nm}$) showed very poor photocolourability even if unweathered. Luminous transmittance changes ΔY_0 of about 5 % and about 15 % for **[GG / 3 % Photo L]** and **[GG / 1 % Red PNO]**, respectively,

were measured. After 2 h of Suntest they completely lost their photochromic properties showing a residual ΔY_{2h} of lower than 1 %.

A similar behaviour was found for **Blue C** ($\lambda_{max} = 620 \text{ nm}$) within the **GG** matrix, whereby the initial colorability was much higher, with ΔY_0 values of over 16 % and about 40 % for concentrations of 1 % and 3 %, respectively. Nonetheless, again after 2 h of Suntest irradiation there was no significant photochromic activity left. To be sure that the observed very low photo fatigue resistance was not provoked by the chosen matrix, also matrix **GB** was investigated. In that case the colorability of unirradiated samples was even worse: for **[GB / 1 % PNO]** a ΔY_0 of about 9 % was found, **[GB / 3 % Photo L]** and **[GG / 1 % Photo L]** showed a coloration of $\Delta Y_0 = 5 \%$ and about 3 %, respectively. For **[GB / 1 % Blue C]** and **[GB / 3 % Blue C]** coatings ΔY_0 was 8 % and over 20%, respectively. For all samples the photochromic activity after 2 h of Suntest was lower than 1 %.

Blue A ($\lambda_{max} = 610 \text{ nm}$) was also tested in both matrices at 1 % and 3 % concentrations. The very low initial activity, i.e., a ΔY_0 of about 1.5 % and over 3 % for samples with 1 % and 3 % dye, respectively, within the GG matrix, (and even less in the GB matrix) made that dye uninteresting for further investigations. However, its photostability was better than for the three dyes mentioned above. Even after 6 h of irradiation the photochromic activity seemed to be unchanged.

Blue D was found to have a better coloration than Blue A: for **GG** coatings doped with 3 % dye ΔY_0 was about 14 % and for a concentration of 1 % more than 7 % were found. For **GB** samples the coloration was similar: Incorporation of 1 % and 3 % of Blue D resulted in ΔY_0 values of about 5 % and more than 16 %, respectively. After 12 hours in the Suntest the photochromic activity of **[GB / 1 % Blue D]** was completely lost (ΔY_{12} below 1 %). Samples doped with 3 % of dye achieved that level after 16 hours, as did GG samples doped with 1 % of Blue D. After 24 hours of irradiation **[GG / 3 % Blue D]** coatings were inactive with a ΔY_{24} below 4 %.

It can be concluded that the fatigue resistance of physically doped materials, that have been irradiated directly, was by far too low to be of interest for ophthalmic applications.

6.2.2. Dyes chemically incorporated within GG and GB matrices

The dyes WW ($\lambda_{\max} = 510$ nm), gr. Blue D ($\lambda_{\max} = 620$ nm), gr. Blue A ($\lambda_{\max} = 610$ nm), gr. Photo L ($\lambda_{\max} = 430$ nm), and gr. Blue C ($\lambda_{\max} = 610$ nm with a shoulder at about 410 nm) were introduced in the coating solution already during the synthesis (see Figure 6.16) in order to allow for their capability to co-hydrolyse with the polysiloxane precursors. Due to its hydroxyethyl substituent, which is able to participate in the sol-gel reaction and hydrogen bonding, the chromene WW is also treated as a graftable dye. Chromophore concentrations of 1 % and 3 % of weight were used with respect to the solids of the coating solution. The mass of silylated side chain was not taken into account in the mass calculations, in order to make sure that identical chromophore concentrations were realised for physically incorporated dyes and their silylated analogs.

Graftable Photo L doped coatings were characterised by relatively low coloration depth. For the **[GG / 1 % gr. Photo L]** and **[GB / 1 % gr. Photo L]** samples the photochromic activity was only about 5 %. In the case of **[GG / 3 % gr. Photo L]** and **[GB / 3 % gr. Photo L]** coatings ΔY_0 values of about 15 % and 10 %, respectively, were found. However, in that latter case strong colour change was perceptible because of low spectral transmittance at the maximum of the dye absorption. **GB** based samples have no more photochromic activity left after 4 hours of suntesting. GG samples doped with gr. Photo L are more stable; coatings containing 1 % of dye are degraded after 8 hours, which for 3 % samples did not occur before 16 hours.

Photochromic activities of 25 % and 20 % were measured for **[GG / 3 % gr. Blue A]** and **[GB / 3 % gr. Blue A]** coatings, respectively. Irradiation in the Suntest led to the loss of their photochromic activity after 28 and 32 hours for the GB based ($T_{50\%} = 20$ h) and GG based samples ($T_{50\%} = 12$ h), respectively.

The red chromene **WW** was also tested for its colorability and photo fatigue within **GG** and **GB** matrices. The dye (3 %) showed poor coloration, with a ΔY_0 of about 6 % and poor stability in GB matrix samples that were found to have no more photochromic activity after 4 hours of irradiation. When the dye was entrapped in the GG matrix (3 %) a much higher photochromic activity and stability was found. An initial ΔY_0 value of 45 % was observed producing a deep red tint, that completely disappeared after 24 hours irradiation ($T_{50\%} = 9$ h).

Excellent colorability characterises **graftable Blue C**. For samples based on the **GG** matrix system, ΔY_0 values of about 20 % and 37 % were measured for 1 % and 3 % dye concentrations. The photochromic activity amounted to more than 32 % for 1 % **GB** coatings and reached $\Delta Y_0 = 50$ % for 3 % samples. Unfortunately, gr. Blue C turned out to be fairly unstable in the weathering experiments. All four compositions completely lost their photochromic response after 4 hours of irradiation.

Graftable Blue D at 1 % concentration within a **GG** coating showed a photochromic activity of about 25 %, whereas for a [**GB / 1 % gr. Blue D**] sample only about 18 % were measured. In the case of 3 % concentration the photochromic activity of gr. Blue D was much higher: **GG** and **GB** coatings showed ΔY_0 values of 38 % and 30 %, respectively. UV light irradiation decreased the photoactivity also in this case. [**GB / 1 % gr. Blue D**] samples showed no more photochromic activity after 32 hours of irradiation. The corresponding 3 % samples were inactivated after 40 hours ($T_{50\%} = 24$ h). GG based coatings doped with gr. Blue D seemed to be most UV stable system. They completely lost their photochromism only after 40 h ($T_{50\%} = 20$ h, 1 % of dye) and 68 h ($T_{50\%} = 32$ h, 3 % of dye).

GA10 and **GAD** matrix systems were also included in the dye-matrix compatibility investigations. In this series only concentrations of 3 % of dye were employed. It is obvious from the aforementioned GG and GB matrix investigation that coatings doped with 1 % have poorer colorability and stability. The GA10 coating sol comprises 10 mol% of 3-aminopropyltriethoxysilane, calculated with respect to a total of 100 % of silanes and crosslinkers. Also variations with 5 mol% (GA5) and 15 mol% (GA15) were tested. Unfortunately, extreme short gelation times made processing of the GA15 system impossible. GA5 based coatings doped with 3 % of Blue D or gr. Blue D are less stable than GA10 based ones; they lost half of their photochromic activity much earlier: $T_{50\%}^{GA5} = 20$ h and $T_{50\%}^{GA5} = 24$ h in case of Blue D and gr. Blue D, respectively. Thus, for the further investigation it was focused on the GA10 matrix system.

6.2.3 Dyes physically incorporated within GA10 and GAD

The **Red PNO-GA10** formulation had almost no coloration in the unweathered state ($\Delta Y_0 = 1\%$). Therefore, its photo fatigue was not assessed. The colorability of **Red PNO** within the **GAD** matrix is better, although only 5% were achieved. Coatings based on the GAD system with 3% of Red PNO or **Photo L** ($\Delta Y_0^{\text{GAD}} = 3\%$) lost their activity after 6 hours of Suntest (possibly already earlier, due to the duration of the first weathering period). The stability of **Photo L** is not any better within the **GA10** system. It lost its photochromic properties after 4 hours of irradiation. Additionally, it showed a low coloration of about 3% in unweathered samples.

Blue C did not exhibit good photo fatigue resistance within the **GA10** (ΔY_0^{GA10} approx. 13%) nor within the **GAD** (ΔY_0^{GAD} approx. 15%) matrix. After 4 hours of irradiation the photochromic activity of the investigated coatings was completely destroyed.

The stability of samples doped with **Blue A** was only slightly better. They lost their activity after 8 h Suntest in the **GA10** system, whereas samples based on the **GAD** system lost their activity only after 16 h. However, the extreme low ΔY_0 value (about 1 – 2%) and a comparably fast (see paragraph 6.3 Kinetics) bleach back reaction makes the achieved results unreliable.

GAD-Blue D coating formulations led to a photochromic activity of about 11%. For the GAD matrix system $T_{50\%}$ was about 8 h, and after 18 hours of UV light irradiation there was no more photochromic activity observed. The **GA10** matrix system seemed to be particularly suitable for **Blue D**. Coatings doped with 3% of the dye ($\Delta Y_0 = 15\%$) lost half of their initial activity after $T_{50\%} = 24$ h.

6.2.4. Dyes chemically incorporated within GA10 and GAD

The red chromene **WW** showed low activity and poor stability within the **GA10** ($\Delta Y_0^{\text{GA10}} = 5\%$) and **GAD** ($\Delta Y_0^{\text{GAD}} = 5\%$) systems. After 6 hours of UV irradiation there was no photochromic coloration left.

The **GA10-gr. Blue D** formulation led to coatings with relatively high photochromic activity with a ΔY_0 value of about 32%. **GAD** based coatings showed an even stronger luminous transmittance change, i.e., more than 38% at the same dye concentration. **GA10** and **GAD** matrix coatings doped with 3% of **gr. Blue D** were

very stable. They still possessed over 60 % and 75 % of their initial ΔY_0 , respectively, after 32 hours in the Suntest. For both the **GA10** and **GAD** systems $T_{50\%}$ was reached after 38 hours of exposure.

Gr. Blue A retains over 75 % of its initial ΔY_0 value in **GA10** based coatings, with an initial activity of 14 %. $T_{50\%}$ was reached after 44 hours of irradiation.

The **GA10** based sample doped with **gr. Photo L** showed an initial luminous transmittance change of about 10 %, however, during the first 4 hours of UV irradiation it completely lost its photochromic properties.

It was found that the **photochromic colorability** strongly depends on the way of incorporation into the matrix. Silylated dyes (covalently grafted) are characterised by much higher luminous/spectral transmittance changes than the analogous

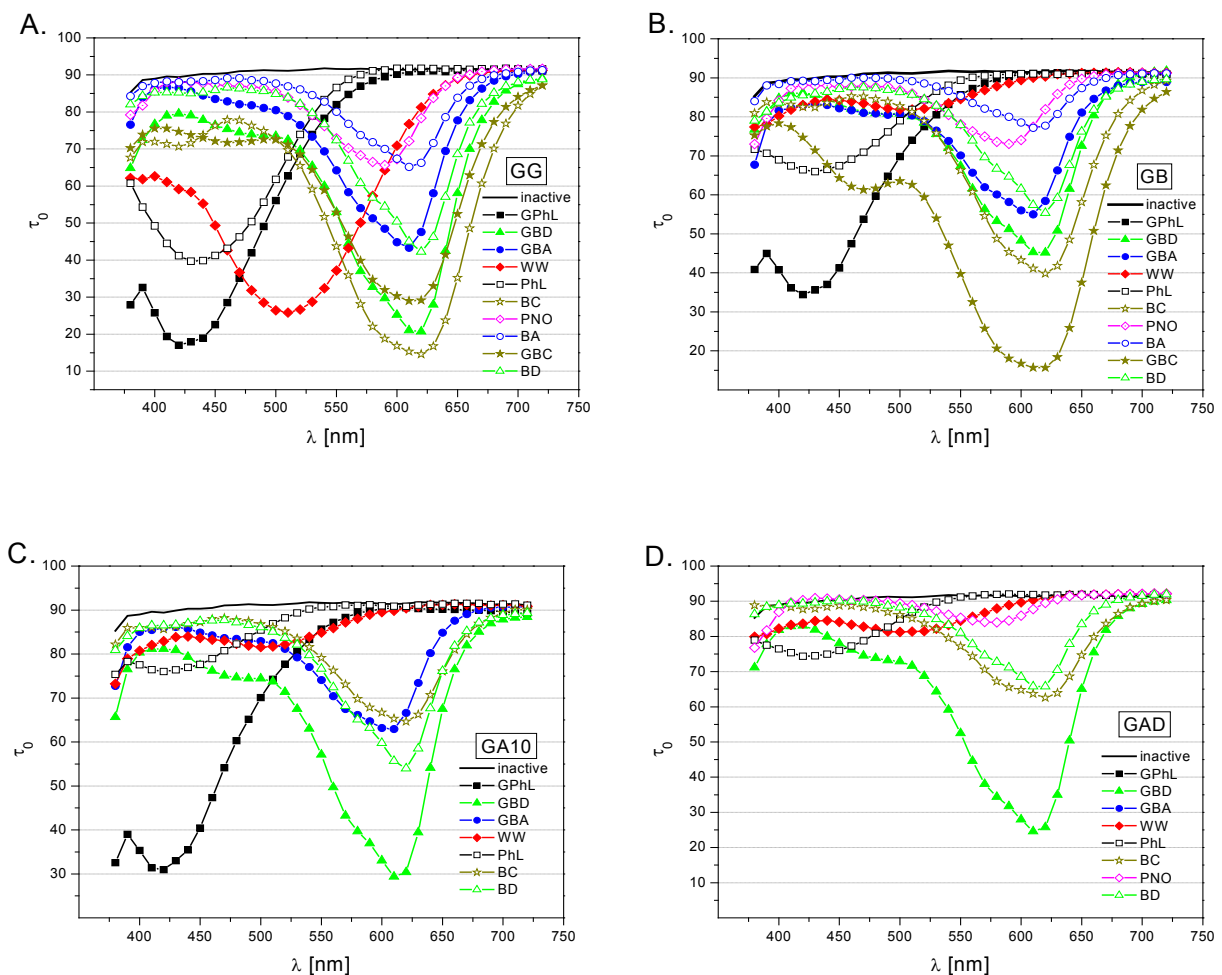


Figure 6.17. Initial photochromic colorability of coatings doped with photochromic dyes (Blue A, Blue C, Blue D, Photo L, PNO, WW, gr, Photo L, gr. Blue A and gr. Blue D – in a concentration of 3 %) based on **A. GG**, **B. GB**, **C. GA10** and **D. GAD** matrix systems.

physically incorporated species. This phenomenon could be observed particularly well in the case of Blue A and gr. Blue A: the physically incorporated dye exhibited an extremely poor coloration in GB, GA10 and GAD matrices, while the silylated species showed high photochromic activity in all of them. The difference in the coloration depth is also marked for other non-graftable/graftable dye pairs (Figure 6.17).

Besides, the host material properties affect the photochromic response, which is due to the interaction of the matrix free volume with the closed or open molecular forms of the dyes. The formation of zwitterionic open merocyanines is favoured in a more polar matrix, which can be observed when comparing GG and GB matrices (Figure 6.17 A and B). Free volume with a non-acidic environment favours the closed forms leading to a lower coloration within GA10 and GAD matrices (Figure 6.17 C and D). This phenomenon can distinctly be seen for the spirooxazine Blue A, the substituted spirooxazine Red PNO and the chromene WW, that showed very poor colorability or even a lack of it in non-acidic matrix compositions.

The Photo fatigue behaviour of photochromic dyes within different matrix systems was investigated after prolonged UV irradiation (Figure 6.18). Obviously,

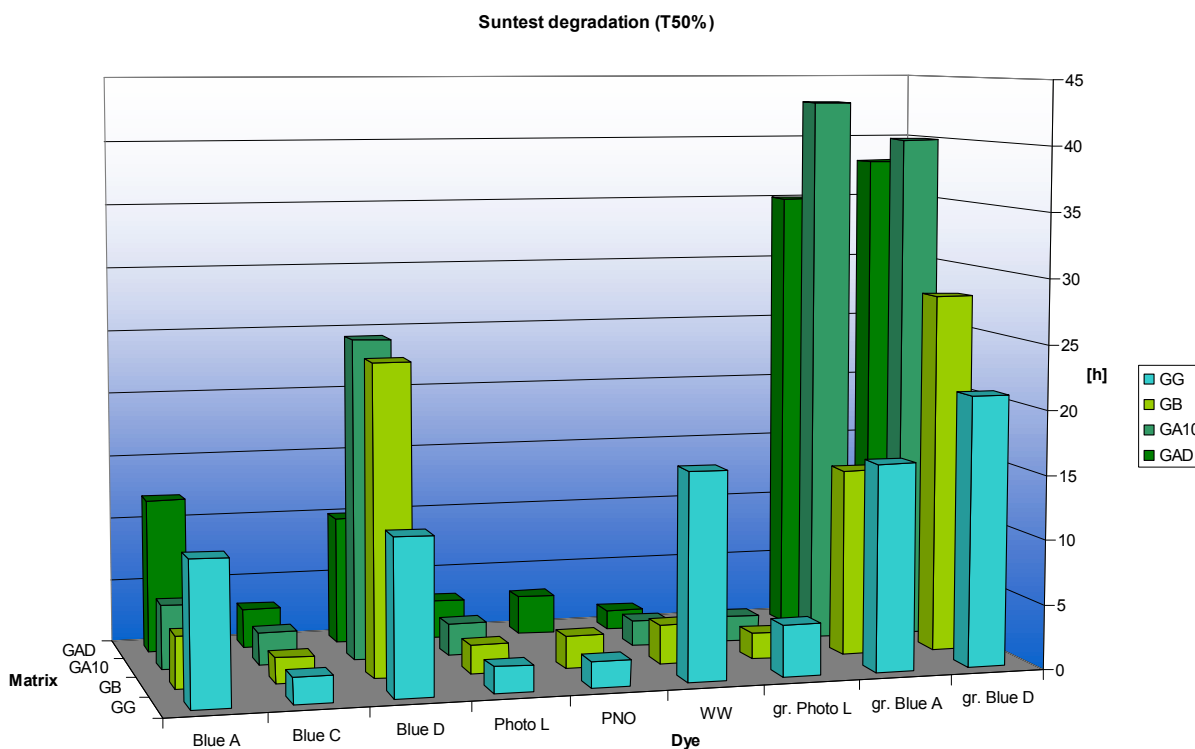


Figure 6.18. Photodegradation of photochromic coatings (Blue A, Blue C, Blue D, Photo L, PNO, WW, gr, Photo L, gr. Blue A and gr. Blue D – concentration of 3 %) based on GG, GB, GA10 and GAD matrix systems after prolonged UV light irradiation, T50% - time needed for a loss of 50 % of the initial photochromic activity.

methylation of the indoline moiety of the spirooxazine increased the stability of the photochrome as was observed for Blue D and Blue A. The spiro-isoindoline (Blue C) was found to be extremely unstable. Substitution on the naphthooxazine moiety (PNO), which caused a hypsochromic shift of the absorption maximum, led to a significant decrease of the photostability. Chromenes (Photo L, gr. Photo L, WW) were characterised by strong photo fatigue, with the GG system (rigid) appearing to be the most suitable matrix for these compounds. A significant advantage of silylated dyes can be derived directly from prolonged UV irradiation testing (Figure 6.18).

The stability of grafted species was increased by a factor of 2 or more compared with that of physically entrapped ones. It is assumed that grafting prevented (or at least hindered) aggregation, crystallisation or diffusion processes, even if the dye was incorporated in concentrations up to 10 %, which is not possible for unsilylated dyes [167]. At higher concentrations, usually softening of the coatings occurs, as well as aggregation and blooming. The physical properties of the coatings with grafted dyes, however, were very similar to those of the pure host material [118]. Moreover, immobilisation of molecules minimises the probability of a contact with degradation products or impurities.

Matrix factors also influenced the photostability of photochromes. Providing the direct environment for the photochromophores, the host material characteristics were found to be extremely important for the dye degradation behaviour. A rigid matrix with many carboxylic sites (GG) was a suitable system for the chromenes. In the case of spirooxazines the less acidic and softer matrices (GA10, GAD) were more adequate, which is probably associated with a faster bleach back reaction. Non-acidic materials are not compatible with the spirooxazine merocyanines, which is believed to be the species predominantly attacked by active oxygen or OH- groups during irradiation.

Besides the main objective of this work to develop stabilisation concepts for photochromic coatings, a side aspect was to create neutral tint photochromic films with high coloration. This would require one dye that strongly absorbs in the whole visible range or a mixture of dyes that each absorb in another part of the visible spectrum. Taking both colorability and photochromic stability into consideration, it seems that Blue D and gr. Blue D are the most promising blue-switching dyes. The red chromene WW can be also considered as a stable dye (showing good coloration

only within the GG matrix). The yellow-switching dyes were of extremely low stability and are not suitable for use in photochromic coatings for ophthalmic products.

6.2.5. Commercially available dyes

As a reference, besides the dyes provided by Great Lakes Chemical also some commercially available dyes were tested with respect to their colorability and photo fatigue in sol-gel derived spun poly(organo)siloxane coatings. The standard coating thickness was about 5 μm .

Reversacol® dyes (Robinson Co., UK) are members of the spironaphthooxazine and naphthopyran families. Three dyes were tested, i.e., Midnight Grey and Misty Grey, the grey tints of which cover most of the visible spectrum, and Ruby, a red-switching dye. The GG system was expected to be the most suitable matrix, because of its high compatibility with other spirooxazines and naphthopyrans. Coatings doped with 3 % of dye were spun on glass plates (Table 6.7) and their absorption spectra measured. MD and RB showed a quite good coloration depth with an initial photochromic activity of $\Delta Y_0 = 40\%$ (Figure 6.19 A), whereas MS' activity was only about $\Delta Y_0 = 10\%$ with no perceptible absorption maximum. A very pale grey tint was observed for that sample. The photo fatigue resistance of RB and MS was rather low.

Table 6.7. GG matrix system coatings on glass plates doped with Reversacol dyes.

Sample name	Reversacol dye	λ_{max} [nm]
GG-MD	Midnight Grey	580
GG-MS	Misty Grey	whole visible spectrum
GG-RB	Ruby	430 (530)

After only 5 hours of irradiation in the Suntest (Figure 6.19 B) they have lost more than 80 % of their initial colorability. The photochromic activity of MD doped layers dropped below 10 % within 10 hours in the Suntest.

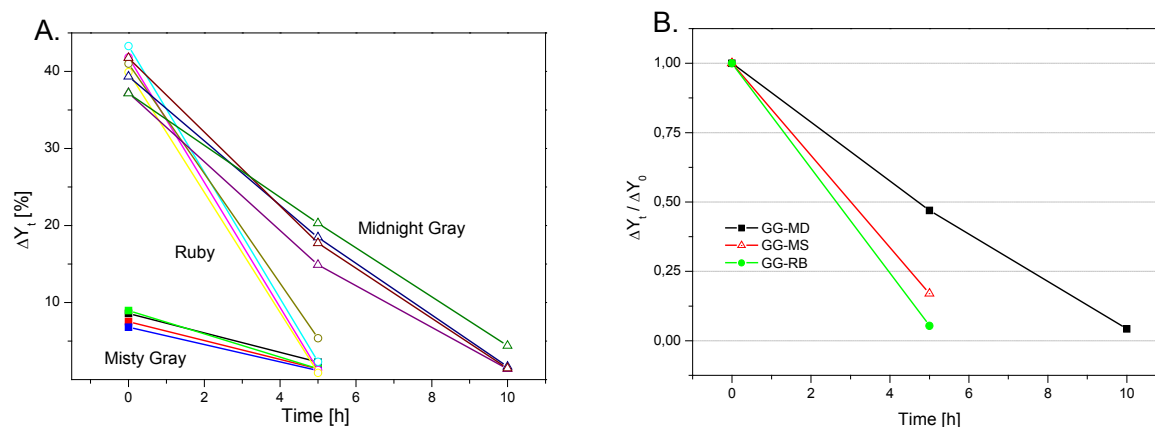


Figure 6.19. Photodegradation of Reversacol dyes: Midnight Grey, Misty Grey and Ruby after irradiation in the Suntest (A– absolute loss of photochromic activity, B – relative loss of photochromic activity after UV irradiation; for the labels meaning see Table 6.7).

As a second reference also dyes purchased from PPG Co. (USA) were tested for their colorability and photo fatigue within the GG matrix system. As for the Reversacol® dyes the coatings were doped with 3 % of dye (Table 6.8). The dyes 5-3 (B) and 33612 (D) had poor photochromic activity with approx. $\Delta Y_0 = 8 \%$ and $\Delta Y_0 = 15 \%$, respectively. For the dye 5-68 (A) the value reached about 30 %. Dye 5-83 (C) was found to have the best colorability of all PPG dyes with a ΔY_0 value of about 40 % (Figure 6.20 A). Sample GG-B showed no more photochromic activity after 4 hours of Suntest irradiation. At the same time the samples GG-A and GG-D lost over 75 % of their initial colorability. Only sample GG-C showed a relatively good photo fatigue rate: it lost 75 % of the initial photochromic activity after 16 hours of UV irradiation.

Table 6.8. GG matrix system coatings on glass plates doped with PPG dyes.

Sample name	PPG dye	λ_{\max} [nm]
GG-A	5-68	470
GG-B	5-3	435
GG-C	5-83	490
GG-D	33612	615

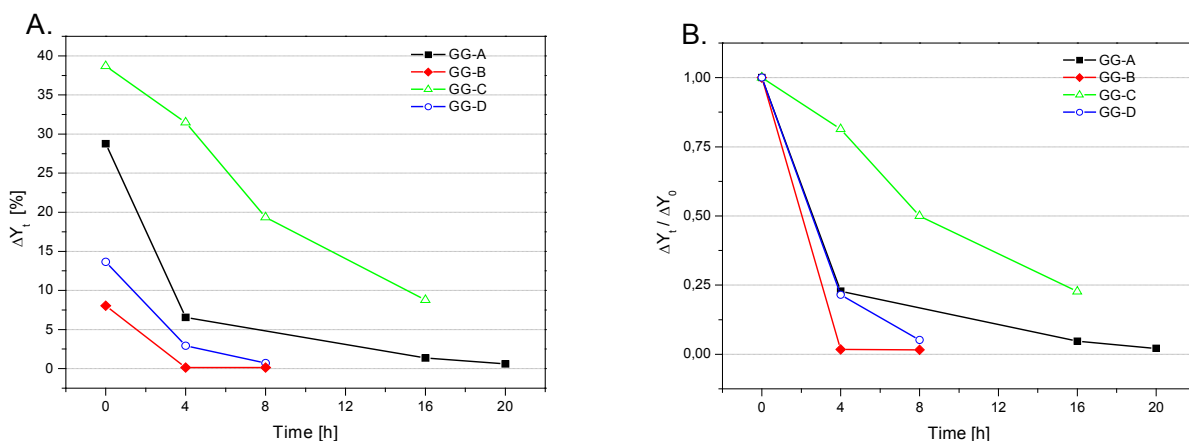


Figure 6.20. The degradation of PPG Co. dyes: 5-68, 5-3, 5-83, 33612 after irradiation in the Suntest (A. – absolute loss of photochromic activity, B. – relative loss of photochromic activity after UV irradiation, for the labels meaning see Table 6.8).

It was obvious that, at least in the investigated matrix system, commercially available dyes did not show better colorability or photo fatigue than the Variacrol® dyes primarily used in this work.

6.2.6. Alternative matrix systems

Besides the standard formulations GG, GB, GA10 and GAD also other matrix compositions were tested as hosts for photochromic dyes. Additionally, also physical properties such as adhesion or top coating ability (with other lacquers) were evaluated.

The GEB system's main components were GLYMO and ethyltriethoxysilane (ETES) in a molar ratio of 0.7 : 0.3. This matrix system was modified through the addition of fluorosilane components (e.g. tridecafluoro-1,1,2,2-tetrahydrooctyltriethoxysilane) to form matrix BIF. Such systems were expected to be suitable hosts for spirooxazine dyes since the fluoro component had been claimed to be particularly favourable for decreasing the photo fatigue of photochromic dyes [164-166].

Both, hardness and adhesion of coatings doped with 3 % of gr. Blue D, Blue D or gr. Blue A were registered (Table 6.9). The systems GEB and BIF were found to be

harder than other matrices, but their adhesion on glass and CR39® was not satisfactory.

Table 6.9. Microhardness and adhesion properties of photochromic coatings based on the GEB and BIF systems.

Matrix System	Dye	Hardness [N/mm ²] (+/-)	Adhesion (PC, CR39, glass)	Thickness [μm] (+/-)
GEB	Blue D, 3%	102.9 (3.96)	Gt4, Gt5, Gt 1	2.1 (0.13)
BIF	Blue D, 3%	152 (12.42)	Gt2, Gt2, Gt1	2.9 (0.12)
BIF	gr. Blue A, 3%	187 (12.03)	Gt0, Gt3, Gt2	13.3 (1.01)
BIF	gr. Blue D, 3%	200.9 (5.63)	Gt0, Gt4, Gt5	14.8 (0.1)

The photochromic activity of Blue D is lower in the BIF matrix than in the GEB system: approx. 20 % and 15 % were found, respectively. After prolonged irradiation in the Suntest, no positive influence of the fluoro component was observed: sample [BIF / 3 % Blue D] (with fluorocomponent) degrades almost as fast as [GEB / 3 % Blue D] (no fluorocomponent) (Figure 6.21 A).

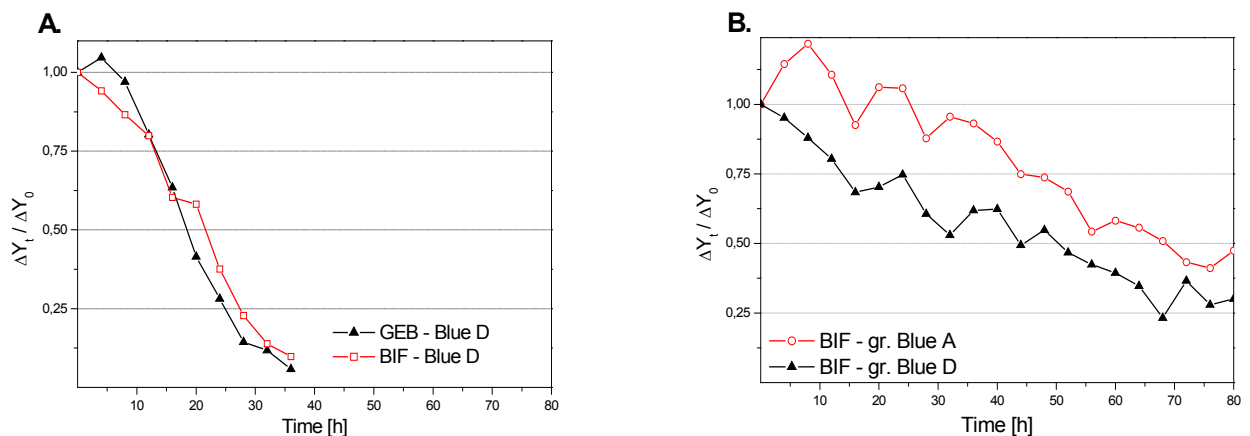


Figure 6.21. Degradation curve after prolonged UV irradiation of **A.** GEB and BIF based coatings doped with 3 % of Blue D and **B.** BIF coatings doped with 3 % of gr. Blue A and gr. Blue D.

Both, graftable Blue A and graftable Blue D were characterised by low colorability ($\Delta Y_0 = 11\%$ and $\Delta Y_0 = 14\%$, respectively) but high stability within the BIF matrix (Figure 6.21 B), where the high thickness (over $13\ \mu\text{m}$) of the layers is certainly considered to be an additional stabilisation factor. BIF based coatings showed some

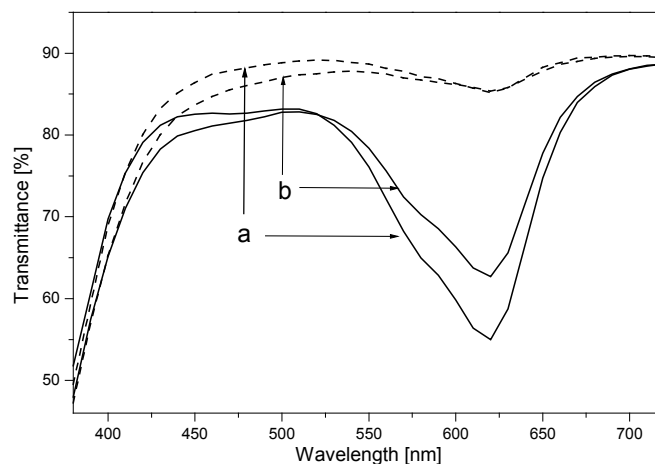


Figure 6.22. Transmittance spectra of gr. Blue D within BIF film: a. direct after preparation, b. after 24 h of UV irradiation; solid lines - activated states, dashed lines – non-activated states.

remaining coloration in the bleached state. In the absence of UV radiation some of the photochromophores were present in their merocyanine form and the coatings appeared coloured (Figure 6.22). Probably the high hardness (ca. $200\ \text{N}/\text{mm}^2$) hindered the mobility of the photochromes and prevented the complete back reaction. An unfadeable coloration of non-activated photochromic materials is a great disadvantage for practical use. Moreover, GEB/BIF systems were found to have short gelation times, which in practice aggravates processing.

Some alternatives to AMEO were taken into consideration, i.e., (aminoethylaminomethyl)phenylethyltrimethoxysilane (PHA), 3-(2-aminoethylamino) propylmethyltrimethoxysilane (ADA), and (N-methylaminopropyl)trimethoxysilane (MAT). However, the matrix systems GPHA, GADA and GMAT resulting therefrom showed extremely fast gelation, which again rendered the processing difficult. Consequently, the produced coatings had very poor optical quality and a rough surface, so that the evaluation of their thickness and hardness was not possible.

GADA and GMAT coatings showed a yellow discoloration and were therefore excluded from the further investigations. Thus, the photochromic activity of Blue D (3 %) was only investigated in GPHA. A photochromic activity of about 12 % and a degradation of 50 % after 20 hours of UV irradiation were comparable to standard matrix systems used in this work.

6.2.7. Other factors that influence coloration and photo fatigue

Photochromic activity and photo fatigue of organic photochromes are known to depend on both the dyes' properties and their environments, which in this work were hybrid sol-gel derived organopolysiloxanes. A good compatibility between both of them is a fundamental prerequisite, however, other factors may influence the coloration and stability of photochromic coatings as well.

Curing temperature and time influence the physical properties of the matrix system (see: paragraph No. 6.1.2. Matrix characterisation) as well as the photochromic characteristics of investigated coatings. GG- based samples doped with a mixture of 3 % of WW and 4 % of gr. Blue D were cured at different temperatures (between 100 °C and 225 °C) for variable periods of time (from 2 minutes to 40 minutes). The photoactivities of the incorporated dyes decreased with increasing curing temperature (Figure 6.23). It is assumed that the increasing connectivity and hence rigidity of the matrix hindered the photochromic reaction. However, the coloration depth of samples that were cured for only 2 minutes at 200 °C - 225 °C was comparable to that of samples cured at lower temperatures (100 °C - 125 °C) for longer times. Probably, the thermal degradation of dyes is responsible for the decrease in colorability. Short curing at high temperature led to hard coatings (see paragraph No. 6.1.2 Matrix characterisation) with good coloration depth. Unfortunately, the photo fatigue of such coatings ($T_{50\%} = 16$ h) was higher than found for samples cured at 100 °C - 125 °C ($T_{50\%} = 24$ h).

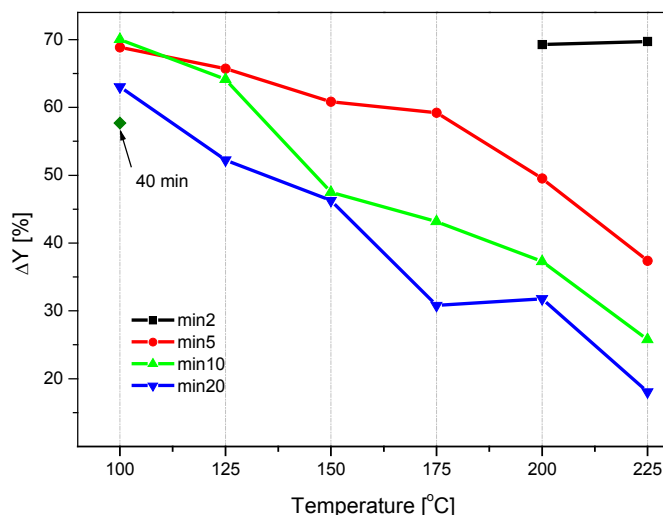


Figure 6.23. Photochromic activity of GG based coatings doped with a mixture of 3 % WW and 4 % gr. Blue D.

The **coating thickness** was also investigated as one of many possible factors that might have some influence on the photochromic activity and the rate of photodegradation. GG sols doped with 3 % of Blue D were spun on glass plates with variable numbers of revolutions per minute, in order to realise different thicknesses. As expected from the Lambert-Beer-law [107], the coating thickness and the coloration depth correlated (Table 6.10). However, the observed increase in ΔY_0 with increasing thickness was lower than the theoretically expected increase. It is assumed that some saturation was effectively present due to shielding of the incident UV radiation by activated chromophores in the top layer.

Table 6.10. Photochromic activity (ΔY_0) of [GG / 3 % Blue D] coatings with varied thickness (**d**).

d [μm]	3.65	4.63	4.67	5.19	5.38	5.7	6.14	6.61	8.06	10.5	10.72
	+/- 0.2	+/- 0.22	+/- 0.13	+/- 0.32	+/- 0.09	+/- 0.3	+/- 0.09	+/- 0.2	+/- 0.4	+/- 0.45	+/- 0.42
ΔY₀	28.58	27.03	27.63	29.37	26.44	29.19	28.82	33	34.31	36.12	37.74

Figure 6.24 shows the course of the photochromic activity loss upon Suntest irradiation with the coating thickness. According to the photo fatigue results of the test series mentioned above, one can assume that the thinnest layers are the least photostable (Figure 6.24). The thickness of the coatings is not expected to have an

influence on their microhardness, which could change the photochrome degradation rate, so potential differences in the dye stability must be related to the film thickness.

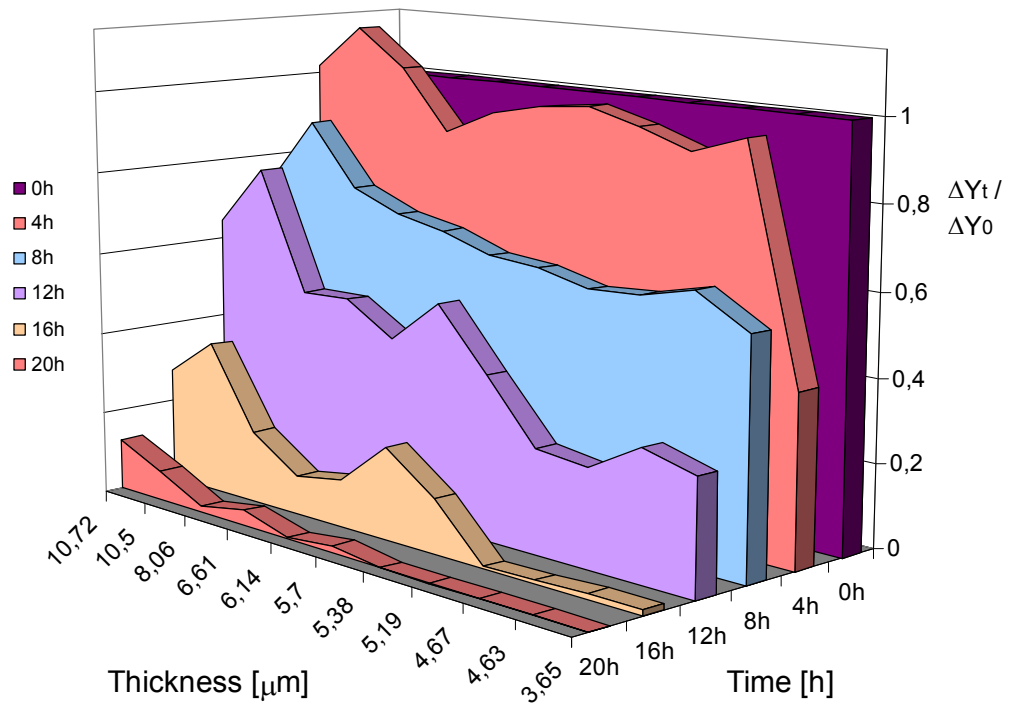


Figure 6.24. Degradation after prolonged UV irradiation (Suntest) for coatings of varied thickness.

A certain “depot-effect” may be effective as well. Activation and subsequent degradation of deeper located molecules would be possible only after deactivation of molecules situated at the very surface of the coating.

UV light source and irradiation periods could, probably being the main degradation factors, influence the photo fatigue behaviour of photochromes. Xenon lamps of the Suntest device imitate the spectrum of natural sunlight, involving besides visible light also short wavelengths down to 290 nm. Therefore, a QUV Weathering Tester with an emission maximum at 351 nm was additionally used to study the influence of the irradiation source on the degradation rate. Also irradiation periods of the Suntest experiments were varied. [GG / 3 % Blue D] and [GG / 3 % Photo L] coatings were exposed in the Suntest for 20 h, all at once and in 4 hours periods.

It was found that there were almost no differences in photodegradation behaviour of samples irradiated in the Suntest and those tested in the QUV device (Figure 6.25 A).

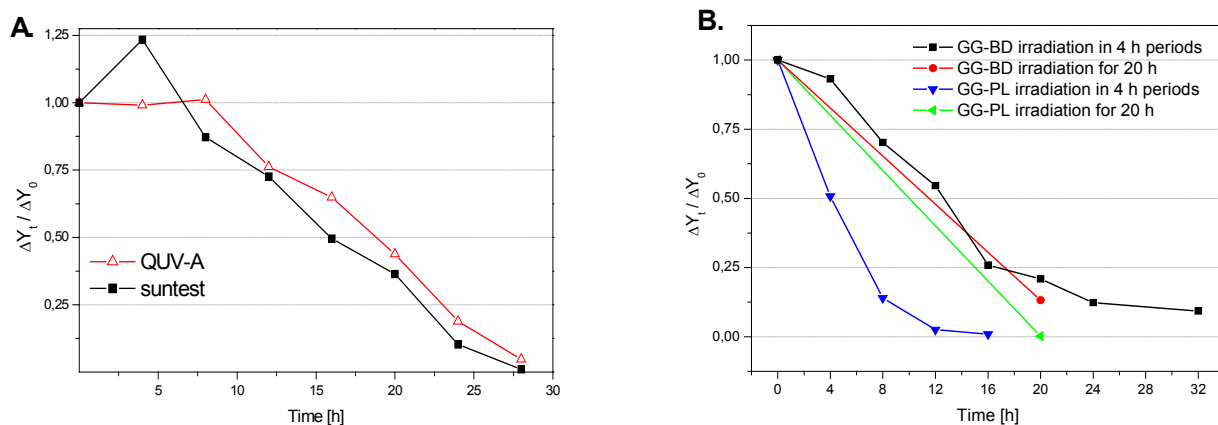


Figure 6.25. Influence of irradiation conditions on the degradation rate: **A.** Blue D doped GG coatings within Suntest and QUV Weathering Tester; **B.** Suntest irradiation of [GG / 3 % Blue D] and [GG / 3 % Photo L] coatings for 20 hours: all at once and in 4 hours periods.

Possibly the influence of the different wavelength distributions was compensated by the influence of temperature (not more than 40 °C in the case of Suntest, for QUV Tester about 52 °C), which causes a slightly faster degradation. Division of the irradiation time did not have any influence on the degradation rate, however “all at once” irradiation might have led to imprecise definition of sample life time as was obvious for the Photo L doped samples (Figure 6.25 B).

Coloration and stability of photochromes depend on many factors. The most important ones are the incorporation method and the matrix compatibility. Graftable dyes chemically bonded to organopolysiloxane backbones were about 10 times more degradation resistant than their unsilylated analogues. As can be seen for example for the WW dye (very good coloration and stability only in the GG matrix) the host material system has to be tailored according to the dye properties. Some matrix compositions were rather unsuitable in terms of processing. Gentle reaction and curing conditions were favourable for good photochromic performance.

6.3 Kinetics

A photochromic “on/off” reaction caused by UV light can be reversed thermally in the case of SO and chromenes. The rate of the reversion is controlled by a number of factors, one of the most important being the matrix or liquid solution in which the photochromic organic molecule is dissolved. The polarity of the medium seems to have a decisive influence [95].

The newly developed coatings are mainly tailored for a use in sun protection eyewear. In this context the kinetics of the colour change is very important. Too fast coloration or decoloration cannot be resolved by the human eye; too slow responses can be a handicap when rapid changes of ambient light conditions occur e.g.: on moving from outdoor to indoor.

For the investigation of the switching kinetics coated glass samples were irradiated “in situ” in the measurement chamber of a colorimeter by means of a UV lamp (HBO 200 W Hg lamp) (Figure 6.26).

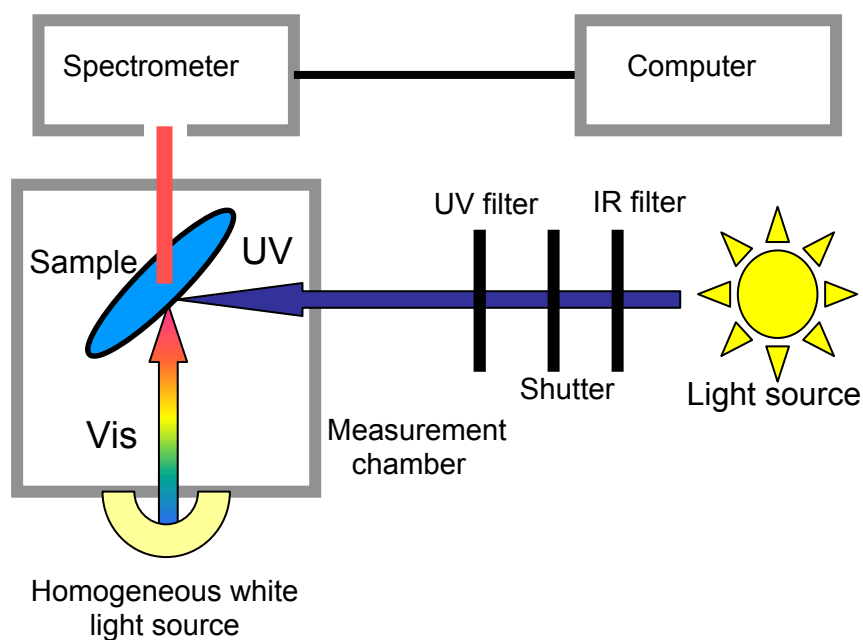


Figure 6.26. The “in situ” kinetics measurement set up.

A spin coated glass microscope slide was placed with an angle of 45° in the measurement chamber, so that the UV beam did not interfere with the white light beam in the spectrometer. The IR water filter cut off the thermal IR fraction of the Hg emission. A UV filter was inserted in order to exclude very short wavelengths, i.e. UV radiation that is not common in the natural sunlight spectrum. The change in luminous transmittance was determined in intervals of 2 seconds during activation as

well as during bleaching. Besides dyes prepared by Great Lakes Chemical, commercially available dyes from Robinson company (Reversacol®) were also investigated as references.

The kinetics of the thermal back reaction in solution is of first order, whereas the reaction in amorphous solids deviates from first-order kinetics. The rate constant of the bleach back reaction in solution increases with temperature and is generally larger in polar solvents than in nonpolar solvents [163].

Generally, the dyes showed slower reactions when entrapped in hybrid polymers as compared to corresponding solutions in organic solvents (Table 6.11). This was particularly evident for the bleaching processes. Nonetheless, the differences were rather small and indicated a high degree of mobility for the incorporated chromophores.

Table 6.11. Half life times for sample coloration and decoloration (t_a - activation time, needed for achieving 50 % of maximum absorption; t_f – fading time; both in seconds); physically entrapped dyes in various matrices and solvents.

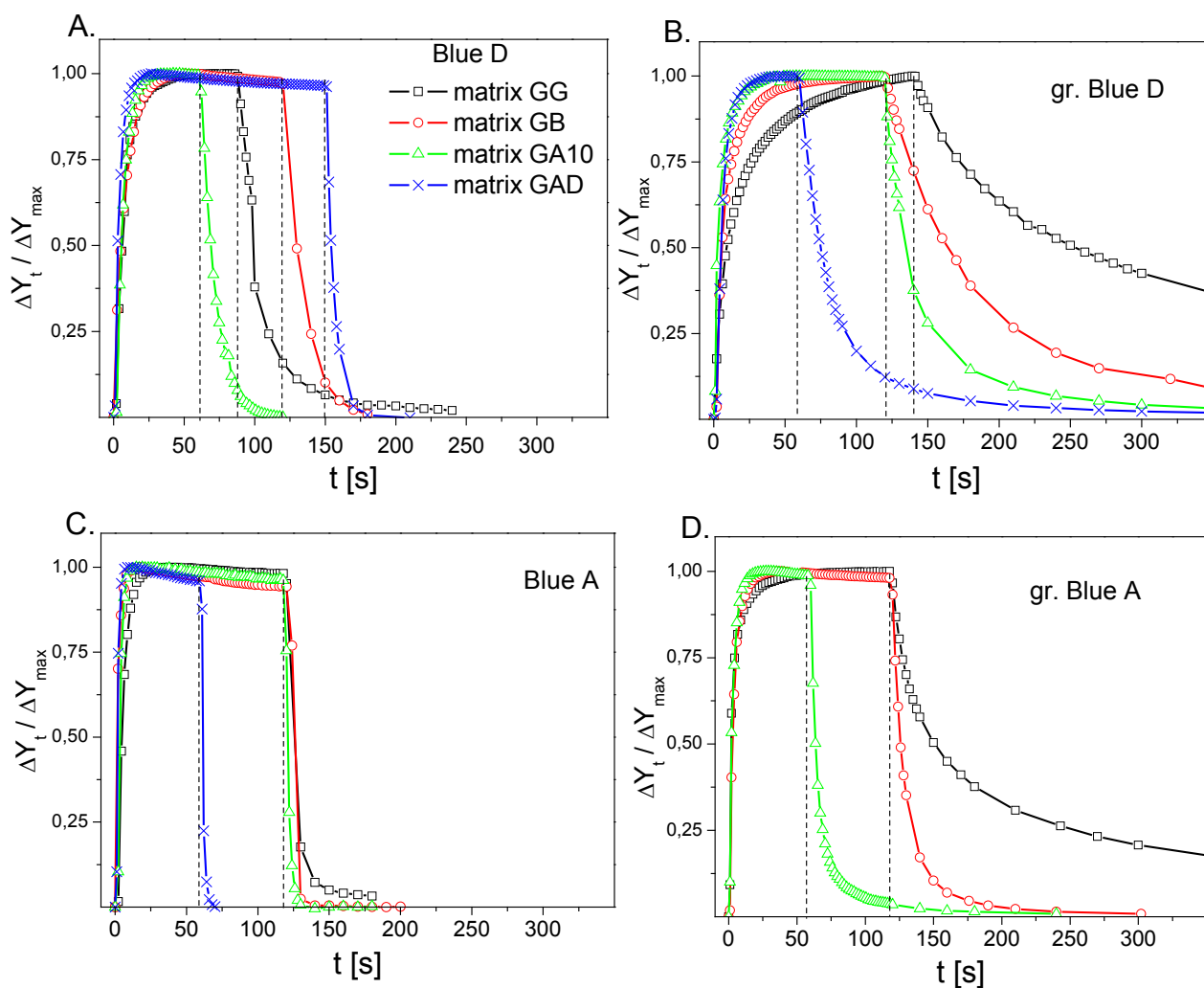
	GG		GB		GA10		GAD		MeOH [72]		hexane [72]	
	t_a	t_f	t_a	t_f	t_a	t_f	t_a	t_f	t_a	t_f	t_a	t_f
Blue A	4.7	5.8	1.4	6.2	3.4	3.2	1.7	2.6	2	1	3	4
Blue C	20.5	93.6	10.3	63	14.7	28.6	9	23.9	---	---	---	---
Blue D	6.2	9	5.3	9.6	5.5	8.9	2.9	4.2	6	12	4	4
PNO	3.9	2.8	3.7	5.2	4.1	1.8	2.2	2.2	2	1	2	>24
Photo L	5.5	10	7.4	9.1	3.9	7.5	3.8	5	6	11	5	12

Table 6.12. Half life times for sample coloration and decoloration (t_a - activation time, needed for achieving 50 % of maximum absorption; t_f – fading time; both in seconds); covalently bonded dyes in different matrices.

	GG		GB		GA10		GAD	
	t_a	t_f	t_a	t_f	t_a	t_f	t_a	t_f
gr. Blue A	1.8	33	2.8	8	1.9	5.5		
gr. Blue D	9.01	113.4	5.8	44.3	2.7	14.8	5	15
gr. Photo L	5.4	31.7	5.3	11.5	1.5	10.6		
WW	7.5	129.1	4.8	57	5.8	26.6	---	---

It was evident that a covalent bonding of the dye in the matrix noticeably slows down the “off - reaction“, probably due to sterical hindrance and the restricted mobility of the chromophore, i.e., restricted ability to re-orientate within the free volume of the matrix (Table 6.12).

Fast on- and off- kinetics were observed in particular when the dye was physically entrapped in softer host materials. The determined bleaching curves could be mathematically fitted by means of a second order exponential decay function (Figure 6.27 A-J). Indications of complex kinetics, which would be expected for a material having domains of different polarity (see paragraph No. 6.1.3 Polarity of hybrid polymer materials), could not be found.



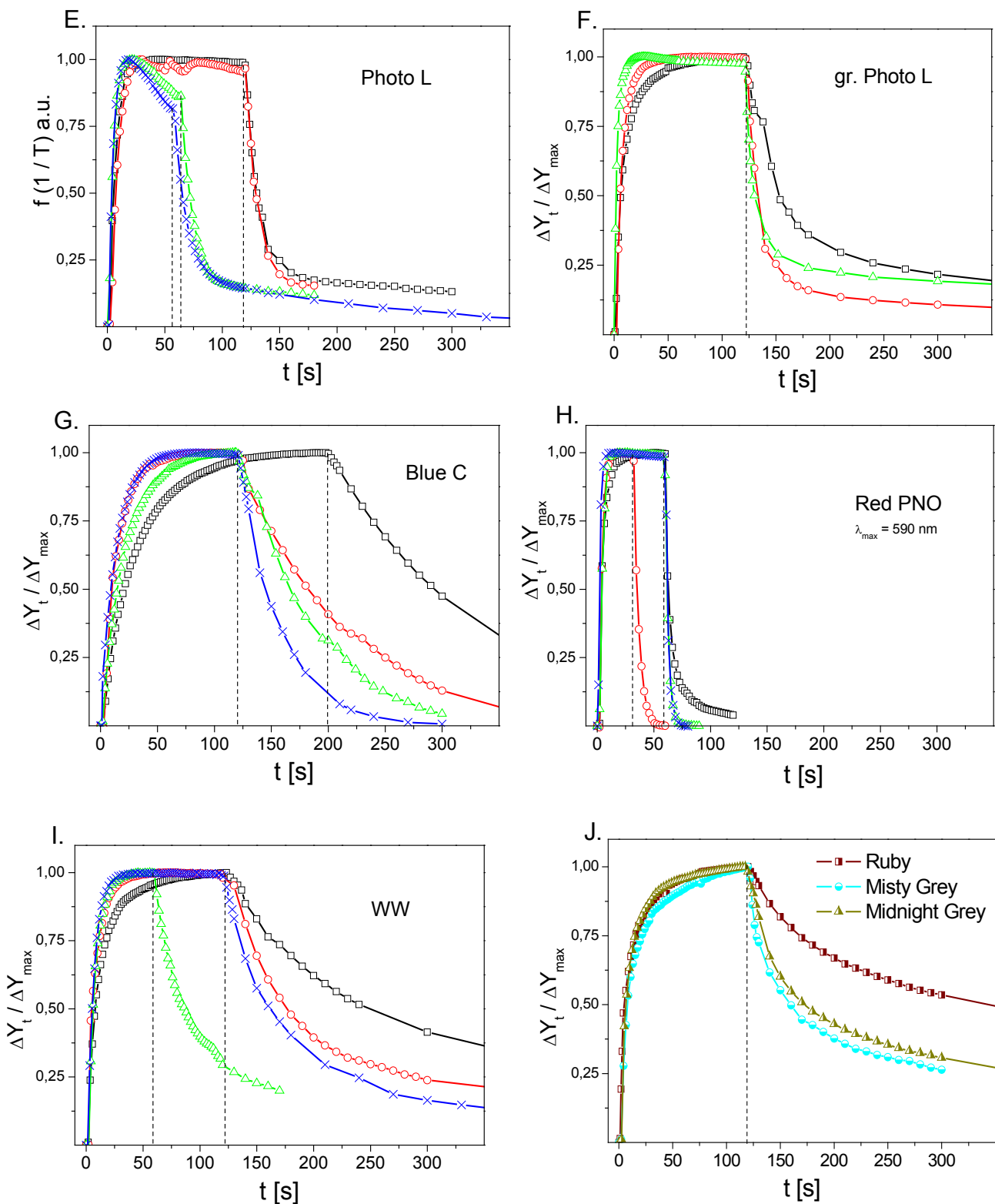


Figure 6.27. Kinetic behaviour of photochromic coatings. UV light was switched on at $t_0 = 0$ s and shut off at t_1 (indicated with dashed lines). Photochromic dyes **A.** Blue D, **B.** graftable Blue D, **C.** Blue A, **D.** graftable Blue A, **E.** Photo L, **F.** graftable Photo L, **G.** Blue C, **H.** Red PNO and **I.** WW, within GG (black squares), GB (red circles), GA10 (green triangles) and GAD (blue crosses) coatings on glass; **J.** commercial Reversacol® dyes within GG coatings. Exact values of activation (t_a) and fading (t_f) times are to be found in Table 6.11 and 6.12.

It can be seen that the matrix characteristics (both rigidity and polarity) have a strong influence on the switching kinetics. Moreover, the large difference between the covalently bonded and physically entrapped dyes is clearly evident, e.g. for the off-reaction of graftable Blue D in the GG system (Figure 6.27 A and B), which proceeded slower by a factor of about 10 as compared to Blue D. Also for other couples of dyes, such as Blue A and graftable Blue A (Figure 6.27 C and D) or Photo L and graftable Photo L (Figure 6.27 E and F), covalent bonding to the siloxane backbone slowed down the bleaching kinetics by a factor of about 3 as compared to the corresponding physically incorporated dyes. This effect is different from an organic polymer matrix where covalently bonded and simply dissolved dyes showed no difference in kinetic behaviour. There was no definite indication of an effect of covalent linkage on the decoloration rate [167]. The hybrid polymer matrices are possibly more rigid and more polar than purely organic ones. The ground state dipole moment of the spiro molecular form is about five times lower than for the merocyanine one [168]. It is conceivable that, on the one hand, the polar carboxylic sites of the host material might have been able to stabilise the opened merocyanine form, thus causing slower bleaching. On the other hand, kinetics is a free volume controlled phenomenon so the back reaction might have been sterically hindered as a result of covalent attachment to a rigid host material.

In the following the kinetics for three photochromic dyes shall be compared: Blue D (1,3,3,5,6-pentamethylspiro-[indolino-naphthoxazine]), Blue-C, a spiro-isoindolinoxazine, analogous in structure to Blue D, and a 5'-morpholino-1,3,3-trimethyl substituted spiro-indolinoxazine (Red PNO). The very fast kinetics surprised in the case of Red PNO (Figure 6.27 A, G and H), i.e., the biggest molecule. In contrast, Blue C seemed to be the most sterically hindered dye during the whole photochromic reaction, being stabilised in the merocyanine form. Kinetics of Blue A, as could be suspected, was faster than for Blue D (Figure 6.27 C and A), which with two methyl groups needs more volume for free structural changes.

WW, a red-switching chromene, was probably also sterically hindered in the decoloration process. Its significantly slow kinetics might have been caused by the relatively big molecular size, however, chemical bonding to the matrix backbone might occurred as well (see before). The observed decrease of photochromic activity for Photo L during activation suggests direct photolysis of the dye molecules taking

place, which might contribute to the low stability of Photo L. Interestingly, covalent bonding prevented that phenomenon (Figure 6.27 E and F).

Independently of the dye used, host systems based on GA10 and GAD offer conditions for faster switch on/off photochromic reactions. In almost all cases, samples based on the GG matrix, which is the hardest one, show the slowest kinetics. Although it could not be directly confirmed by the polarity investigations, the GG matrix contains polar carboxylic sites, whereas GA10 and GAD were more basic and less polar. The GB matrix is analogous to GG but less rigid because of the lower fraction of inorganic domains present in the hybrid polymer structure.

The commercially available Reversacol® dyes (a red one, Ruby and two grey ones, Misty Grey and Midnight Grey) showed only low photocolorability in the GG matrix. Their kinetics were comparable to those of the Variacrol® dyes (Figure 6.27 J). They achieved 50 % of the maximum colorability in several seconds ($t_{a(\text{Ruby})} = 4.9 \text{ s}$, $t_{a(\text{Misty Grey})} = 8.1 \text{ s}$, $t_{a(\text{Midnight Grey})} = 6.4 \text{ s}$) and faded to 50 % in dozens of seconds ($t_{f(\text{Ruby})} = 223.5 \text{ s}$, $t_{f(\text{Misty Grey})} = 39.5 \text{ s}$, $t_{f(\text{Midnight Grey})} = 52.6 \text{ s}$). The commercially available Transition lens activated and faded in $t_a = 8.2 \text{ s}$ and $t_f = 121.2 \text{ s}$, respectively.

Kinetics depend on the dye molecular structure as well as on the matrix characteristics. Chemically bonded dyes switch distinctly slower than physically incorporated ones. More polar matrices favour the coloured forms while the softer systems cause less sterical hindrance in spiro-ring open/close reactions. This is evident for the faster switching of photochromes incorporated within GA10 and GAD systems when compared to GG. The investigated photochromic coatings show slightly faster kinetics than the commercial products, however, they still comply with physiological advisable activation and fading times.

6.4. Electron Spin Resonance Measurements

Electron spin resonance (ESR) spectroscopy, giving information about the electronic structure (the presence of unpaired electrons), involves the experimental observation of transitions between magnetic sublevels of a sample exposed to a magnetic field. In the case of spiro-compounds a biradical form, which partially leads to degradation products, should be present. The concentration of that merocyanine form might explain different degradation behaviour. Further investigations on photochromic dyes in solution or as single crystals were used as a proof for the biradical photochromic ring opening reaction after irradiation. Campredon et al. succeeded in trapping biradical species of unsubstituted spiro-compounds with nitric oxide [169]. With three simple line spectra and g factors between $g=2.0041$ and $g=2.0042$ for spiro(indolino-naphthooxazines) and between $g=2.0045$ and $g=2.0046$ for spiro(indolino-benzopyrans), ESR activity was detected after as well as before UV irradiation. Low concentration suggested that although biradicals are present in solutions of the photochromic compounds, the species are not on the main reaction pathway. They might instead be involved in the photodegradation of the spiro-compounds. Nitro-substituted spiro-compounds form radical anions. The ESR spectra of some 6'-nitrospiro(indolino-benzopyrans) in form of three quartets (factor g between $g=2.0047$ and $g=2.0048$) indicated that the extra electron is localised on the nitrospiropyran moiety [169]. Other investigations point out that photodegradation has not only radical origin [72, 170,171].

Bulk samples based on GG, GB, GA10, GAD and SiO₂ matrices were investigated by means of ESR spectroscopy. The samples were doped with 3% of Blue D, gr. Blue D, Blue A, Blue C, Photo L, gr. Photo L, Red PNO, and WW. The SiO₂ sample was stored for three days at room temperature after a 15 minutes treatment in an ultrasonic bath. All other samples were stored after synthesis for only one day at room temperature. Gelled samples were dried at 125 °C for 20 minutes, afterwards crushed and sieved. The fractions with particle sizes between 250 µm and 500 µm were used. Measurements were made on unirradiated samples, and after irradiation for 1 h, 4 h and 9 h with a mercury lamp placed in a distance of 40 cm from the sample. The investigation was repeated with irradiated samples, which were kept in the dark for 24 h. In almost all cases radical activity was evident.

It was possible to recognise single signals with a g factor in the range between $g = 2.0025$ and $g = 2.005$ after Hg irradiation for almost all samples. Typical signals were of regular Lorentzian shapes and similar to each other with only a few exceptions (Figure 6.28).

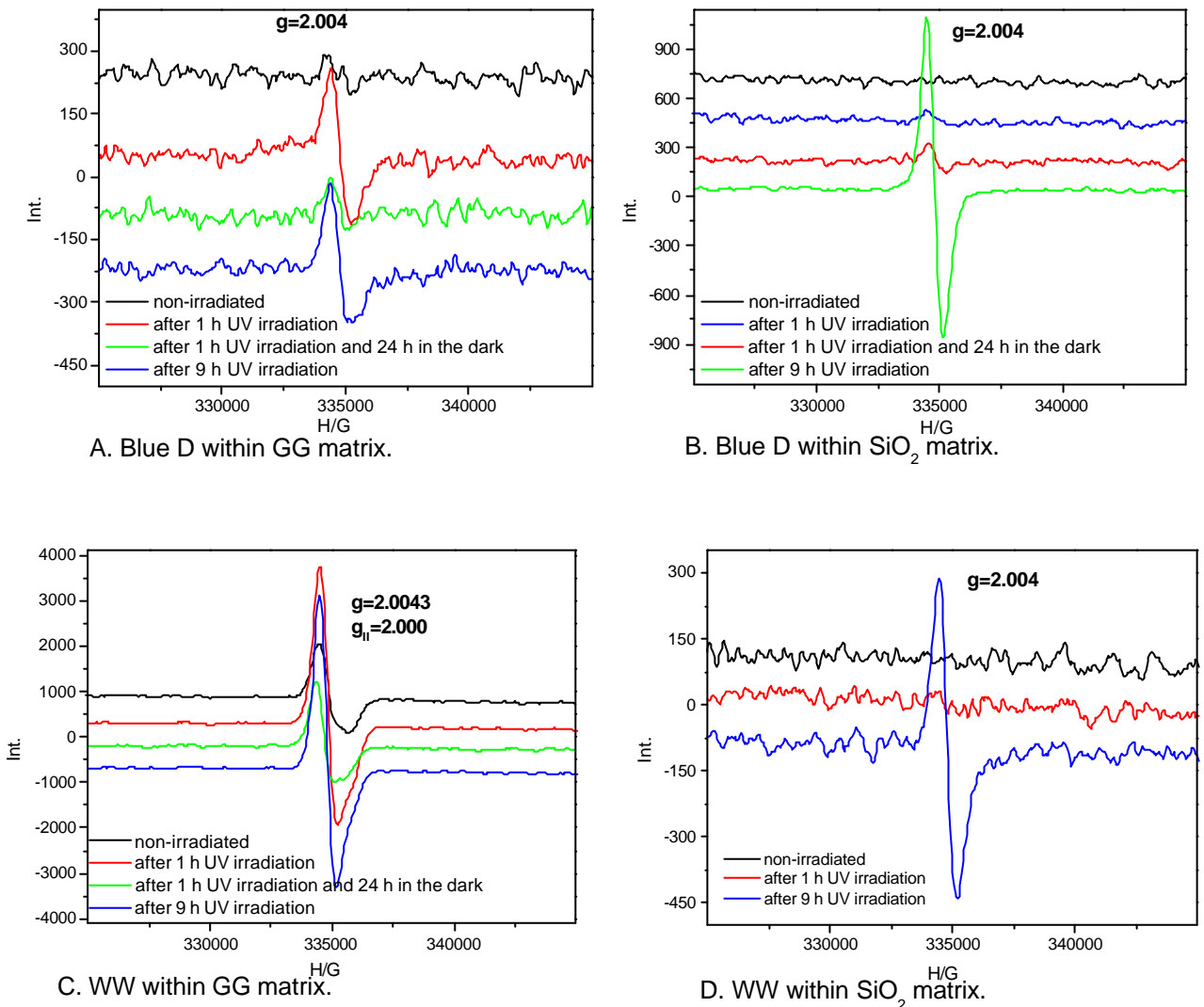


Figure 6.28. ESR spectra of GG and SiO_2 bulk samples doped with photochromic dyes: Blue D within **A.** GG matrix and **B.** SiO_2 matrix; WW within **C.** GG matrix and **D.** SiO_2 matrix; spectra taken from non-irradiated samples, after 1 h UV-Vis irradiation, after 1 h UV-Vis irradiation and 24 h storage in the dark and after 9h UV-Vis irradiation.

The magnetic centres observed in the samples are assumed to be rather stable and renewable. Even after 24 h in the dark they were present to some extent. The intensities of the ESR signals decreased with lower concentration of free electrons, but after repeated irradiation they achieved the initial level.

In the case of the organically modified siloxanes some free radicals were observed also in non-irradiated powders. The intensity of these signals rose after irradiation (Figure 6.29). Interestingly, already in the pure matrix samples ESR signals were detected. Therefore, also pure and doped SiO_2 matrices were included in the investigations. Very strong resonances for the chromene WW doped samples need to be emphasised.

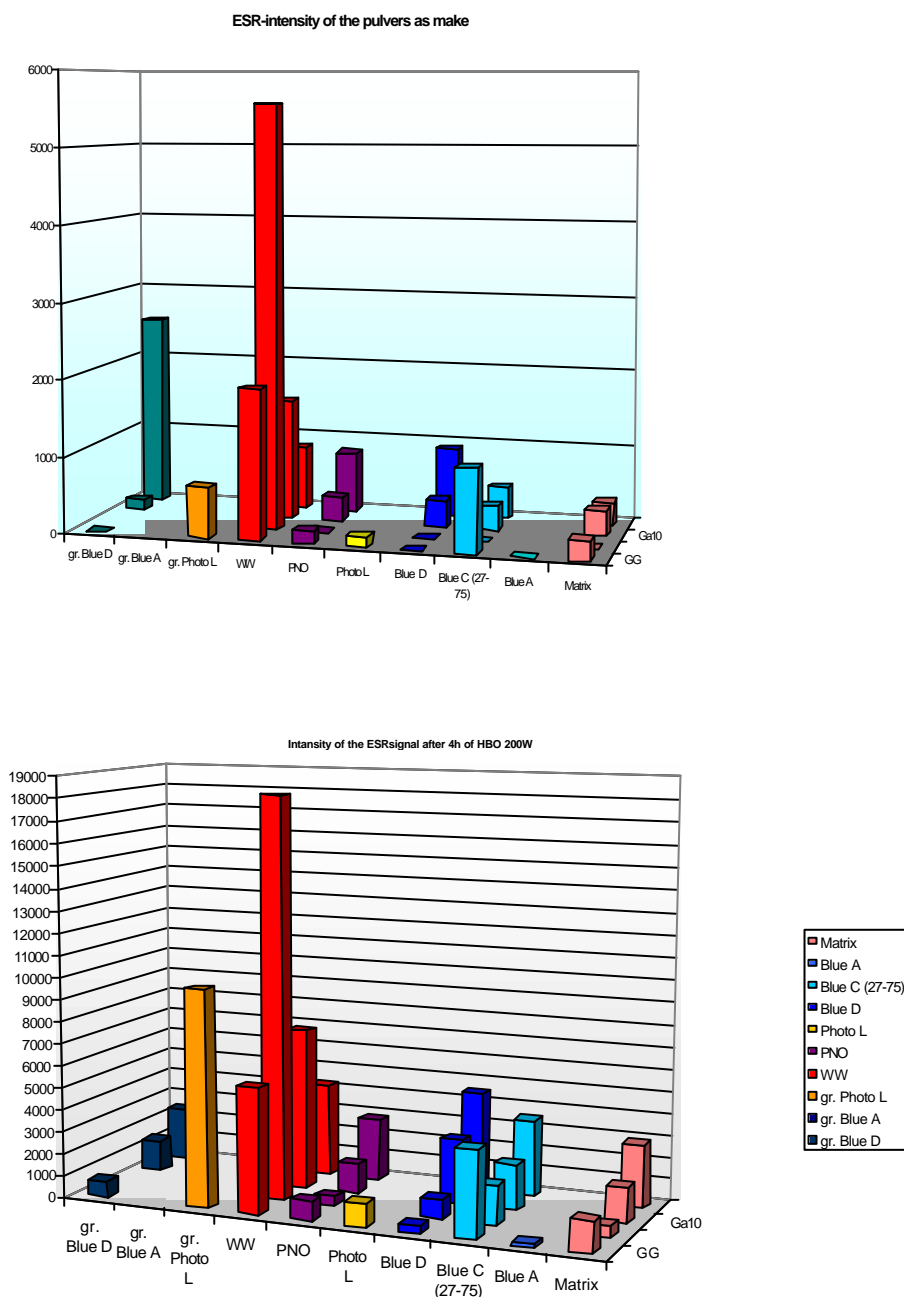


Figure 6.29. ESR signal intensities for GG, GB, GA10, GAD matrices and listed dyes before (A.) and after (B.) 4 h of UV-Vis irradiation.

The exact g factors (Table 6.13 to 6.17) were very near to that of a free electron. This suggests that the observed radicals might have had no defined structure. This could mean that they were released during irradiation, or electrons being present before were not located anymore on one molecular site.

Table 6.13. Presence of radicals in GG based samples as revealed by ESR spectroscopy, before (g, A) and after 4 h UV-Vis irradiation (g_i , A_i); A, A_i – signal intensities.

Dye	g	A	g_i	A_i	A_i / A
Matrix	2.0047	265	2.0046	1400	5.28
BA	---	---	2.00446	157	---
BD	---	---	2.00435	373	---
PL	2.0041	137	2.00436	1050	7.66
BC	2.0039	1088	2.0046	3925	3.61
SBD	---	---	2.00427	717	---
SPL	2.00392	658	2.00453	9812	14.90
WW	2.0043	1965	2.0042	5666	2.88
PNO	2.0042	174	2.0045	884	5.08

Table 6.14. Presence of radicals in GB based samples as revealed by ESR spectroscopy; pure GB matrix - signal asymmetrical, wider bottom; GB-WW – signal asymmetrical, smaller bottom; A, A_i – signal intensities.

Dye	g	A	g_i	A_i	A_i / A
matrix	---	---	2.0047	515	---
BC	---	---	2.0044	1728	
BD	---	---	2.0044	843	---
PNO	---	---	2.0042	448	---
WW	2.0046	5570	2.0046	18200	3.27

Table 6.15. Presence of radicals in GA10 based samples as revealed by ESR spectroscopy; Ga10-SBD – signal with shorter and wider top; GA10-WW – signal asymmetrical, smaller bottom; GA10-BD - two signals after irradiation.

Dye	g	A	g_i	A_i	A_i / A
matrix	2.0043	338	2.0047	1563	4.62
BC	2.0039	319	2.0043	2034	6.47
BD	2.0039	360	2.004	2943/1000	8.18
SBD	2.0027	135	2.004	1434	10.62
PNO	2.0037	323	2.0047	1318	4.08
WW	2.0046	1584	2.0047	7320	4.62

Table 6.16. Presence of radicals in GAD based samples investigated by ESR spectroscopy; GAD-SBD – signal asymmetrical after irradiation; GAD-BD – two signals after irradiation.

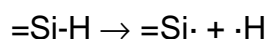
Dye	g	A	g_i	A_i	A_i / A
matrix	2.0048	300	2.0045	2860	9.53
BC	2.0039	427	2.0045	3492	8.18
BD	2.0045	908	2.005	4493/ 960	4.95
SBD	2.0025	2550	2.003	2400	0.94
PNO	2.0041	790	2.0042	2855	3.61
WW	2.0041	844	2.0043	4254	5.04

Table 6.17. Presence of radicals in SiO₂ based samples as revealed by ESR spectroscopy.

Dye	g	A	g_i	A_i
BA	---	---	2.0041	182
BC	---	---	2.0047	1084
BD	---	---	---	---
SBD	---	---	2.0043	150
PL	---	---	---	---
SPL	---	---	---	---
PNO	---	---	2.0039	160
WW	---	---	---	---

It could be derived that the observed signal originated from a mobile dye radical. The presence of the ESR signals in unirradiated pure matrix samples and the increase of their intensity after irradiation, suggested that not only dye molecules were related to the development of magnetic centres.

It is very difficult to define the structure of a paramagnetic ion only from its paramagnetic susceptibility, especially for complicated molecules with multiple electrons [172]. Sharp signals without a dissolved structure can be caused by anisotropy of the radicals' environment. Natural enzymatic systems show ESR signals without fine structure and with g factors around 2.004. This was interpreted as unlocalised free electrons that migrate in the hydrogen and peptide network till they meet an acceptor. Only in this way the oxidation-reduction reaction between two distantly separated molecules can be accomplished. Sharp ESR signals are common for polymers with conjugated double bonds independently from linearity or spacial structures. Those signals are single Lorentzian function-shaped lines with g factors between $g = 2.003$ and $g = 2.006$. For polymers without double bonds one observes no ESR activity at all. The signal intensity increases with the length of the conjugated system. The presence of an extra bright ESR signal indicates some additional free radicals, which are entrapped in the polymer network. Radicals are resulting from intra- and intermolecular connections. It was shown that single ESR signals are typical also for some dyes with complex conjugated systems. Usually they are sharp and symmetric with g factors similar to the pure spin value ($g = 2.0023$). In that case free electrons could originate from intercharge complexes [172]. In practice, an orbitally unpaired electron should be bound to one or more nuclei, therefore the g factor of such an electron will change and in the case that an unpaired electron will interact with the magnetic moments of the neighbouring nuclei that make up the radical, hyperfine coupling is registered [173]. Some ESR investigations were made on UV-irradiated silica gels and showed different ESR spectra depending on the starting alkoxides. In case of xerogels obtained by acidic hydrolysis of triethoxysilane similarly shaped ESR signals with a low g factor (ca. $g = 2.001$) can be observed. This single sharp signal was assigned to an Si E' centre, which originates from photolysis:



In other cases more complicated spectra were obtained probably due to the photolysis of the functional groups at the silicon position, such as Si-H, Si-CH₃, Si-OC₂H₅ and residual solvent interactions [174].

In this work the silica matrix seemed to give no intrinsic signal. The asymmetrical or doubled signals obtained for some sample compositions (GB-matrix asymmetrical, wider bottom; GB-WW – asymmetrical, smaller bottom; Ga10-SBD – top smaller and wider; GA10-WW – asymmetrical, smaller bottom; GA10-BD - two associated signals after irradiation; GAD-SBD – asymmetrical; GAD-BD – two associated signals after irradiation) suggest the presence of a possible additional free electron. In the case of WW and graftable Blue D they could be associated with free dye molecules, in Blue D with more or less matrix free space. For almost all irradiated samples the value of the g factor grew slightly, suggesting that the surrounding of the free radical was becoming more defined, i.e., the whole system became more isotropic. It is possible that stiffer networks restricted the radicals in their movements. The especially high ESR intensities for graftable dyes and WW may be explained by prolonged conjugated systems. Surprisingly high radical concentrations were present in samples with good photostability such as graftable Blue D within GG and GAD matrices or WW within the GG matrix. Although for the pure matrices after irradiation one could distinctly observe higher radical concentrations (GG: by a factor of 5.28, GA10: by a factor of 4.62, GAD: by a factor of 9.53 times), they were still lower than for doped samples. For dyes with fast and very fast bleaching kinetics such as Red PNO, Photo L and Blue C, intensities changed only little after irradiation. Possibly the measurements took too long to record all of the magnetic centres before recombination took place.

As a summary it can be stated that in the investigated samples magnetic activities were evident. Higher conjugated systems such as the chromene WW exhibited higher ESR activities. Systems with fast kinetics showed distinctly lower ESR intensities after irradiation than other dyes. The concentration of radical species rose after UV-Vis irradiation and was renewable. For some systems, the radical species were very stable. The g factor and the simple structure of the ESR signals suggested that the electrons existed in an anisotropic surrounding, i.e. moving freely in the molecular network, which changed slightly after irradiation. The high intensities found for samples with the best photostability disagree with results achieved for solutions or single crystals of spiro-compounds, where a high concentration of

radicals was correlated with strong photodegradation. However, the reduction of the concentration of present excited dye molecules should lead to an enhancement of photochromes stability, which could explain this discrepancy.

6.5. Optimisation

The degradation of photochromes in solution has been investigated by various authors. UV radiation and interactions of excited or/and ground-state oxygen with the photomerocyanine form were identified as the main degradation factors [94, 96]. Moreover, it was found that the exclusion of ambient oxygen and/or quenching of its excited states decreases the photo fatigue of SO and SP tested within a range of solvents [95, 175, 176]. DABCO (or its derivatives) as a singlet-oxygen quencher improves the photostability of spiro[indoline-naphthoxazine] in solution by a factor of two [72]. Light stabilisers such as HALS [177] also influence the photo fatigue of SO and SP positively.

The degradation rate of photochromic ophthalmic lenses has to be quite low to fulfil customer expectations. Statistically, eyeglasses are replaced every 2 years. Theoretically, the average half life time for such a product should not be shorter than 500 h, which, however, cannot be met even by new generation photochromic glasses [9]. As can be seen from the results presented in the previous chapters, the half life time of the coatings was by far lower and thus had to be optimised. Besides any kind of matrix modification [178], also other stabilisation concepts such as introduction of stabilisers or reduction of ambient oxygen permeation were attempted. The stability of a photochromic article is the main issue with regard to its application for commercial exploitation.

The temporary increase of photochromic activity observed after a short UV irradiation period instead of immediate activity dropping, that can be noticed for almost all tested samples, is a common phenomenon observed not only within the present work [141].

6.5.1. Stabilisers

To decrease the photo fatigue of spirooxazine dyes, some ultraviolet stabilisers and excited state quenchers can be used, e.g. organonickel complex stabilisers, or some members of the class of hindered amine light stabilisers (HALS). HALS such as Tinuvin 770 (T770), Enam 121 and Enam 129, with their tetra-methyl-piperidine group as a radical quenching moiety, are also known to show antagonism with acidic compounds, which is a great advantage for the acid-sensitive

spirooxazines [9, 179]. HALS were originally developed as light stabilisers for plastic materials [177], but are now used as multifunctional additives, since they have been found to work as radical trapping agents, antioxidants, heavy metal deactivators, hydroperoxide decomposers, and so on [180]. Conventional UV stabilisers, such as benzophenones or triazoles, are not applicable within photochromic systems because they absorb in the same UV light range as do SO, which hinders photochromic coloration. Excited states of oxygen or the matrix material, which are formed during UV irradiation, can accelerate the degradation rate of photochromes. Organometal complexes as excited state quenchers, preferably singlet oxygen quenchers, increase the photostability of organic photochromic compounds [120]. The most suitable compounds are salts or chelates of nickel. Some synergistic effects between different types of stabilisers are expected [177].

In the present work several additives were tested concerning their stabilisation efficiency: excited state quenchers such as 3-methylpyrazoline, silylated 3-methylpyrazoline, graftable 3-methylcoumarine and a Ni-organocomplex (Q84), the singlet oxygen quencher 1,8-diazabicyclo[5.4.0]undec-7-ene (DABCO-I), and the hindered amine light stabilisers Tinuvin 770, Enam 121, and Enam 129 (Figure 5.2). All of them were examined within GG, GB, and GA10 matrices for stabilisation of gr. Blue D (3 %) doped coatings on glass. The molar ratio of dye to stabiliser was 1 : 2.

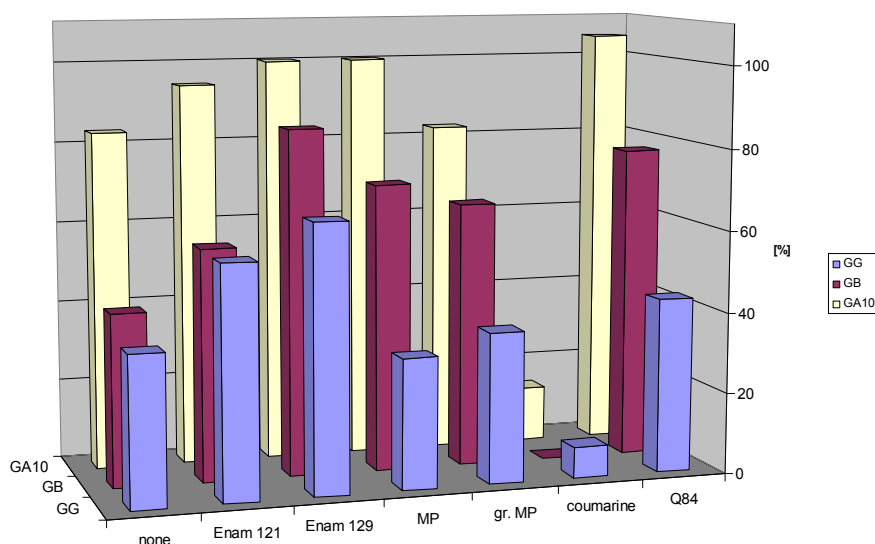


Figure 6.30. Relative remaining photochromic activity after 24 h of UV light irradiation for GG, GB, and GA10 coatings doped with 3 % of gr. Blue D combined with selected stabilisers: Enam 121, Enam 129, 3-methylpyrazoline (MP), graftable 3-methylpyrazoline (gr. MP), graftable 3-methylcoumarine, nickel organocomplex (Q84) and with no stabiliser added (as reference).

The activity of the investigated coatings was decreased by a few percent when MP and gr. MP were added. For GG based samples, the photochromic activity of an unstabilised coating was $\Delta Y_0^{GG} = 32\%$, whereas with MP as additive only $\Delta Y_0^{GG}(MP) = 28\%$ were achieved. Differences in the photochromic activity of unirradiated samples within other matrices and for samples doped with gr. MP were found to be of the same order of magnitude.

After 24 h of UV irradiation the relative remaining photochromic activity (with regard to unirradiated coatings) was estimated for gr. Blue D (Figure 6.30). Enam 129 clearly enhanced the stability of the investigated systems, i.e. for the GG and GA10 based coatings by about 78 % and 20 %, respectively (difference between ΔY values of unstabilised and stabilised samples after 24 h of UV irradiation). For the GB based sample the fatigue of the Enam 129 doped coating is half as strong as compared to the unstabilised one. Q84, Enam 121 and 3-methylpyrazoline stabilised the photochrome very well. In general, for samples (comparable coating thickness for all investigated samples; see: Appendix 1) comprising stabilisers, the remaining colorability after 24 hours of UV light irradiation is 20 % up to 60 % better than for unstabilised ones. It should be noted that, the presence of 3-methylcoumarine increased the rate of degradation.

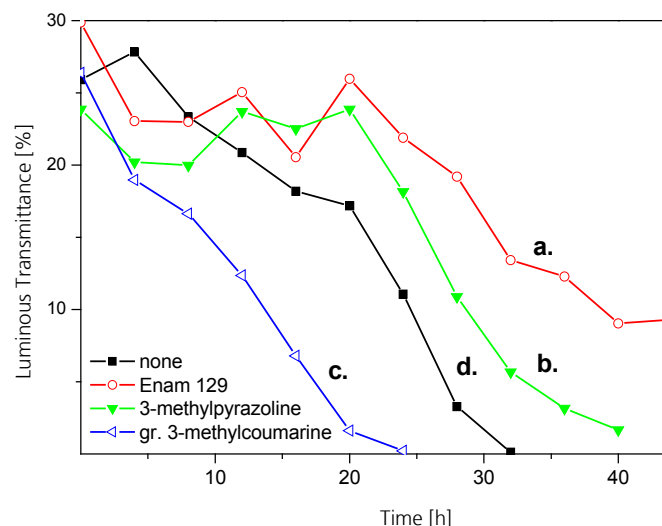


Figure 6.31. Degradation of gr. Blue D doped coatings based on the GB system: a. Enam 129, b. 3-methylpyrazoline, c. gr. 3-methylcoumarine and d. without stabilisers.

The GB matrix was found to be the most suitable one for the application of stabilisers (Figure 6.31). A stability enhancement of 35 % (Enam 121) up to 100 % (Enam 129) indicated that the added compounds performed best in this system. Remaining acidic moieties were probably deactivated through the addition of enamine stabilisers. This was not necessary in the case of GA10 matrix, where Q84 (excited state quencher) was most efficient.

It is obvious that molecules possess different mobility in solution and in a solid matrix, suggesting that the free volume of the reaction medium is important for a high efficiency of stabilisers.

The system compatibility and stabilisation effects of the above mentioned compounds were also tested for coatings containing the red-switching chromene WW (3 %). However, its coloration and life time within the GB ($\Delta Y_0 = 6\%$, $T_{50\%} = 2\text{ h}$), GA10 ($\Delta Y_0 = 2\%$, $T_{50\%} = 2\text{ h}$), and GAD ($\Delta Y_0 = 5\%$, $T_{50\%} = 2\text{ h}$) matrices could not be improved. Only in the case of the GG system, WW presented good photochromic activity, with a ΔY_0 value above 40 %, even for samples with added Enam 129 and Q84. The photo fatigue of WW, however, was decreased through the presence of

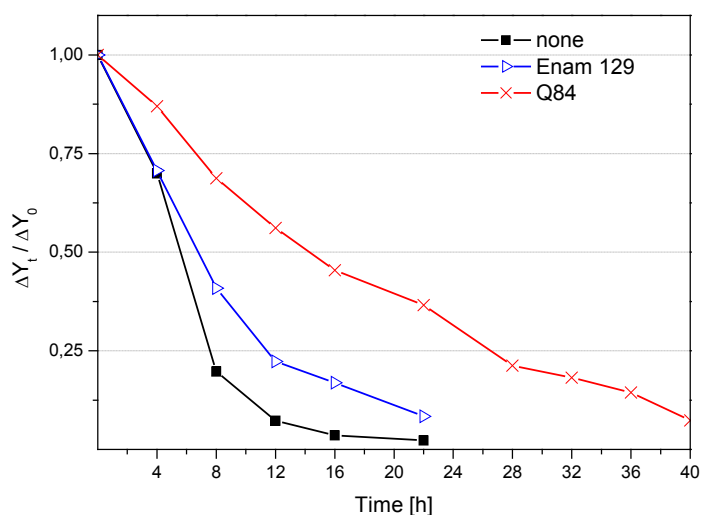


Figure 6.32. Loss of photochromic activity after UV light irradiation for chromene WW (3 %) within the GG matrix system with no stabiliser and with Enam 129 or Q84.

the latter. Its photochromic half-life time was achieved after $T_{50\%}(\text{Q84}) = 12\text{ h}$ with a linear loss of coloration, other than was observed for the undoped coating (Figure 6.32).

6.5.2. Coating stacks

A. Multiple coating stacks with stabilisers

The absence of oxygen in its ground/excited state in the solution of a photochromic dye increases its photostability very distinctly [96]. To decrease the photo fatigue of photochromes, a physical barrier for ambient oxygen by means of an additional top coating was applied in addition to the chemical stabilisers described in the previous chapter. For that purpose the so-called particle lacquer (PL) a nanoparticle containing sol derived from the GG system was used. The incorporated silica nanoparticles enhance the hardness and abrasion resistance of the parent matrix system, which is advantageous with regard to scratch protection of the other relatively soft matrices. The PL system was not doped with photochromes in this work.

Tinuvin 770 (T770), DABCO-I and Q84 were used for the stabilisation of gr. Blue D, Blue D and WW within the GG matrix. Different stabiliser concentrations (0.25 n, 0.5 n, 1 n and 2 n with respect to the molar amount (n) of dye) were attempted in order to define the proper dye to stabiliser ratio. To achieve a good stabilisation effect, a minimum stabiliser quantity of 1 : 1 (molar ratio of dye to stabiliser) was necessary. For higher concentrations only slight improvements were noticed. In case of DABCO-I, a molar ratio of 1 : 2 (dye to stabiliser) seemed to be the most effective. If not pointed out explicitly, stabilisers were added with the above mentioned concentrations.

The presence of a PL top coating alone increases the stability of photochromes by about 30 % relatively to a corresponding single-layer system without stabilisers. The addition of stabilisers in combination with ambient oxygen protection by means of a top layer is particularly beneficial for the photo fatigue behaviour. The best stabilisation could be achieved for the double layer system [GG / 3 % Blue D // PL] with addition of T770. The photochromic half life time ($T_{50\%}$) was raised to 32 hours. DABCO-I in a molar ratio of stabiliser to dye of 1 : 1 ($T_{50\%}$ = 24 h) seemed to be more appropriate as excited state quencher for Blue D than Q84, which gave almost no stabilisation. Also, for a double-layer coating doped with a mixture of gr. Blue D (3 %) and WW (3 %) DABCO-I causes the best stabilisation, whereby in the case of a one-layer coating containing gr. Blue D a similar

improvement of photo fatigue is created by Q84. The stabilisation effect of graftable Enam 121, Enam 129, 3-methylpyrazoline, gr. 3-methylpyrazoline, gr. 3-methylcoumarine and Q84 (Ni organocomplex) on the violet-switching mixture of Blue D (4 %) and WW (3 %) within a double-layer GG // PL coating was also

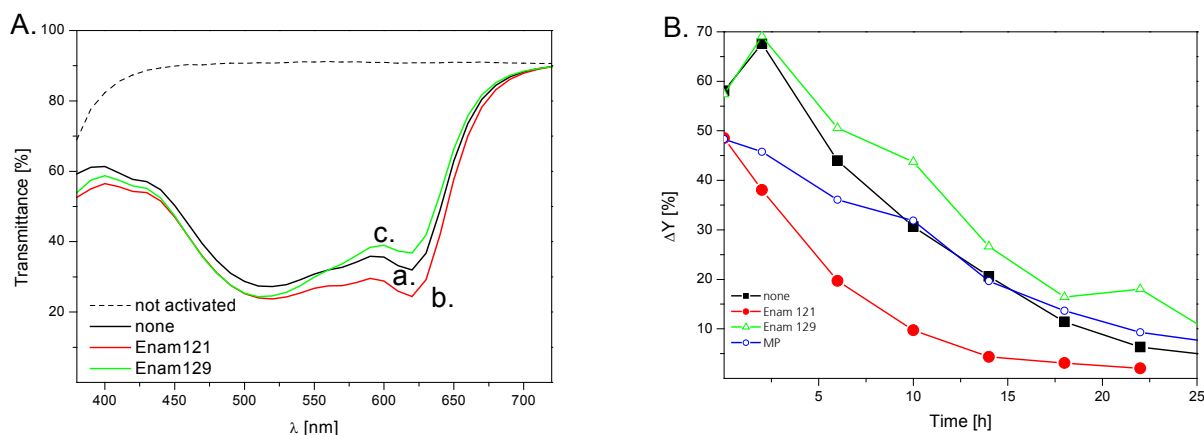


Figure 6.33. Photochromic characterisation of double-layer coatings based on GG matrix with mixture of Blue D (4 %) and WW (3 %) and with or without stabiliser; PL was applied as top coating: A. Coloration of not irradiated coatings with non stabiliser (a.), with Enam 12 (b.) and Enam 129 (c.); B. loss of luminous transmittance after UV irradiation for coatings without stabiliser, with Enam 121, Enam 129 and 3-methylpyrazoline.

investigated. Such coatings were characterised by very high luminous transmittance changes. Up to $\Delta Y_0 = 60\%$ were observed (Figure 6.33 A) for unstabilised samples and samples doped with Enam 121 and Enam 129. The other stabilisers lowered the photochromic activity. The stabilisation efficiency of the additives was generally lower in double-layer compared to single-layer systems. After 26 hours of UV light irradiation only the coatings doped with Q84 and Enam 129 still showed a higher activity (about 60 %) than the corresponding coatings without stabiliser (see: Appendix 1, Table 2). It should be noted that for all coatings a 50 % loss of photochromic activity ($T_{50\%}$) took place after almost the same UV irradiation periods: $T_{50\%}(\text{none}) = 12 \text{ h}$, $T_{50\%}(\text{Q84}) = 15 \text{ h}$, $T_{50\%}(\text{Enam 129}) = 16 \text{ h}$. The coumarine compound had no harmful effect on the system stability (Figure 6.33 B), as was the case for single-layer coatings. For the mixture of gr. Blue D (4 %) and WW (3 %) incorporated within a GG matrix, the beneficial effect of the top coating was evident, especially when Q84 was present. Both factors improved the photostability of the investigated system by more than 100 % compared to the unstabilised single-layer coating system!

The stability of photochromes within the GAD matrix system, opposite to other matrix systems, was surprisingly affected by the presence of PL as top coating. Nonetheless, the chemical stabilisation of gr. Blue D (3 %) within the single-layer system worked, especially when a HALS (T770) was employed. This was obviously not the case in double-layer systems (Figure 6.34), where lower photostability than in unstabilised single-layer coatings was observed.

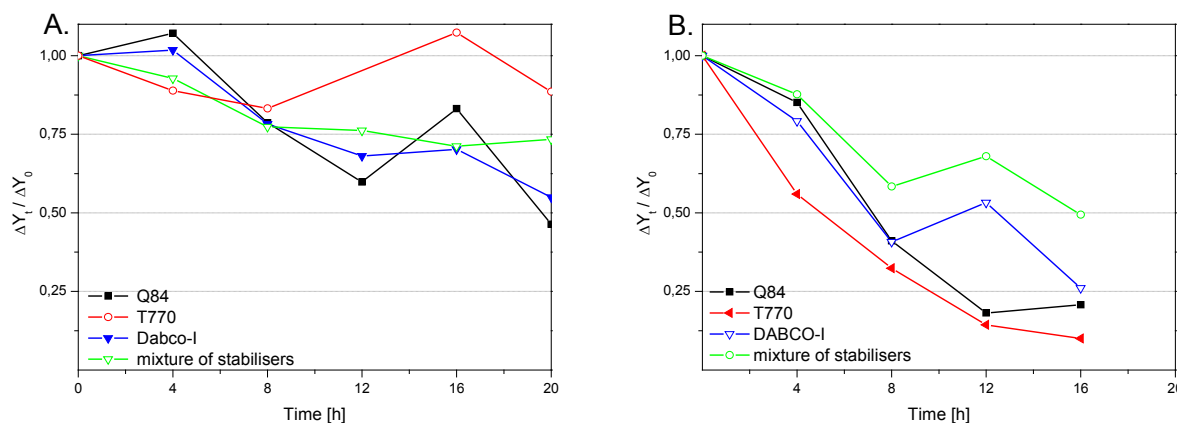


Figure 6.34. Degradation of gr. Blue D (3 %) within the GAD matrix system. Added stabilisers: Q84, T770, DABCO-I and a mixture of these; A. without and B. with top layer.

The addition of a mixture of all stabilisers further improved the fatigue behaviour of the double-layer coatings. Stabilisation through an excess amount of excited state quenchers (Q84, DABCO-I) would suggest that, for photochromic coating stacks based on the GAD matrix, the presence of singlet oxygen and other excited molecules is most harmful. For a single-layer system, UV light stabilisation by HALS (T770) was the most effective method (Figure 6.34).

B. Multiple coating stacks with stabilisers and anti-reflective (AR) coating

Commercially available ophthalmic products are most often equipped not only with a hard anti-scratch (AS) coating, but also with an anti-reflective (AR) coating. Usually, AR coatings are inorganic, oxidic multilayer stacks, whereby also sol-gel derived hybrid materials can be applied [9, 32, 109, 137]. Materials mostly used are SiO_x and TiO_x .

For the realisation of samples with the most suitable coating composition showing a tint as neutral as possible, a high photochromic activity and a low photo fatigue (see Appendix 2, Tables 1-5) commercially available ophthalmic lenses made of CR39[®] were chosen as substrates.

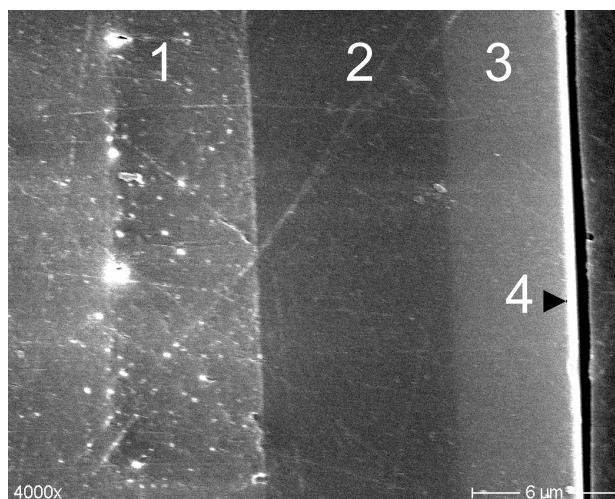


Figure 6.35. Cross section SEM image of a CR39[®] lens (1) equipped with a double-layer coating system (2 and 3) and AR coating (4).

It is known that SiO_x / polysiloxane coating stacks show low oxygen permeation rates. Therefore, an oxidic AR top coating of proprietary composition was employed to realise an oxygen barrier on top of the photochromic coating stacks. Figure 6.35 demonstrates the build-up of such a system.

Double-layer coating systems (top coating: PL) based on GG (kat1_AR, kat3, kat4_AR, and kat5), GB (kat10, kat12, kat17_AR and kat19_AR) and GA10 (kat14 and kat20_AR) were doped with a dye mixture of gr. Blue D (4 %) and WW (3 %) and a stabiliser mixture (T770, Q84 and DBCO-I). A part of the samples was cured at 180 °C for 5 minutes (kat4_AR, kat5, kat12 and kat19_AR; see Appendix 2, Tables 1 and 2). A beneficial influence of the anti-reflective coating on the stability during prolonged UV light irradiation was well noticeable (Figure 6.36). The photochromic activity dropped to 50 % of the initial coloration after approx. T_{50%} = 30 h of UV light irradiation for lenses without AR equipment (Figure 6.36 A). For samples equipped with the AR coating T_{50%} was reached only after 60 h of irradiation. Coating stacks based on the GB and GA10 matrices even showed photochromic half life times of

80 h and 95 h, respectively (Figure 6.36 B). Different curing conditions did not have a distinct influence on the photo fatigue, but samples cured at higher temperature appeared to be slightly less stable. For example, after 24 hours of irradiation, kat3 still showed 52 % of its initial photochromic activity, while kat5 (analogous to kat3, but

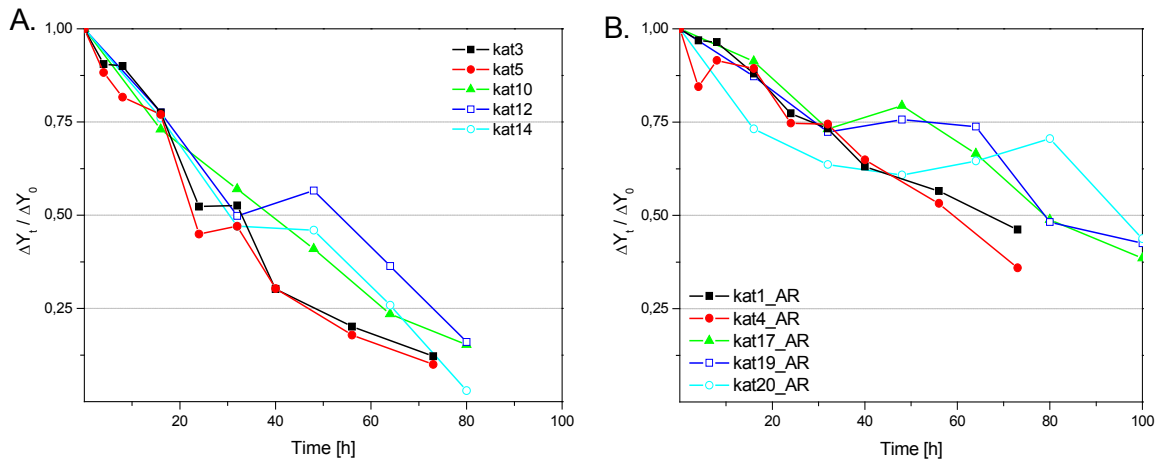


Figure 6.36. Degradation rate for double-layer coating systems based on GG, GB and GA10 matrix systems doped with gr. Blue D (4 %), WW (3 %) and a stabiliser mixture, A. without and B. with AR coating; sample labels: see text and Appendix 2, Tables 1 and 2.

cured at 180 °C) showed only 45 %. This tendency was recognisable for all matrix systems, independent of the presence of the AR coating (Appendix 2, Tables 1 - 2).

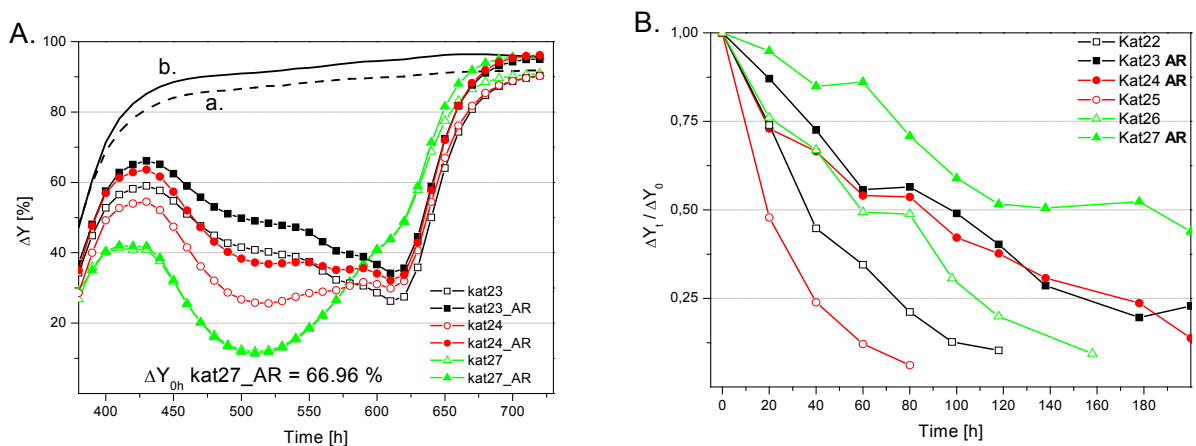


Figure 6.37. Photocolorability in the unweathered state (A.; transmittance of inactive samples: a. without and b. with AR coating) and B. degradation curves for multi-layer coatings based on the GG system doped with gr. Blue D (4 %) and/or WW (3 %), without and with AR equipment; sample labels: see text and Appendix 2, Table 3.

Samples with incorporated mixtures of gr. Blue D and WW (4 % and 3 %) were characterised by very high initial luminous transmittance changes up to 60 % (Appendix 2, Tables 1-3), which is in the range of the coloration depth typical for commercial photochromic products. The presence of the AR coating was associated with a decrease in photochromic activity, which was probably caused by the heat treatment the samples underwent during PVD application (about 80 °C for 65 minutes). On the other hand, also a decreased amount of UV light penetrating through the coating stack might have been the reason for the lower photocolorability (Figure 6.37 A). Nonetheless, by AR equipment the transmittance of samples in the non-activated state was increased from about 80 % (without AR coating) to more than 90 % (samples with AR coating) (Figure 6.37 A).

Double-layer coating systems (top coating: PL) based on the GG matrix (kat22, kat23_AR, kat24_AR, and kat25) and doped with gr. Blue D (4 %) and WW (3 %) without stabilisers were also investigated. Samples kat24_AR and kat25 were cured at 160 °C for 5 minutes (see Appendix 2, Table 3). For the samples kat26 and kat27_AR photochromic dyes were separated. Two independent layers were applied, one containing gr. Blue D and a second one containing the red chromene. An interstage heating treatment step was necessary. The whole system was top coated with PL and finally equipped with the AR system (kat27_AR, Appendix 2, Table 3). The absence of stabilisers within the coating stacks based on the GG system (kat22-25) seemed to be of no importance for the stability of the investigated systems when an AR layer was applied. They lost half of their photochromic activity only after 80 h of UV light irradiation (Figure 6.37 B), which is similar to chemically stabilised systems. However, the lack of chemical stabilisers strongly increased the photo fatigue in samples without AR coating (Figures 6.36 A and 6.37 B).

By separation of the dyes the photo stability could enormously be enhanced. Sample kat26 (without AR protection) is as stable as chemically stabilised and AR coated samples (Figures 6.36 B and 6.37 B). Besides an excellent initial photochromic activity of $\Delta Y_{0h} = 67\%$ (Figure 6.37 A), it still keeps 30 % of its photocolorability after 96 hours of UV light irradiation ($T_{50\%} = 60$ h). A multiple-coating system of the same composition with an additional AR coating also exhibited a high ΔY_{0h} value of 67 %, and lost half of its initial photochromic activity only after 180 h of UV light irradiation! However, degradation did not proceed linearly and after 120 h of suntesting its coloration actually had dropped to almost 50 % (Figure 6.37 B). It is

assumed that both the isolation from degradation products as well as the separation from excited states of activated photochromophores are very efficient stabilisation factors. Both gr. Blue D and WW produced high radical concentrations, when UV irradiated (see paragraph No. 6.4 ESR measurements). Space separation of dyes connected with exclusion of ambient oxygen and chemical UV light protection were efficient techniques to produce a photochromic coating system with strong colorability and a low photo fatigue.

The GAD matrix system was used as a “base” coating for multiple-layer compositions with spatially separated photochromes (samples kat28 - kat59, Appendix 2 Table 4). Blue D (5 %) and gr. Blue D (3 %) were additionally stabilised with Q84. To achieve a neutral tint also a yellow dye, gr. Photo L (3 %), was incorporated within the upper GG based layer, also containing the red chromene WW (3 %). DABCO-I, as a suitable stabiliser for WW, was added to that second layer. The photochromic double-layer was equipped subsequently with the top coatings, i.e., PL and AR coatings. The photodegradation rates of these samples after prolonged UV irradiation are shown in Figure 6.38.

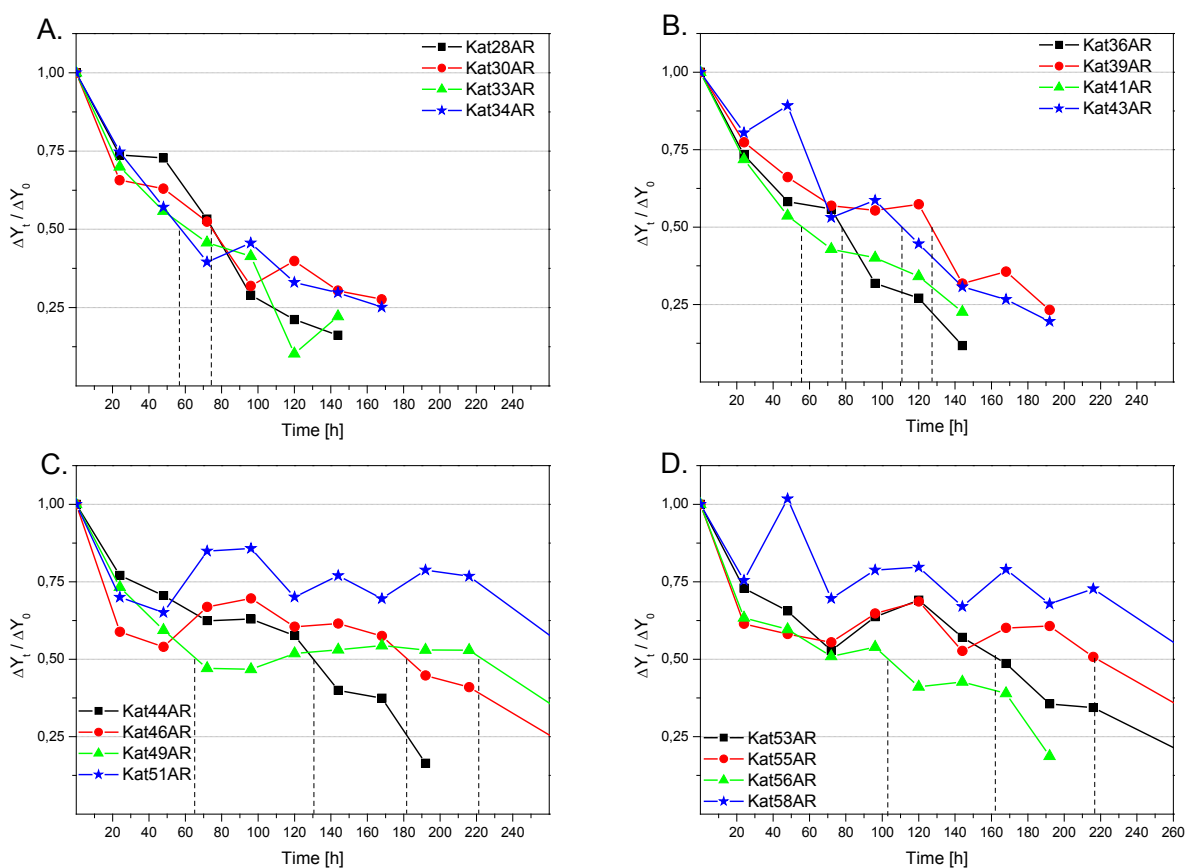


Figure 6.38. Relative loss of photochromic activity after prolonged UV irradiation for GAD // GG // PL // AR samples with spatially separated dyes and AR layer; for sample labels see Appendix 2 Table 4.

A high concentration of Blue D (5 %) could not match the better stability of gr. Blue D within the GAD matrix (Figure 6.38 A and C). Nonetheless, the addition of stabilisers (Q84 in the case of Blue D and DABCO-I for WW or WW / gr. Photo L mixtures) enhanced the photostability of the photochromic systems (Figure 6.38 A and B) to half life times higher than 100 h (samples kat39_AR and kat43_AR). Stabilised coating compositions based on gr. Blue D and the GAD matrix (added Q84, samples kat53_AR – kat58_AR) as well as WW or a mixture of WW and gr. Photo L (added DABCO-I, samples kat55_AR and kat58_AR) in GG matrix kept more than 50 % of their initial coloration even after 200 h Suntest (Figure 6.38 D)! The photochromic activity of unweathered samples was good (average ΔY_0 higher than 50 %), with exception of chemically stabilised coatings comprising a mixture of WW and gr. Photo L, where ΔY_0 was lower than 30 % (Appendix 2 Table 4). Unfortunately, the absorption characteristics of the investigated coatings changed after irradiation in the Suntest. As an example, the absorption at $\lambda_{\max} = 615$ nm (gr. Blue D or Blue D) was more durable than that at $\lambda_{\max} = 510$ nm (WW) (Figure 6.39 A – F). The lower stability of the red dye, especially in samples with high concentrations thereof, led upon irradiation, to coatings that were more bluish instead of the initial purple tint.

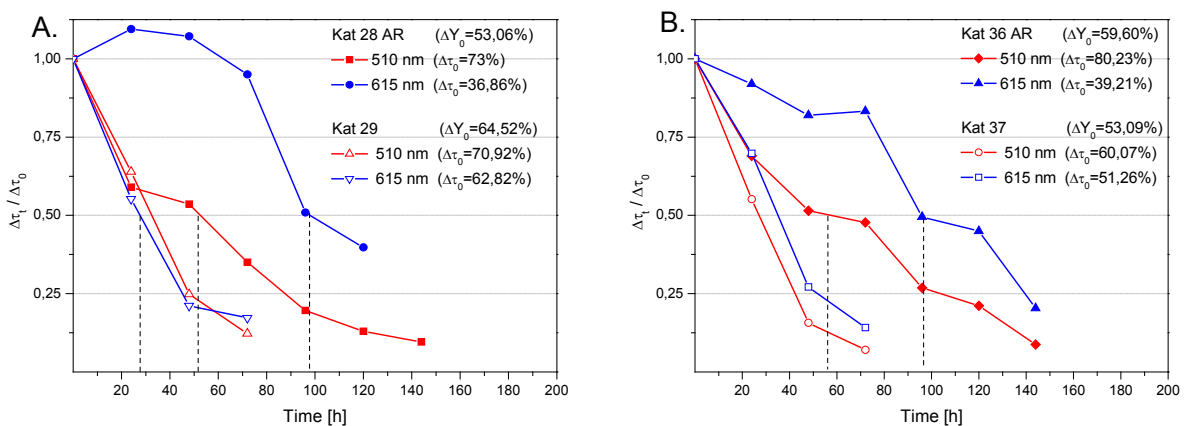


Figure 6.39. Relative change of spectral transmittance at $\lambda_{\max} = 615$ nm and $\lambda_{\max} = 510$ nm for selected multi-layer coating compositions; for samples labels see Appendix 2 Table 4.

It seemed that the AR coating increased the stability of WW only for stabiliser-free coatings, as was observed in the case of samples kat44_AR – kat47 and kat52 - kat55_AR (Figure 6.39 C and D; Figure 6.39 E and F).

Some coating stacks doped with blue photochromes only (Blue D and gr. Blue D) were also evaluated. Their initial coloration produced a deep blue tint, which is considered to provide proper protection against excessive daylight (Figure 6.40). A photochromic activity of about 40 % was achieved through a

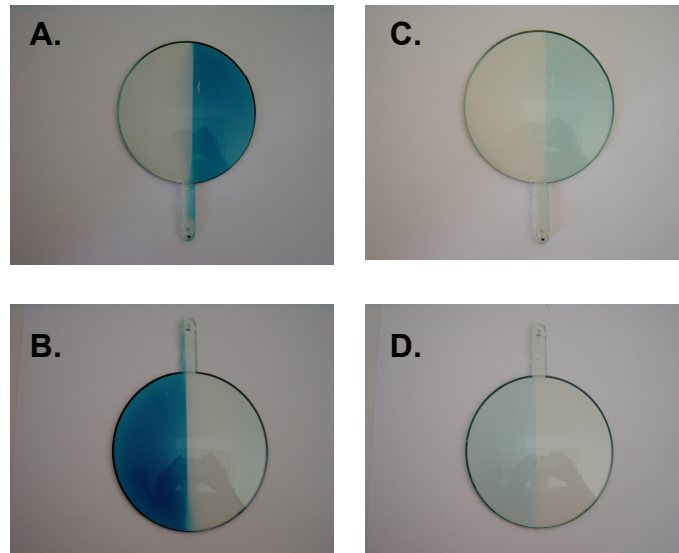


Figure 6.40. Photochromic coatings on bis-phenol-A polycarbonate lenses: coloration directly after UV irradiation (A. and B.) and 3 minutes after switching off the UV source (C. and D.); coatings compositions: [GG / 6 % gr. Blue D] (A.) and [GG / 4 % gr. Blue D + 2 % Blue D] (B.).

combination of two dyes or a high concentration of gr. Blue D (up to 6 %) within a one-layer GG system. It is remarkable that even these high concentrations of graftable dye did not cause any blooming, agglomeration or softening of the matrix.

Blue multi-layer coatings equipped with top coat (PL) and AR coating (kat60_AR – kat75, Appendix 2 Table 5) turned out to have a very good photo stability with half life times up to 270 h in the Suntest (Figure 6.41 A). All these compositions were based on GAD base coatings doped with gr. Blue D (3 %). GA10, GB or GG coatings doped with Blue D (3 %) or gr. Blue D (3 %) were applied as the second photochromic layer. PL and AR top coats finished the coating stack.

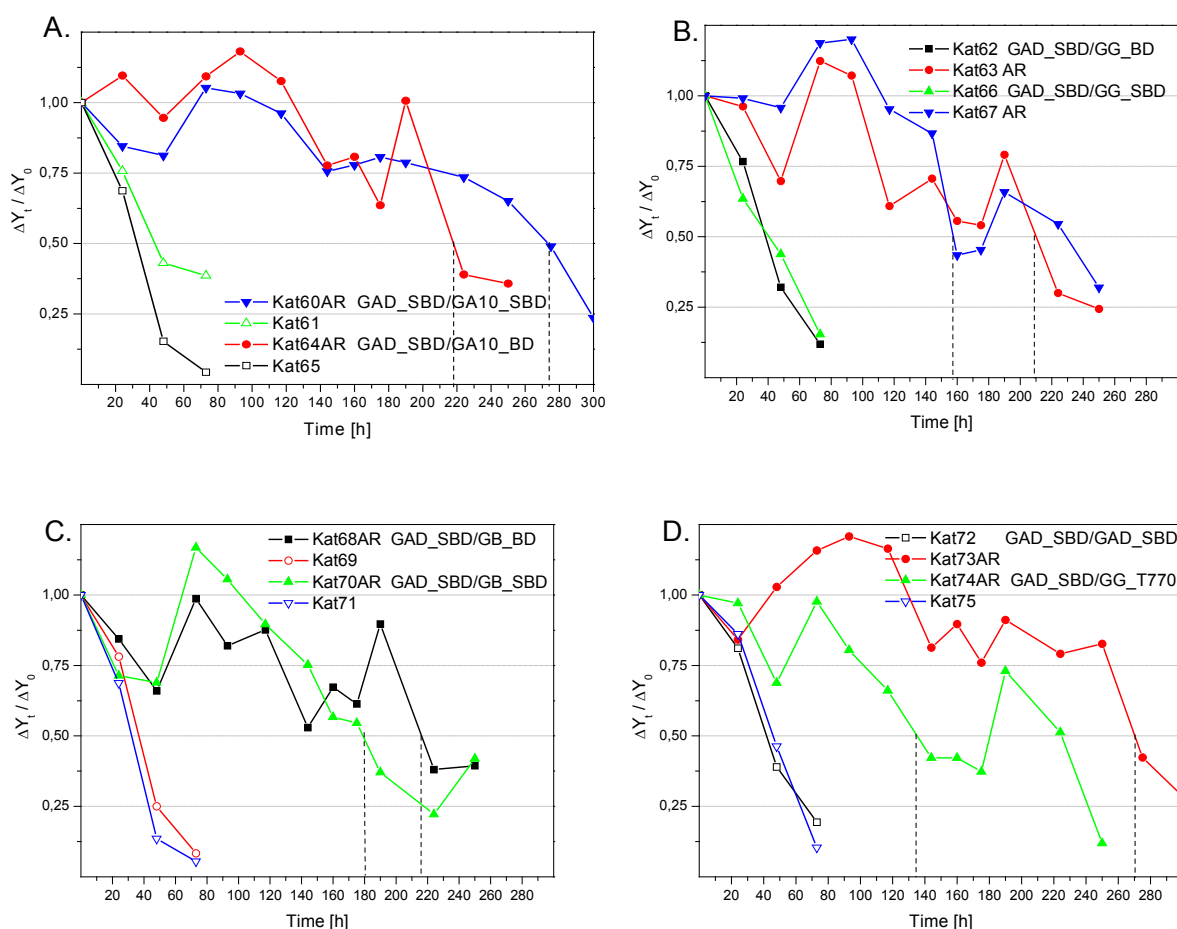


Figure 6.41. Relative loss of photochromic activity after prolonged UV irradiation for samples with blue photochromes, with and without AR layer; for sample labels see Appendix 2 Table 5.

Samples kat60_AR – kat75 (Appendix 2, Table 5) showed the typical stabilisation effect when equipped with an AR coating. The most photostable of the whole series were the samples kat60_AR ($T_{50\%} = 275$ h) and kat73_AR ($T_{50\%} = 270$ h) (Figure 6.41 A and D). There, two rather soft, nonpolar matrix systems GAD and GA10 associated in a multi-layer coating resulted in outstanding stability of gr. Blue D. All other samples were also remarkably stable, with half life times higher than 100 h (Figure 6.41 A – D).

C. Commercial photochromic products

Two commercially available photochromic lenses, a “Varia 3®” lens (imbibed CR39®) and a new generation “Transitions®” lens (coated PC) were investigated as references. They showed very high initial photochromic activity of up to 65 % and half-life times of $T_{50\%}$ (Varia 3) = 150 h and $T_{50\%}$ (Transitions) = 110 h (Figure 6.42).

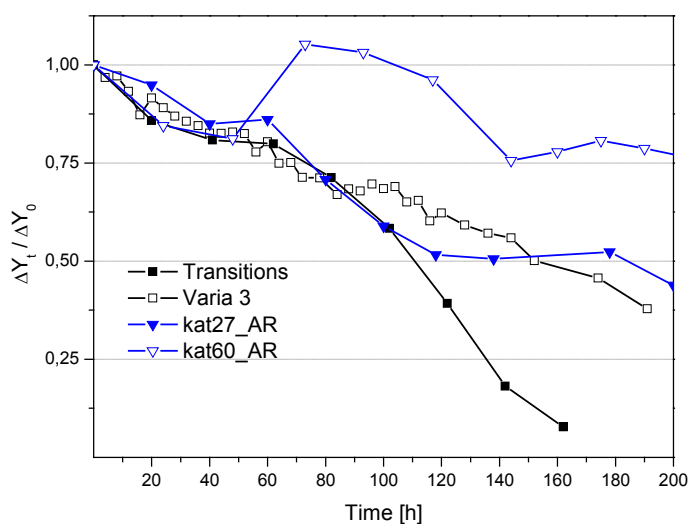


Figure 6.42. Relative loss of coloration after prolonged UV irradiation for commercially available photochromic lenses and for samples kat27_AR and kat60_AR.

Figure 6.42 demonstrates that the older generation Varia 3® lens showed a linear degradation curve with around 35 % of its initial activity left after 200 h of suntesting. The new generation Transitions® coating system behaved very similarly during the first 100 h of irradiation. However, this specimen showed a strong drop in the activity after that period and was completely degraded after 160 h.

In terms of luminous transmittance changes and half life times, the multi-layer coatings kat27_AR and kat60_AR developed in this thesis were comparable to the commercial systems. Kat60_AR still showed 75 % of its initial activity after 200 h which means an even better stability as was observed for the imbibed Varia 3® lens.

The temporary increase of photochromic activity observed after a short UV irradiation period is typical for the tested samples[141] and in may be effective by a certain “depot-effect” (see paragraph No. 6.2 Entrapment of photochromic dyes).

A main drawback, however, consisted in the restricted optical quality of the prepared multi-layer stacks and their tints, that were not neutral. Here, further optimisation would be necessary.

It could be shown that the photochromic dyes used in this work showed different coloration and degradation properties within different kinds of matrices. It was not always adequate to incorporate several dyes together into one coating. To achieve a maximum of photochromic performance, it was beneficial to spatially separate the dyes in different layers of a multi-layer coating. Such coating stacks should be composed of matrix systems of good interfacial compatibility in order to prevent delamination or other adverse effects. Multi-layer coating systems required careful and clean preparation. Interstage curing of the base coating was necessary for the application of the next layer with good optical quality. None of the used matrix systems possessed high hardness, due to the fact that the photochromic activity is suppressed or even reversed in rigid environments. To protect the coatings from scratches and other physical damages, a kind of “anti-scratch” coating is recommended. For that purpose the so-called particle lacquer (PL), an abrasion resistant organopolysiloxane coating with a high concentration of incorporated silica nanoparticles, which also prevents oxygen and water migration was used. Samples comparable to commercial systems in terms of stability and coloration were obtained. These samples comprised a multi-layer build-up with the dyes incorporated within two separate layers, a top coat and an oxidic AR coating, which has been applied by PVD.

7. Conclusions

The aim of this work was to test and tailor new sol-gel derived hybrid polymer coatings for the incorporation of photochromic spirooxazines and chromenes. The development and optimisation of work was performed via two different routes (Figure 7.1), that led to photochromic multi-layer coating systems with coloration depth and photostabilities comparable to commercially available products.

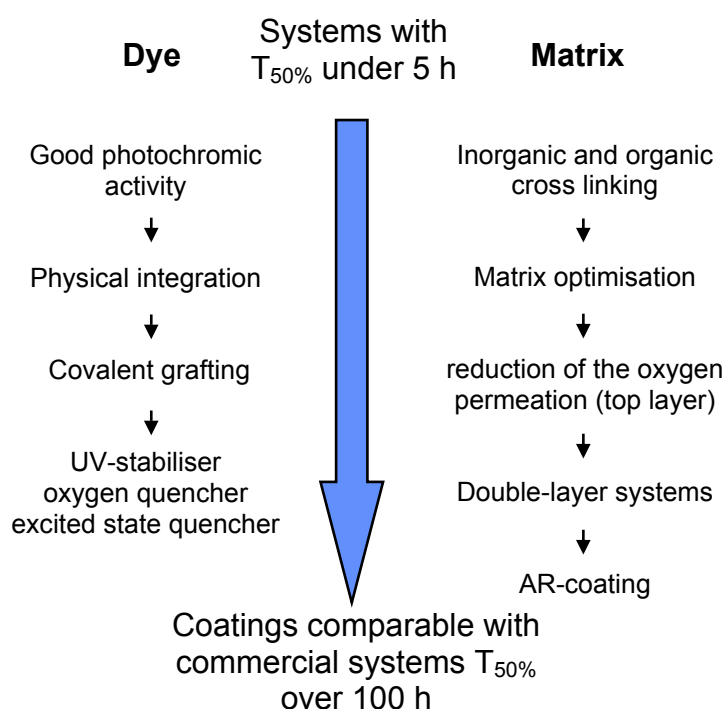


Figure 7.1. Development of photochromic coating systems.

Hybrid sol-gel derived polymers were found to be suitable host materials for photochromic dyes. Matrix properties and the type of entrapment heavily influence the photochromic activity, as well as the degradation rate and the kinetics of incorporated dyes. Dyes incorporated within more polar and rigid matrices were found to show slower kinetics and higher coloration but associated with faster photodegradation. On the other hand, hosts with less polar sites, low residual water concentration and low rigidity are

preferable in terms of photostability. Significant differences were found for physically incorporated and covalently grafted chromophores. Using silylated dyes that can participate in the sol-gel process, the photodegradation rate of the whole system can be decreased as compared to the physically entrapped systems. The higher photostability and slower kinetics for covalently bonded photochromes is probably due to sterical hindrance. Addition of proper stabilisers increases the photostability: The employment of UV light stabilisers, excited state quenchers and HALS was found to be beneficial but not sufficient. Besides the presence of stabilisers, also the reduction of oxygen migration into the coating (by a hard top coat and an inorganic anti reflective coating) strongly increases stability of photochromes. Finally, it was found that the separation of photochromes within two (or more) different layers leads to a further improvement of the coloration and fatigue behaviour of the whole coating stack, presumably by preventing the contact of dye molecules with excited states of other molecules or their degradation products. These latter findings are considered to pave the way for stable photochromic coatings based on hybrid polymers. Future development should be directed towards more photostable yellow and red switching dyes.

The results of the present investigations should help to choose the most suitable molecular environments for the tested photochromes in terms of photostability, kinetics and activity, which is considered relevant with respect to potential applications, in particular in the ophthalmic sector. Furthermore, the interesting combination of properties of this type of materials offers a large potential with regard to many applications, such as coatings for sunglasses, radiation protectors, filters, sunroofs, reversible markings, printing applications and smart textiles.

8. Zusammenfassung - Summary in German

Das Ziel dieser Arbeit war es, neue, über das Sol-Gel Verfahren hergestellte Beschichtungsmaterialien zu entwickeln, die als Matrices für photochrome Spirooxazine und Chromene geeignet sind. Die Entwicklungs- und Optimierungsarbeit erfolgte über zwei Routen (Abb. 7.1) und führte zu komplexen photochromen Mehrschichtaufbauten, deren Einfärbungs- und Photostabilitätseigenschaften mit kommerziell erhältlichen Produkten vergleichbar sind.



Abb. 7.1. Entwicklung von photochromen Beschichtungs-Systemen.

Über das Sol-Gel Verfahren hergestellte hybride Polymere stellen geeignete Wirtsmaterialien für photochrome Farbstoffen dar. Die Eigenschaften der Matrix und die Einbauweise beeinflussen sowohl die photochrome Aktivität, als auch die Degradationsgeschwindigkeit und Kinetik der eingebauten Farbstoffe. Farbstoffe integriert in rigide Matrices höherer Polarität zeigen geringere Schaltgeschwindigkeit und stärkere Einfärbung, jedoch verknüpft mit höherer Degradationsgeschwindigkeit.

Andererseits Matrixmaterialien mit eher unpolarem Charakter, niedriger Konzentration an Restwasser, und niedriger Rigidität sind zu bevorzugen, wenn gute Photostabilität erreicht werden soll. Wesentliche Unterschiede bestehen zwischen chemisch angebondenen und physikalisch eingebauten Farbstoffen. Durch den Einsatz von silylierten Farbstoffen, die am Sol-Gel-Prozess partizipieren können, kann eine Verringerung der Photodegradationsgeschwindigkeit im Vergleich zu physikalisch eingebauten Farbstoffen erreicht werden. Höhere Photostabilität und langsamere Schaltkinetik sind vermutlich auf sterische Hinderung zurückzuführen. Der Zusatz geeigneter Stabilisatoren erhöht die Photostabilität: Der Einsatz von UV-Stabilisatoren, Excited State Quenchern und HALS ist vorteilhaft aber nicht ausreichend. Neben der Präsenz von Stabilisatoren, führt auch die Verringerung der Sauerstoffpermeation (durch eine harte Deckschicht und eine reflexionsmindernde PVD-Beschichtung) zu einer Stabilitätserhöhung. Schließlich wurde gefunden, dass die räumliche Trennung der Farbstoffe in zwei (oder mehr) unabhängigen Schichten ebenfalls die Färbetiefe und Photoresistenz der Beschichtungen erhöhte, vermutlich dadurch, dass der Kontakt von Farbstoffmolekülen mit angeregten Zuständen anderer Moleküle oder ihren Degradationsprodukten verhindert oder zumindest eingeschränkt wird. Diese Befunde können den Weg für stabile photochrome Beschichtungen auf der Basis von Hybridpolymeren ebnen. Weiterer Optimierungsbedarf wird in den bisher erzielbaren Farbtönen gesehen. Zukünftige Entwicklungen sollten sich auf photostabilere gelb und rot schaltende Farbstoffe konzentrieren.

Die Ergebnisse der vorgelegten Untersuchungen können bei der Auswahl der am besten geeigneten, molekularen Umgebung für erprobte Photochrome in Bezug auf Photostabilität, Kinetik und Aktivität helfen. Dies ist von großer Bedeutung im Hinblick auf mögliche Anwendung vor allem im ophthalmischen Bereich. Darüber hinaus bergen die interessante Eigenschaftskombinationen dieser Art von Materialien großes Potential für ein weites Feld möglicher Anwendungen (Sonnenbrillen, Strahlungsschutz, Filter, Sonnendächer, schaltbare Markierungen, Druck, Textilien).

8. References

1. M. Klessinger, J. Michl, "Lichtabsorption und Photochemie organischer Moleküle", Weinheim, VCH, NY, 1989, p. 398-402.
2. P. Suppan, "Chemia i Swiatlo", PWN, Warszawa, 1997, p. 13-39.
3. S. E. Braslavsky, Phytochrome in "Photochromism. Molecules and Systems", H. Dürr, H. Bouas-Laurent (Eds.), Elsevier, 2003.
4. G. H. Brown, in "Photochromism" G. H. Brown (Ed.), Wiley, 1971, p. 2-12.
5. http://ehs.unc.edu/training/self_study/laser/eye.html
6. R. Marks, M. Staples, G. G. Giles, Int. J. Cancer 53 (1993) 585-590.
7. D. H. Sliney, J. Photochem. Photobiol. B: Biology 64 (2001) 166-175.
8. P. H. Gies, C. R. Roy, S. Toomey, A. McLennan, Mutation Research 422 (1998) 15-22.
9. J. C. Crano, W. S. Kwak, C. N. Welch, Spirooxazines and their use in photochromic lenses, in "Applied Photochromic Polymer Systems", C. B. McArdle (Ed.), Blackie & Son Ltd, New York, 1992, 31-79.
10. E. Fisher, Y. Hirshberg, J. Chem. Soc., 1952, 4522-4524.
11. A. Lightstone, T. Lightstone, A. Wilkins, Ophthal. Physiol. Opt. Vol. 19, No. 4 (1999) 279-285.
12. C. J. Brinker, G. W. Scherer, Sol-Gel Science: The Physics and Chemistry of Sol-Gel Processing, Academic Press Inc., San Diego, 1990.
13. J. D. Mackenzie, E. Bescher, J. Sol-Gel Sci. Technol. 27 (2003) 7-14.
14. K.-C. Song, J.-K. Park, H.-U. Kang, S.-H. Kim, J. Sol-Gel Sci. Technol. 27 (2003) 53-59.
15. D. Levy, S. Einhorn, D. Avnir, J. Non-Cryst. Solids, 113 (1989) 137-145.
16. C. Sanchez, B. Lebeau, F. Ribot, M. In, J. Sol-Gel Sci. Technol. 19 (2000) 31-38.
17. G. Kickelbick, Prog. Polym. Sci. 28 (2003) 83-114.
18. H. K. Schmidt, ACS Symp. Ser. 360 (1988) 333-344.
19. ORMOCER[®]s - trademark of Fraunhofer-Gesellschaft zur Förderung der Angewandten Forschung e.V., Germany.
20. K. H. Haas, Adv. Eng. Mater. 9 (2000) 571-582.
21. C. Sanchez, F. Ribot, B. Lebeau, J. Mater. Chem. 9 (1999) 35-44.
22. N. Nishiyama, T. Asakura, K. Horie, J. Coll. Inter. Sci. 124 (1988) 14-21.
23. K. Gigant, U. Posset, G. Schottner, L. Baia, W. Kiefer, J. Sol-Gel Sci. Technol. 26 (2003) 369-373.
24. A. Jitianu, A. Britchi, C. Deleanu, V. Badescu, M. Zaharescu, J. Non-Cryst. Solids 319 (2003) 263-279.
25. C. Sanchez, G.-J. de A. A. Soler-Illia, F. Ribot, T. Lalot, C. R. Mayer, V. Cabuil, Chem. Mater. 13 (2001) 3061-3083.
26. D. Levy, New J. Chem. 18 (1994) 1073-1086.
27. X. D. Sun, X. J. Wang, W. Shang, J. J. Song, M. G. Fan, E. T. Knobbe, J. Sol-Gel Sci. Technol. 9 (1997) 169-181.
28. D. Levy, D. Avnir, J. Phys. Chem. 92 (1988) 4734-4738.
29. Y. Chujo, Current Opt. Solid State Mater. Sci., 1 (1996) 806-811.
30. G. Schottner, Chem. Mater. 13 (2001) 3422-3435.
31. K. H. Haas, S. Amberg-Schwab, K. Rose, Jahrbuch Oberflächen-Technik, 55 (1999) 183-198.
32. G. Schottner, K. Rose, U. Posset, J. Sol-Gel Sci. Technol. 27 (2003) 71-79.
33. J. Kron, G. Schottner, K. J. Deichmann, Thin Solid Films 392 (2001) 236-242.
34. C. Ohtsuki, T. Miyazaki, M. Tanihara, Mater. Sci. Eng. C 22 (2002) 27-34.

35. A. Geiger, D. Griebel, R. Herrmann, K. Kuerzinger, Pat. No. WO 03/074420 A1, 2003, Roche Diagnostics GmbH, Fraunhofer-Gesellschaft zur Förderung der Angewandten Forschung e.V..
36. S. Gerlach, Fraunhofer-Institut für Silicatforschung, Jahrestätigkeitsbericht 2002.
37. S. Amberg-Schwab, H. Katschorek, U. Weber, A. Burger, J. Sol-Gel Sci. Technol. 26 (2003) 699-703.
38. M. Pilz, H. Römich, J. Sol-Gel Sci. Technol. 8 (1997) 1071-1075.
39. M. Popall, A. Dabek, M.E. Robertsson, G. Gustafsson, O.-J. Hagel, B. Olsowski, R. Buestrich, L. Cergel, M. Leby, P. Kiely, J. Joly, D. Lambert, M. Schaub, H. Reichl, 48th IEEE Electronic Components and Technology Conference (Cat.No.98CH36206). Seattle, WA (US) May 25-28, 1998, 1018-1025.
40. R. Houbertz, L. Fröhlich, M. Popall, U. Streppel, P. Dannberg, A. Bräuer, J. Serbin, B.N. Chichkov, Adv. Eng. Mater. 5 (2003) 551-555.
41. W. Que, X. Hu, Thin Solid Films, 436 (2003) 196-202.
42. T. Itou, H. Matsuda, Key Eng. Mater. 150 (1998) 67-76.
43. G. Schottner, J. Kron, K. J. Deichmann, J. Sol-Gel Sci. Technol. 13 (1998) 183-187.
44. Aldrich, Fluka, Sigma and Supelco Chiral Products Catalog, 1997, p. 250.
45. F. Samson, Surface and Coatings Technol. 81 (1996) 79-86.
46. J. M. Urreaga, M. C. Matias, V. Lorenzo, M. U. de la Orden, Mater. Lett. 45 (2000) 293-297.
47. H. Selhofer, R. Müller, Thin Solid Films 351 (1999) 180-183.
48. T. L. Phison, Chem. News. 43 (1881) 283.
49. E. ter Meer, Ann. Chem. 181 (1876) 1.
50. H. Dürr, in "Photochromism: Molecules and Systems" H. Dürr, H. Bouas-Laurent (Eds.), Elsevier, 2003, p. 1-15.
51. E. Wolf, H. K. Camenga, Z. Phys. Chem. 107 (1977) 21-38.
52. A. Weller, Z. Electrochem. 60 (1956) 1144-1147.
53. S. Yamamoto, K. H. Grellmann, Chem. Phys. Lett. 85 (1982) 73 -79.
54. B. Schilling, J. P. Synder, J. Am. Chem. Soc. 97 (1975) 4422-4424.
55. S. J. Cristol, R. L. Snell, J. Am. Chem. Soc. 80 (1958) 1950 – 1954.
56. H. Dürr, Photochromism of Dihydroindolizines and Related Systems, in: "Organic Photochromic and Thermochromic Compounds", J. C. Crano, R. Guglielmetti (Eds.), Plenum Press, NY, 1999.
57. W. H. Armistead, S. D. Stookey, Science 144 (1964) 647.
58. M. Mennig, K. Fries, M. Lindenstruth, H. Schmidt, Thin Solid Films 351 (1999) 230-234.
59. R. Facht, M. Müller, H. Bürger, A. Kriltz, GlasTechnol. Ber.Glass Sci. Technol. 71 (1998) 243-246.
60. T. R. Zhang, W. Feng, R. Lu, C. Y. Bao, T. J. Li, Y. Zhao, J. N. Yao, Mater. Chem. Phys. 78 (2002) 380-384.
61. H. Y. Zhang, L. Xu, E. B. Wang, M. Jiang, A. G. Wu, Z. Li, Mater. Lett. 57 (2003) 1417-1422.
62. W. Feng, T. R. Zhang, L. Wei, R. Lu, Y. B. Bai, T. J. Li, Y. Y. Zhao, J. N. Yao, Mater. Lett. 54 (2002) 309 – 313.
63. W. Feng, T. R. Zhang, Y. Liu, R. Lu, G. Guan, Y. Zhao, J. N. Yao, Mater. Chem. Phys. 77 (2002) 294 – 298.
64. Y. He, Z. Wu, L. Fu, C. Li, Y. Miao, L. Cao, H. Fan, B. Zou, Chem. Mater. 15 (2003) 4039-4045.
65. T. He, J. Yao, J. Photochem. Photobiol. C: Photochem. Rev. 4 (2003) 125-143.

66. C. D. Gabbutt, T. Gelbrich, J. D. Hepworth, B. M. Heron, M. B. Hursthouse, S. M. Partington, *Dyes Pigm.* 54 (2002) 79-93.
67. P. Bamfield, "Chromic phenomena: Technological applications of colour chemistry", RSC, 2001.
68. B. van Gemert, D. Knowles, *PPG Technol. J.* 1 (1995) 11-17, PPG Industries.
69. T. Nakabayashi, N. Nishi, H. Sakuragi, *Sci. Prog.* 84 (2001) 137-156.
70. S. Jockusch, N. J. Turro, F. R. Blackburn, *J. Phys. Chem. A* 106 (2002) 9236-9241.
71. W. Zhao, E. M. Carreira, *J. Am. Chem. Soc.* 124 (2002) 1582-1583.
72. V. Malatesta, Photodegradation of Organic Photochromes, in: "Organic Photochromic and Thermochromic Compounds", J. C. Crano, R. Guglielmetti (Eds.), Plenum Press, NY, 1999.
73. H. Dürr, *P. Appl. Chem* 73 (2001), 639-665.
74. Y. Liang, A. S. Dvornikov, P. M. Rentzepis, *J. Mater. Chem.* 10 (2000) 2477-2482.
75. A. M. Asiri, *J. Photochem. Photobiol. A: Chem.* 159 (2003) 1-5.
76. M. A. Wolak, N. B. Gillespie, C. J. Thomas, R. R. Birge, W. J. Lees, , J. *Photochem. Photobiol. A: Chem.* 147 (2002) 39-44.
77. R. Matsushima, M. Nishiyama, M. Doi, *J. Photochem. Photobiol. A: Chem.* 139 (2001) 63-69.
78. A. Heynderickx, A. M. Kaou, C. Moustrou, A. Samat, R. Guglielmetti, *New J. Chem.* 27 (2003) 1425-1432.
79. F. Sun, F. Zhang, F. Zhao, X. Zhou, S. Pu, *Chem. Phys. Lett.* 380 (2003) 206-212.
80. J. Ern, A. T. Bens, H.-D. Martin, K. Kuldova, H. P. Trommsdorff, C. Kryschi, *J. Phys. Chem. A* 106 (2002) 1654-1660.
81. H. Nakashima, M. Irie, *Macromol. Chem. Phys.* 200 (1999) 683-692.
82. H. Dürr, Pat. No. DE 19834940 A1, 1998.
83. H. Rau, in "Photochromism: Molecules and Systems" H. Dürr, H. Bouas-Laurent (Eds.), Elsevier, 2003, p. 165-192.
84. E. Ortyl, R. Janik, S. Kucharski, *Eur. Polym. J.* 38 (2002) 1871-1879.
85. C. Schulz, H. Dürr in "Photochromism: Molecules and Systems" H. Dürr, H. Bouas-Laurent (Eds.), Elsevier, 2003, p. 193-209.
86. H. Ono, C. Osada (Fuji) US Pat. No. 3562172 (1971)
87. G. Arnold, H. P. Vollmer, German Oten. 1927849, 1970.
88. R. C. Bertelson, Photochromic Processes Involving Heterolytic Cleavage in "Photochromism", G. H. Brown (Ed.), Wiley, 1971, p. 45-432.
89. H. Dürr, Y. Ma, G. Cartellaro, *Synthesis* 3 (1995) 294-298.
90. T. Deligeorgiev, S. Minkovska, B. Jejiaskova, S. Rakovsky, *Dyes Pigm.* 53 (2002) 101-108.
91. A. Samat, V. Lokshin, K. Chamontin, D. Levi, G. Pepe, R. Guglielmetti, *Tetrahedron* 57 (2001) 7349-7359.
92. X. Li, Y. Wang, T. Matsuura, J. Meng, *J. Photochem. Photobiol. A: Chem.* 161 (2004) 201-213.
93. R. Nakao, T. Horii, Y. Kushino, K. Shimaoka, Y. Abe, *Dyes Pigm.* 52 (2002) 95-100.
94. R. Gautron, *Bull. Soc. Chim. Fr.* 1968, 3200- 3204.
95. C. Salemi, G. Giusti, R. Guglielmetti, *J. Photochem. Photobiol. A: Chem.* 86 (1995) 247-252.
96. Y. N. Malkin, T. B. Krasieva, V. A. Kuzmin, *J. Photochem. Photobiol. A: Chem.* 49 (1989) 75-88.

97. G. Baillet, G. Giusti, R. Guglielmetti, *J. Photochem. Photobiol. A: Chem.* 70 (1993) 157-161.
98. C. Salemi-Delvaux, B. Luccioni-Houze, G. Baillet, G. Giusti, R. Guglielmetti, *Tetrahedron*, 37 (1996) 5127-5130.
99. V. Malatesta, R. Millini, L. Montanari, *J. Am. Chem. Soc.* 117 (1995) 6258-6264.
100. R. A. Kopelman, S. M. Synder, N. L. Frank, *J. Am. Chem. Soc.* 125 (2003) 13684-13685.
101. R. Richert, H. Bässler, *Chem Phys. Lett.* 116 (1985) 302-306.
102. B. H. Lee, J. H. Kim, M. J. Cho, S. H. Lee, D. H. Choi, *Dyes Pigm.* 61 (2004) 235-242.
103. J. Ratner, N. Kahana, A. Warshawsky, v. Krongauz, *Ind. Eng. Chem. Res.* 35 (1996) 1307-1315.
104. B. Schaudel, C. Guermeur, C. Sanchez, K. Nakatani, J. A. Delaire, *J. Mater. Chem.* 7 (1997) 61-65.
105. N. Y. C. Chu, *Solar Energy Mater.* 14 (1986) 215-221.
106. V. Malatesta, P. Allegrini, L. Crisci (Enichem Synthesis S.p.A.) US Pat. No.: 5242624, 1993.
107. G. Gauglitz "Photophysical, photochemical and photokinetic properties of photochromic systems", in "Photochromism: Molecules and Systems" H. Dürr, H. Bouas-Laurent (Eds.), Elsevier, 2003, p. 15-63.
108. R. J. Hovey, N. Y. C. Chu, P. G. Piusz, C. H. Fuchsmann (American Optical) US Pat. 4215010 (1980).
109. T. Sakagami, K. Machida, Y. Fujuii, N. Arakawa, N. Murayama (Kureha) US Pat. 4756973 (1988).
110. H.-J. Suh, W.-T. Lim, J.-Z. Cui, H.-S. Lee, G.-H. Kim, N.-H. Heo, S.-H. Kim, *Dyes Pigm.* 57 (2002) 149-159.
111. S.-H. Kim, H.-J. Suh, J.-Z. Cui, Y.-S. Gal, S.-H. Jin, K. Koh, *Dyes Pigm.* 53 (2002) 251-256.
112. S.-H. Kim, S.-W. Choi, J.-H. Kim, S.-H. Jin, Y.-S. Gal, J.-H. Ryu, J.-Z. Cui, K. Koh, *Dyes Pigm.* 50 (2001) 109-115.
113. S.-R. Keum, S.-M. Ahn, S.-H. Lee, *Dyes Pigm.* 60 (2004) 55-59,
114. A. Leautic, A. Dupont, P. Yu, R. Clement, *New J. Chem.* 25 (2001) 1297-1301.
115. K. Nakatani, P. Yu, *Adv. Mater.* 13 (2001) 1411-1413.
116. Y. Einaga, M. Taguchi, G. Li, T. Akitsu, Z. Gu, T. Sugai, O. Sato, *Chem Mater.* 15 (2003) 8-10.
117. W. S. Kwak, J. C. Crano, 1996, PPG Industries, Inc.
118. A. Klukowska, U. Posset, G. Schottner, M. L. Wis, C. Salemi-Delvaux, V. Malatesta, *Mat. Sci.*, 20 (2002) 95-104.
119. M. Mennig, K. Fries, M. Lindenstruth, H. Schmidt, proceedings of 2nd International Conference on Coatings on Glass (1998) 333-337.
120. M. Mennig, K. Fries, H. Schmidt, *Mat. Res. Soc. Symp. Proc.* 576 (1999) 409-414.
121. L. Hou, H. Schmidt, *Mater. Lett.* 27 (1996) 215-218.
122. L. Hou, H. Schmidt, *J. Mater. Sci.* 31 (1996) 3427-3434.
123. G. Schottner, J. Kron, U. Posset (Fraunhofer-Gesellschaft zur Förderung der Angewandten Forschung e.V.) Pat. No. DE 10025906 A1.
124. L. Crisci, W. Giroladini, V. Malatesta, M. L. Wis (Great Lakes Chemical) US pat. No. US 6414057 B1, 2002.
125. R. C. Bertelson, Application of Photochromism, in: "Photochromism", G. H. Brown (Ed.), Wiley, 1971, p. 733-815.

126. H. G. Heller, IEEE Proceedings, 130 (1983) 209-211.
127. J.-S. Lin, Eur. Polym. J. 39 (2003) 1693-1700.
128. Y.-R. Yi, I.-J. Lee, J. Photochem Photobiol A: Chem. 151 (2002) 89-94.
129. K. Ock, N. Jo, J. Kim, S. Kim, K. Koh, Syn. Meter. 117 (2001) 131-133.
130. B. Osterby, R. D. McKelvey, L. Hill, J. Chem. Ed. 68 (1991) 424-425
131. H.-J. Suh, S.-H. Jin, Y.-S. Gal, K. Koh, S-H. Kim, Dyes Pigm. 58 (2003) 127-133.
132. S. Y. Ju, D.-I. Kwon, S.-J. Min, K.-D. Ahn, K. H. Park, J.-M. Kim, J. Photochem. Photobiol. A: Chem. 160 (2003) 151-157.
133. P. Fisher, Opinion on Transitions. publication of Transition Optical, Alta Vision Labs (Fisher Optical), 1, 1995.
134. J. D. Basil, C.-C. Lin, R. M. Hunia (PPG Industries) US Pat. No. 4799963, 1989.
135. R. A. Smith (Transitions Optical, Inc.) US Pat. No. 5624757, 1997.
136. R. W. Walters, K. J. Stewart (PPG Industries) Pat. No. EP 1200512 A1, 2002.
137. C. N. Welch, E. M. King, L. G. Anderson, R. Daughenbaugh, K. J. Stewart (PPG Industries) Pat. No. WO 2003037998, 2003.
138. C. Knox, W. McDonald, F. Mallak, (Transitions Optical, Inc.) WO Pat. No.: 2004/044626 A1, 2004.
139. H. Dürr, Praxis d. Naturwiss. - Chem. 40 (1991) 22-28.
140. N. Y. C. Chu, 4n+2 systems: spirooxazine, in: "Photochromism: Molecules and Systems", H. Dürr, H. Bouas-Laurent (Eds.), Elsevier, 2003, p. 493-509.
141. V. Malatesta, U. Posset, private communications.
142. DIN 53 151 (German Industrial Specification).
143. U. Posset, M. Lankers, W. Kiefer, H. Steins and G. Schottner, Appl. Spectrosc. 47 (1993) 1600.
144. L. E. Scriven, Mater. Res. Soc. Symp. Proc., 121 (1988) 717-729.
145. A. Goumri, J. Yuan, E. L. Hommel, P. Marshall, Chem. Phys. Lett. 375 (2003) 149-156.
146. K. Gigant, U. Posset, G. Schottner, Appl. Spectrosc. 56 (2002) 762-769.
147. H. C. Marsmann, in: P. Diehl, E. Fluck, R. Kosfeld, (Eds.). NMR 17: Oxygen-17 and Silicon-29, Springer, Berlin, 1981.
148. R. B. Taylor, B. Parbhoo, D. M. Fillmore, Nuclear Magnetic Resonance Spectroscopy, in: The Analytical Chemistry of Silicones, A. Lee Smith (Ed.), Wiley, New York, 1991.
149. Y. S. Chiu, K. H. Wu, T. C. Chang, Eur. Poly. J. 39 (2003) 2253-2259.
150. W-D. Herzog, M. Messerschmidt, NMR-Spektroskopie fuer Anwender, VCH, Weinheim, New York, Basel, Cambridge, Tokyo, 1995.
151. T-H. Lee, E-S. Kang, B-S. Bae, J. Sol-Gel Sci. Technol. 27 (2003) 23-29.
152. R. Di Maggio, L. Fambri, P. Mustarelli, R. Camprostrini, Polymer 44 (2003) 7311-7320
153. G. Sciaini, D. E. Wetzler, J. Alvarez, R. Fernandez-Prini, M. L. Japas, J. Photochem. Photobiol. A: Chem. 153 (2002) 25-31.
154. B. Dunn, J. I. Zink, Chem. Mater. 9 (1997) 2280-2291.
155. A. F. Lagalante, R. J. Jacobson, T. J. Bruno, J. Org. Chem 61 (1996) 6404-6406.
156. P. Makedonski, M. Brandes, W. Grahn, W. Kowalsky, J. Wichern, S. Wiese, H.-H. Johannes, Dyes Pigm. 61 (2004) 109-119.
157. E. Casassa, G. Fonrodona, A. de Juan, Inorg. Chim. Acta 187 (1991) 187-195.
158. I. Baraldi, G. Brancolini, F. Momicchioli, G. Ponterini, D. Vanossi, Chem. Phys. 288 (2003) 309-325.

159. H. Wang, E. Borguet, K. B. Eisenthal, *J. Phys. Chem. B* 102 (1998) 4927-4932.
160. C. Reichardt, *Chem. Rev.* 94 (1994) 2319-2358.
161. E. M. Kosower, 80 (1958) 3253-3270.
162. V. G. Luchina, I. Yu. Sychev, A. I. Shienok, N. L. Zaichenko, V. S. Marevtsev, *J. Photochem. Photobiol. A* 93 (1996) 173-178.
163. T-W. Shin, Y-S. Cho, Y-D. Huh, K. D. Lee, W. Yang, J. Park, I-J. Lee, *J. Photochem. Photobiol. A: Chem.* 137 (2000) 163-168.
164. L. Hou, B. Hoffmann, H. Schmidt, M. Mennig. *J. Sol-Gel Sci. Technol.* 8 (1997) 923-926.
165. L. Hou, H. Schmidt, B. Hoffmann, M. Mennig. *J. Sol-Gel Sci. Technol.* 8 (1997) 927-929.
166. L. Hou, B. Hoffmann, M. Mennig, H. Schmidt. *Sol-Gel Production, Key Eng. Mater.* 150 (1998) 41-48.
167. V. A. Krongauz, Environmental effects on organic photochromic systems, in: "Photochromism Molecules and Systems" H. Dürr, H. Bouas-Laurent (Eds.), Elsevier, 2003, p. 793-821.
168. M. Bletz, U. Pfeifer-Fukumura, V. Kolb, W. Baumann, *J. Phys. Chem. A* 106 (2002) 2232-2236.
169. M. Campredon, R. Guglielmetti, A. Samat, A. Alberti, *J. Chim. Phys.* (91 (1994) 1830-1836.
170. V. Malatesta, C. Neri, M. L. Wis, L. Montanari, R. Millini, *J. Am. Chem. Soc.* 119 (1997) 3451-3455.
171. V. Malatesta, C. Neri, M. L. Wis, *Mol. Cryst. Liq. Cryst.* 298 (1997) 145-150.
172. L. A. Blumenfeld, W. W. Wojewodski, A. G. Siemionow, "Zastosowanie elektronowego rezonansu paramagnetycznego w chemii", PWN, Warszawa, 1967.
173. N. J. Turro, M. H. Kleinman, E. Karatekin, *Angew. Chem. Int. Ed.* 39 (2000) 4436-4461.
174. K. Matsui, M. Motegi, K. Ito, *Nucl. Instr. Meth. Phys. Res. B* 116 (1996) 253-256.
175. V. Malatesta, M. Milosa, R. Millini, L. Lanzini, P. Bortolus, S. Monti, *Mol. Cryst. Liq. Cryst.* 246 (1994) 303-310.
176. A. A. Firth, D. J. McGarvey, T. G. Truscott, *Mol. Cryst. Liq. Cryst.* 246 (1994) 295-298.
177. F. Gugumus, *Polym. Deg. Stab.* 50 (1995) 101-116.
178. A. Klukowska, U. Posset, G. Schottner, A. Jankowska-Frydel, V. Malatesta, *Mat. Sci.*, 22 (2004) 188-199.
179. N. Y. C. Chu (American Optical Corporation) Pat. No.: US 4720356, 1988.
180. H. Yamashita, Y. Ohkatsu, *Polym. Degrad. Stab.* 80 (2003) 421-426.

Appendix 1

Table 1. GG, GB and GA10 coatings doped with 3 % of gr. Blue D and containing different stabilisers (Enam 121, Enam 129, 3-methylpyrazoline (MP), graftable 3-methylpyrazoline (gr. MP), 3-methylcoumarine, nickel-organocomplex (Q84)), their thickness and photochromic activity: ΔY_{0h} , ΔY_{24h} and remaining percentual activity after 24 h of UV irradiation (T_{24h}); δ_{n-1} – thickness standard deviation.

Sample		Ave. Thickness [μm]	δ_{n-1} [μm]	ΔY_{0h} [%]	ΔY_{24h} [%]	T_{24h} [%]
Matrix	Stabiliser					
GG	none	4.94	0.06	30	11	37
GG	Enam 121	5.57	0.09	30	17	57
GG	Enam 129	5.90	0.24	26	17	65
GG	MP	5.03	0.17	25	8	32
GG	gr. MP	5.30	0.07	27	10	37
GG	coumarine	4.61	0.07	26	2	8
GG	Q84	5.30	0.06	30	13	43
GB	none	4.21	0.14	26	11	42
GB	Enam 121	4.16	0.13	28	16	57
GB	Enam 129	5.59	0.53	27	23	85
GB	MP	3.38	0.33	24	17	71
GB	gr. MP	3.44	0.05	26	17	65
GB	coumarine	3.62	0.23	26	----	----
GB	Q84	4.41	0.31	22	17	77
GA10	None	5.84	0.03	24	20	83
GA10	Enam 121	4.14	0.07	18	17	94
GA10	Enam 129	3.93	0.09	16	16	100
GA10	MP	3.71	0.15	13	13	100
GA10	gr. MP	3.55	0.01	17	14	82
GA10	coumarine	4.69	0.17	22	3	14
GA10	Q84	5.03	0.20	18	19	1

Table 2. Characteristics (thickness and photochromic activity: ΔY_{0h} , ΔY_{24h} and remaining percentual activity after 26 h of UV irradiation (T_{26h})) of double layer systems [GG / 4 % Blue D + 3 %] (base coat) // [PL / no dye] (top coat), with different stabilisers in the base coat (Enam 121, Enam 129, 3-methylpyrazoline (MP), graftable 3-methylpyrazoline (gr. MP), 3-methylcoumarine, nickel-organocomplex (Q84)).

stabiliser	Average thickness [μm] (δ_{n-1})			Luminous Transmittance		T_{26h} [%]
	Basic layer	Both layers	Top layer	ΔY_{0h}	ΔY_{26h}	
none	5.19 (0.49)	10.20 (0.87)	5.07 (0.39)	63	11	17
Enam 121	6.23 (0.44)	10.04 (1.27)	3.83 (0.82)	49	2	4
Enam 129	7.65 (0.23)	12.81 (0.65)	5.16 (0.72)	58	15	26
MP	5.17 (0.12)	8.51 (0.28)	3.32 (0.33)	42	6	14
gr. MP	6.63 (0.19)	10.68 (0.54)	3.75 (0.20)	32	4	13
coumarine	6.84 (0.33)	11.21 (0.41)	4.36 (0.27)	48	9	19
Q84	4.95 (0.11)	8.63 (0.07)	3.68 (0.08)	33	9	27

Appendix 2

Table 1. List of single-layer coating compositions stabilised with mixtures of T770, Q84 and DABCO-I (with a molar ratio of dye : T770 : Q84 : DABCO-I as 1 : 1 : 1 : 2) ; additional top coat PL and AR layer (“AR” in the label). CR39[®] lenses were used as substrates.

	Matrix	Dyes mixture	Curing	ΔY_{0h} [%]	ΔY_{24h} [%] ($\Delta Y_{24h} / \Delta Y_{0h}$ [%])	ΔY_{72h} [%] ($\Delta Y_{72h} / \Delta Y_{0h}$ [%])
Kat1_AR	GG	gr. Blue D 4 %; WW 3 %	125 °C / 20 min.	52.77	40.81 (77)	24.38 (46)
Kat3	GG	gr. Blue D 4 %; WW 3 %	125 °C / 20 min.	56.56	29.59 (52)	6.88 (12)
Kat4_AR	GG	gr. Blue D 4 %; WW 3 %	180 °C / 5 min.	54.67	40.85 (75)	19.62 (36)
Kat5	GG	gr. Blue D 4 %; WW 3 %	180 °C / 5 min.	59.43	26.71 (45)	5.92 (10)

Table 2. List of single-layer coating system compositions stabilisers added T770, Q84 and DABCO-I (with a molar ratio of dye : T770 : Q84 : DABCO-I as 1 : 1 : 1 : 2); additional top coat PL and AR layer (“AR” in the label). CR39[®] lenses were used as substrate.

	Matrix	Dyes mixture	Curing	ΔY_{0h} [%]	ΔY_{48h} [%] ($\Delta Y_{48h} / \Delta Y_{0h}$ [%])	ΔY_{96h} [%] ($\Delta Y_{96h} / \Delta Y_{0h}$ [%])
Kat10	GB	gr. Blue D 4 %; WW 3 %	125 °C / 20 min.	61.8	25.32 (41)	----
Kat11	GB	gr. Blue D 4 %; WW 3 %	125 °C / 20 min.	61.25	22.03 (36)	----
Kat12	GB	gr. Blue D 4 %; WW 3 %	180 °C / 5 min.	60.08	34.01 (57)	----
Kat13	GB	gr. Blue D 4 %; WW 3 %	180 °C / 5 min.	63.25	27.25 (43)	----

Kat14	GA10	gr. Blue D 4 %; Blue D 2 %	125 °C / 20 min.	37.24	17.13 (46)	
kat15	GA10	gr. Blue D 4 %; Blue D 2 %	125 °C / 20 min.	36.32	22.26 (61)	9.63 (27)
Kat16_AR	GB	gr. Blue D 4 %; WW 3 %	125 °C / 20 min.	56.72	39.29 (69)	15.6 (27)
Kat17_AR	GB	gr. Blue D 4 %; WW 3 %	125 °C / 20 min.	52.97	42.07 (79)	20.4 (38)
Kat18_AR	GB	gr. Blue D 4 %; WW 3 %	180 °C / 5 min.	54.74	36.47 (67)	16.52 (30)
Kat19_AR	GB	gr. Blue D 4 %; WW 3 %	180 °C / 5 min.	53.43	40.42 (76)	22.71 (43)
Kat20_AR	GA10	gr. Blue D 4 %; Blue D 2 %	125 °C / 20 min.	31.32	19.04 (61)	13.7 (44)
Kat21_AR	GA10	gr. Blue D 4 %; Blue D 2 %	125 °C / 20 min.	32.67	21.48 (66)	9.16 (28)

Table 3: List of coating compositions with additional top coat PL and AR layer (“AR” in the label). CR39[®] lenses were used as substrates.

	GG_GBD (4 %) + WW (3 %)	GG_GBD (4 %)	GG_WW (3 %)	Curing	ΔY_{0h} [%] (ΔY_{0h} [%] without AR layer)	ΔY_{48h} [%] ($\Delta Y_{48h} /$ ΔY_{0h} [%])	ΔY_{96h} [%] ($\Delta Y_{96h} /$ ΔY_{0h} [%])
Kat22	+			125 °C / 20 min.	47.37	21.21 (45)	10.02 (21)
Kat23_AR	+			125 °C / 20 min.	45.86 (48.72)	33.27 (73)	22.49 (49)
Kat24_AR	+			160 °C / 5 min.	54.12 (57.01)	36.01 (67)	22.81 (42)
Kat25	+			160 °C / 5 min.	56.89	13.6 (24)	3.5 (6)
Kat26		+	+	125 °C / 20 min.	66.96	44.79 (67)	20.51 (31)
Kat27_AR		+	+	125 °C / 20 min.	67.13 (62.63)	57.02 (85)	32.65 (49)

Table 4. List of coating compositions with additional top coat PL and AR layer (“AR” in the label), cured at 125 °C for 20 minutes. CR39® lenses were used as substrates.

	GAD_BD (5%)	GAD_BD (5%) +1n Q84	GAD_GBD (3%)	GAD_GBD (3%) + 1n Q84	GG_WW (3%)	GG_WW (3%) + 2n DABCO-I	GG_WW (3%)_GPL (3%)	GG_WW (3%) GPL (3%) + 2n DABCO-I	ΔY_{0h} [%]	ΔY_{48h} [%] ($\Delta Y_{48h} /$ ΔY_{0h} [%])	ΔY_{96h} [%] ($\Delta Y_{96h} /$ ΔY_{0h} [%])
Kat28_AR	+				+				53.06	36.84 (69)	15.37 (29)
Kat 29	+				+				64.52	14.43 (22)	-
Kat30_AR	+					+			47.83	30.13 (63)	15.28 (32)
Kat 31	+					+			52.82	9.09 (17)	-
Kat 32	+						+		50.35	8.92 (18)	-
Kat33_AR	+						+		46.31	25.85 (56)	19.17 (41)
Kat 34 AR	+						+		39.62	22.6 (57)	18.08 (46)
Kat 35	+						+		43.31	11.61 (27)	6.66 (15)
Kat36_AR		+			+				59.6	34.17 (57)	18.98 (32)
Kat 37		+			+				53.09	11.13 (21)	-
Kat 38		+				+			45.84	12.04 (26)	-
Kat39_AR		+				+			44.24	29.27 (66)	24.49 (55)
Kat 40		+					+		43.66	6.34 (15)	-
Kat41_AR		+					+		42.11	25.16 (60)	16.89 (40)
Kat 42		+					+		36.31	9.76 (27)	10.05 (28)
Kat43_AR		+					+		29.66	17.67 (60)	17.39 (59)
Kat44_AR			+		+				62.1	43.6 (70)	39.10 (63)
Kat 45			+		+				60.36	30.01 (50)	8.24 (14)
Kat46_AR			+			+			54.52	29.44 (54)	37.94 (70)
Kat 47			+			+			46.74	32.47 (70)	9.0 (19)

Kat 48			+					+		36.71	22.17 (60)	21.47 (59)
Kat49_AR			+					+		40.57	24.08 (59)	18.97 (47)
Kat 50			+						+	24.97	17.69 (71)	23.1 (93)
Kat51_AR			+						+	25.16	16.38 (65)	21.58 (86)
Kat 52				+	+					59.3	35.08 (59)	28.52 (48)
Kat53_AR				+	+					39.39	39.92 (101)	38.79 (99)
Kat 54				+				+		50.08	34.68 (69)	27.19 (54)
Kat55_AR				+				+		55.23	32.08 (58)	35.77 (65)
Kat56_AR				+					+	42.3	25.24 (60)	22.82 (54)
Kat 57				+					+	37.27	28.32 (76)	25.73 (69)
Kat58_AR				+					+	29.97	30.2 (101)	23.61 (79)
Kat 59				+					+	29.69	29.66 (100)	27.01 (91)

Table 5. List of coating compositions with additional top coat PL and AR layer (“AR” in the label), cured at 125 °C for 20 minutes. CR39[®] lenses were used as substrates

	GAD_GBD (3%)	GA10_GBD (3%)	GG_BD (3%)	GA10_BD (3%)	GG_GBD (3%)	GB_BD (3 %)	GB_GBD (3 %)	GAD_GBD (6 %)	GG_T770	ΔY_{0h} [%] (without AR layer)	ΔY_{48h} [%] ($\Delta Y_{48h} / \Delta Y_{0h}$)	ΔY_{93h} [%] ($\Delta Y_{93h} / \Delta Y_{0h}$)	ΔY_{253h} [%] ($\Delta Y_{250h} / \Delta Y_{0h}$)
Kat60_AR	+	+								37.27 (43.24)	26.53 (71)	38.46 (103)	24.26 (65)
Kat 61	+	+								46.63	20.01 (43)		
Kat 62	+		+							42.73	13.96 (33)		
Kat63_AR	+		+							28.75	20.05 (70)	30.81	7.0 (24)

										(46.96)		(107)	
Kat64_AR	+			+						22.3 (36.23)	21.09 (95)	28.51 (127)	9.98 (45)
Kat 65	+			+						36.49	5.74 (16)		
Kat 66	+				+					48.50	21.24 (44)		
Kat67_AR	+				+					29.11 (48.12)	27.87 (96)	37.84 (130)	9.31 (32)
Kat68_AR	+					+				35.94 (48.11)	23.71 (66)	29.43 (82)	14.12 (39)
Kat 69	+					+				50.44	12.61 (25)		
Kat70_AR	+						+			39.96 (49.80)	27.52 (69)	42.18 (106)	16.75 (42)
Kat 71	+						+			46.63	6.33 (14)		
Kat 72	+							+		42.85	16.72 (39)		
Kat73_AR	+							+		29.15 (39.52)	30.35 (104)	37.12 (127)	24.38 (84)
Kat74_AR	+								+	36.92 (45.43)	25.4 (69)	29.7 (80)	4.40 (12)
Kat 75	+								+	37.42	17.33 (46)		

Acknowledgements – Danksagung

Der Bayerischen Forschungsstiftung bin ich zu Dank verpflichtet für finanzielle Unterstützung meiner Arbeit in Form eines Stipendiums. An dieser Stelle möchte ich auch Herrn Prof. Dr. Gerd Müller danken für die Möglichkeit, diese Doktorarbeit am Fraunhofer-Institut für Silicatforschung durchzuführen und für sein Interesse am Gelingen dieser Arbeit. Die interessante Themenstellung war mir eine Freude! Herrn Dr. Uwe Posset danke ich für seine Diskussionsbereitschaft und großes persönliches Engagement!

Ich danke auch meinen Eltern und Großeltern für die nicht aufgegebene Hoffnung und das dauerhafte Mitfiebern – bardzo Wam dziekuje!

Für die sehr gelungene Zusammenarbeit will ich mich bei Herrn Dr. R. Bertermann und seinem Team, die Festkörper-NMR-Analysen am Institut für Anorganische Chemie der Universität Würzburg durchgeführt haben und der Frau Dr. A. Jankowska-Frydel, die für Durchführung von ESR-Messungen am Lehrstuhl für Physik der Universität Gdansk zuständig war, herzlich bedanken. Ohne die wertvolle Unterstützung durch Herrn K. Buchner von der Firma Rupp+Hubrach Optik GmbH, der sich um AR-Beschichtungen gekümmert hat, wäre diese Arbeit nicht zu Stande gekommen!

Herrn Prof. Dr. A. Klonkowski danke ich für sein stetes Interesse an meinem wissenschaftlerischen Schicksal.

Allem AWZtlerINen will ich herzlichen Dank aussprechen für das sehr gute Arbeitsklima, viel Unterstützung und ständige Gesprächsbereitschaft (unabhängig vom Thema)! Annette, Angie, Christine, Erika, Heike, Johanna, Katja, Rosa, Sabine, Uli, Achim, Gerhard, Klaus und Uwe, ich habe sehr viel von Euch gelernt.

Besonderer Dank geht an Karine Gigant, Dragan Griebel und Haymo Katschorek, die mich in die Geheimnisse des Doktorandenlebens eingeführt haben. Seb, Steph und Stefan danke ich für sehr nette Begleitung auf diesem Weg.

Für ständige Krisenbekämpfungsbereitschaft will ich mich bei Marta und Kasia (bekannt auch als „die polnischen Schwestern“) bedanken – wielkie dzieki!

Herzlichen Dank geht an Anka, Kamila und Beata für stete Unterstützung von weitem – dziekuje!

Dass ich für einen kurzen Moment Teil an Euren Leben nehmen durfte: Claudine, Sandra, Frank, Gerhard und Roland – herzlichen Dank!

Hanne, danke, dass Du Deine Versprechung gehalten hast!

...und allen, die ich nicht absichtlich vergessen habe – Dankeschön!

Curriculum Vitae - Lebenslauf

Persönliche Daten

Name: Anna Klukowska

Geburtsdaten: geb. am 08.02.1976 in Olsztyn, Polen

Nationalität: polnisch

Familienstand: ledig

Ausbildung

09.83 – 06.91 Szkoła Podstawowa (Grundschule), Nr. 1, Przejazdowo, Polen

09.91 – 05.95 Liceum, Nr. 1, im. Marii Konopnickiej, Pruszcz Gdański, Polen: Abschluss „Abitur“

10.95 – 06.2000 Studium der Chemie an der Fakultät für Chemie, Universität Gdansk, Polen: Abschluss „Magister der Chemie“

10.98 – 06.2000 Studium der Pharmazie an der Fakultät der Pharmazie der Medizinischen Universität, Gdansk, Polen

26.06.2000 Magisterprüfung im Studiengang Chemie

09.99 – 06.2000 Magisterarbeit (Diplomarbeit) „Preparation and investigation of the properties of nanostructural systems“, durchgeführt an der Fakultät für Chemie, Universität Gdansk, Polen

seit 10.2000 Doktorarbeit „Switching Hybrid Polymers with Physically and Covalently Entrapped Organic Photochromes“, durchgeführt am Fraunhofer-Institut für Silicatforschung, Würzburg

Berufstätigkeit

seit 10.2000 Wissenschaftliche Mitarbeiterin am Fraunhofer-Institut für Silicatforschung, Würzburg